THEORY AND APPLICATONS OF CTD RECURSIVE COMB FILTERS

Frank Piazza

NAVAL POSTGRADUATE SCHOOL

Monterey, California

THESIS

THEORY AND APPLICATIONS OF
CTD RECURSIVE COMB FILTERS

by

Frank Piazza

December 1976

Thesis Advisor: T.F. Tao

Approved for public release; distribution unlimited.

SECURITY CLASSIFICATION OF THIS PAGE (When Date Entered)

REPORT DOCUMENTATION PAGE

READ INSTRUCTIONS BEFORE COMPLETING FORM

1. REPORT NUMBER	2. GOVT ACCESSION NO.
3. RECIPIENT'S CATALOG NUMBER	
4. TITLE (and Subtitle) Theory and Applications of CTD Recursive Comb Filters	5. TYPE OF REPORT & PERIOD COVERED Master's Thesis; December 1976
6. PERFORMING ORG. REPORT NUMBER	
7. AUTHOR(s) Frank Piazza	8. CONTRACT OR GRANT NUMBER(s)
9. PERFORMING ORGANIZATION NAME AND ADDRESS Naval Postgraduate School Monterey, California 93940	10. PROGRAM ELEMENT, PROJECT, TASK AREA & WORK UNIT NUMBERS
11. CONTROLLING OFFICE NAME AND ADDRESS Naval Postgraduate School Monterey, California 93940	12. REPORT DATE December 1976
	13. NUMBER OF PAGES 155
14. MONITORING AGENCY NAME & ADDRESS(if different from Controlling Office)	15. SECURITY CLASS. (of this report) Unclassified
	15a. DECLASSIFICATION/DOWNGRADING SCHEDULE

16. DISTRIBUTION STATEMENT (of this Report)

Approved for public release; distribution unlimited.

17. DISTRIBUTION STATEMENT (of the abstract entered in Block 20, if different from Report)

18. SUPPLEMENTARY NOTES

19. KEY WORDS (Continue on reverse side if necessary and identify by block number)

Sampled Analog Devices
Bilinear Z Transform
Standard Z Transform
Signal-to-Noise Ratio
Frequency Spectrum

20. ABSTRACT (Continue on reverse side if necessary and identify by block number)

Both integrator and canceller types of sampled analog comb filters implemented by a canonical second order recursive circuit have been studied experimentally and theoretically. Two 96 stage CTD (charge transfer device) delay lines are used in the experimental study. Theoretically, an analysis based on a modification of the digital recursive filter theory was developed and accounted for the major features of the experimental results.

20.(Abstract continued)

Three comb filter applications have been demonstrated. The first two used the integrator type comb filter for the improvement of the signal-to-noise ratio of a periodic signal contaminated by noise and for the sorting of a periodic signal of selected PRF from other periodic signals. The third application used a canceller type comb filter to eliminate a sinusoidal interference from a desireable signal.

THEORY AND APPLICATIONS OF CTD RECURSIVE COMB FILTERS

by

Frank Piazza
Lieutenant, United States Navy Reserve
A.A.S., Hudson Valley Community College, 1966
B.S.E.E., Rochester Institute of Technology, 1969

Submitted in partial fulfillment of the
requirements for the degree of

MASTER OF SCIENCE IN ELECTRICAL ENGINEERING

from the

NAVAL POSTGRADUATE SCHOOL

December 1976

ABSTRACT

Both integrator and canceller types of sampled analog comb filters implemented by a canonical second order recursive circuit have been studied experimentally and theoretically. Two 96 stage CTD (charge transfer device) delay lines are used in the experimental study. Theoretically, an analysis based on a modification of the digital recursive filter theory was developed and accounted for the major features of the experimental results.

Three comb filter applications have been demonstrated. The first two used the integrator type comb filter for the improvement of the signal-to-noise ratio of a periodic signal contaminated by noise and for the sorting of a periodic signal of selected PRF from other periodic signals. The third application used a canceller type comb filter to eliminate a sinusoidal interference from a desirable signal.

TABLE OF CONTENTS

LIST OF FIGURES..... 7
DEFINITION OF TERMS..... 11
ACKNOWLEDGEMENT..... 12
I. INTRODUCTION..... 13
A. GENERAL..... 13
B. RECURSIVE COMB FILTERS..... 14
C. PURPOSE OF THE STUDY..... 15
D. OUTLINE..... 16
II. THEORY..... 18
A. INTRODUCTION..... 18
B. BASIC TRANSFORM THEORY..... 18
C. TRANSFORMS..... 19
D. TRANSFORM PROPERTIES..... 20
E. PHYSICAL SIGNIFICANCE OF Z^{-1} 23
F. DIGITAL FILTERS VERSUS SAMPLED-ANALOG FILTERS..... 23
G. THE UNIT CIRCLE..... 24
III. FILTER DESIGN..... 26
A. SAMPLED ANALOG FILTER DESIGN..... 26
1. Introduction..... 26
2. Recursive Filters..... 28
3. Estimation of the B Coefficients..... 31
4. Integrator and Canceller Recursive Comb Filters..... 33
5. Coefficient Determination..... 35
6. Filter Design..... 36
B. COMPUTER AIDED FILTER DESIGN..... 39
IV. EXPERIMENTAL FILTER STUDY..... 61
A. CIRCUIT CONFIGURATION..... 61

B. EXPERIMENTAL DATA..... 62
1. Data Analyses..... 81
C. FILTER SELECTION..... 84
V. APPLICATIONS OF THE INTEGRATOR TYPE RECURSIVE COMB FILTERS 1: SIGNAL-TO-NOISE RATIO IMPROVEMENT..... 86
A. INTRODUCTION..... 86
B. FOURIER ANALYSIS AND FILTER CONSIDERATIONS... 86
C. DEVICE SELECTED..... 90
D. SIGNAL-TO-NOISE RATIO MEASUREMENTS..... 105
E. FREQUENCY CONSIDERATION..... 113
F. SNR IMPROVEMENT USING A SECOND ORDER FILTER. 116
G. FIRST ORDER FILTER SNR IMPROVEMENT CURVES.... 117
VI. APPLICATION OF THE INTEGRATOR TYPE RECURSIVE COMB FILTER 2: SELECTION OF PULSE TRAINS..... 121
A. RADAR..... 121
B. ELECTRONIC COUNTERMEASURES..... 121
1. Interference Considerations from the Non-Synchronous Pulse Trains..... 124
2. Frequency Spectrum Considerations..... 126
C. PROBLEMS ENCOUNTERED IN DATA TAKING..... 136
VII. CANCELLER APPLICATIONS AND DEMONSTRATION..... 137
A. BACKGROUND..... 137
B. CANCELLER FILTER DEMONSTRATION..... 138
VIII. SUMMARY AND RECOMMENDATIONS..... 141
A. EXPERIMENTAL RESULTS..... 141
B. THEORETICAL ANALYSIS..... 142
C. APPLICATIONS..... 143
D. CONTINUATION OF THIS RESEARCH..... 144
Appendix A: PULSE TRAIN FOURIER ANALYSIS..... 145
Appendix B: COMPUTER PROGRAM FOR PLOTTING H(Z)..... 148
Appendix C: EXPERIMENTAL DATA FOR SNR GRAPHS..... 150
LIST OF REFERENCES..... 153
INITIAL DISTRIBUTION LIST..... 155

LIST OF FIGURES

2.1 Transform Steppingstones..... 19
2.2 Bilinear Z Mapping..... 24
2.3 Standard Z Mapping..... 25
3.1 Design Methods..... 27
3.2 Zero Location for Low and High Pass Filter..... 30
3.3 Graphically Estimating Pole Zero Location..... 32
3.4 Recursive Comb Filter types..... 34
3.5 b-Plane Triangle of Stability..... 38
3.6 Comb Frequency Spectrum (Theoretical)..... 41
3.7 Comb Frequency Spectrum (Theoretical)..... 42
3.8 Comb Frequency Spectrum (Theoretical)..... 43
3.9 Comb Frequency Spectrum (Theoretical)..... 44
3.10 Comb Frequency Spectrum (Theoretical)..... 45
3.11 Comb Frequency Spectrum (Theoretical)..... 46
3.12 Comb Frequency Spectrum (Theoretical)..... 47
3.13 Comb Frequency Spectrum (Theoretical)..... 48
3.14 Comb Frequency Spectrum (Theoretical)..... 49
3.15 Comb Frequency Spectrum (Theoretical)..... 50
3.16 Comb Frequency Spectrum (Theoretical)..... 51
3.17 Comb Frequency Spectrum (Theoretical)..... 52
3.18 Comb Frequency Spectrum (Theoretical)..... 53
3.19 Comb Frequency Spectrum (Theoretical)..... 54
3.20 Comb Frequency Spectrum (Theoretical)..... 55
3.21 Comb Frequency Spectrum (Theoretical)..... 56
3.22 Comb Frequency Spectrum (Theoretical)..... 57
3.23 Comb Frequency Spectrum (Theoretical)..... 58
3.24 Comb Frequency Spectrum (Theoretical)..... 59
3.25 Comb Frequency Spectrum (Theoretical)..... 60
4.1 Filter Circuit Configuration..... 61

4.2 Comb Frequency Spectrum (Experimental)
and Pole Location..... 65
4.3 Comb Frequency Spectrum (Experimental)
and Pole Location..... 66
4.4 Comb Frequency Spectrum (Experimental)
and Pole Location..... 67
4.5 Comb Frequency Spectrum (Experimental)
and Pole Location..... 68
4.6 Comb Frequency Spectrum (Experimental)
and Pole Location..... 69
4.7 Comb Frequency Spectrum (Experimental)
and Pole Location..... 70
4.8 Comb Frequency Spectrum (Experimental)
and Pole Location..... 71
4.9 Comb Frequency Spectrum (Experimental)
and Pole Location..... 72
4.10 Comb Frequency Spectrum (Experimental)
and Pole Location..... 73
4.11 Comb Frequency Spectrum (Experimental)
and Pole Location..... 73
4.12 Comb Frequency Spectrum (Experimental)
and Pole Location..... 75
4.13 Comb Frequency Spectrum (Experimental)
and Pole Location..... 76
4.14 Comb Frequency Spectrum (Experimental)
and Pole Location..... 77
4.15 Comb Frequency Spectrum (Experimental)
and Pole Location..... 78
4.16 Comb Frequency Spectrum (Experimental)
and Pole Location..... 79
4.17 Comb Frequency Spectrum (Experimental)
and Pole Location..... 80
4.18 Comb Frequency Spectrum (0-400 K Hz)..... 83
4.19 Comb Frequency Spectrum (0-400 K Hz)..... 85
5.1 Pulse Train Frequency Spectrum..... 88
5.2 Integrator Comb Filter Response..... 89

5.3 Comb Filter Frequency Spectrum (Experimental)..... 92
5.4 Pulse train frequency spectrum (PRF=4063 Hz)..... 95
5.5 Input Pulse Train Frequency Spectrum (Experimental). 96
5.6 Input Pulse Train Frequency Spectrum (Experimental). 96
5.7 Input Pulse..... 97
5.8 Filter Input and Output..... 97
5.9 Cancellation of the Input Signal..... 98
5.10 Input Noise Spectrum..... 100
5.11 Output Noise Spectrum..... 101
5.12 Comparison of Input and Output Noise Spectrum..... 103
5.13 Time Domain of Input and Output Noise..... 104
5.14 Network for adding Signal and Noise..... 105
5.15 Signal plus Noise..... 108
5.16 Signal plus Noise..... 108
5.17 Signal plus Noise..... 109
5.18 Signal plus Noise..... 109
5.19 Cancellation of Signal Plus Noise..... 110
5.20 Output Signal Frequency Spectrun..... 110
5.21 Comparison of Input and Output Spectrums..... 111
5.22 Output Frequency Spectrum..... 111
5.23 Output and Input Frequency Response Comparison..... 112
5.24 Pulse Train Plus Noise Frequency Spectrum..... 114
5.25 Filtered Pulse Train plus Noise..... 115
5.26 SNR improvement vs b_1 coefficients..... 118
5.27 Band of Data Variation..... 120
6.1 Pulse Sorting Illustration..... 123
6.2 Interfering Spectral Components..... 125
6.3a Output Frequency Spectrum..... 127
6.3b Input Frequency Spectrum..... 127
6.4 Comparison of input and output Spectral Components.. 128
6.5a Spectral output with two input signals..... 129
6.5b Spectral output with two passed signals..... 130
6.6 Comparison of Figure 6.4 and 6.5..... 130
6.7a Input Spectral Components..... 132
6.7b Output Frequency Spectrum with two input signals... 133

6.8 Comparison of two harmonically related signals..... 135
6.9 Limit of frequency selectivity..... 135
7.1 Frequency response f_{clock}=104.6 KHz..... 139
7.2 Demonstrating the cancellation of a signal..... 140
7.3 Demonstrating the cancellation of a signal..... 140
A.1 Pulse train..... 145

DEFINITION OF TERMS

Several equations are presented throughout this thesis. Many of the terms used in these equations are generally represented in most texts and papers as Greek symbols. To simplify the typing requirements, these terms have been redefined. The following list shows the standard symbols which are used throughout this text.

PI = 3.141592654

f = frequency = 1/T

w = 2*PI*f

e = exp

s = jw

Z = exp(sT)

MHz = Mega Hertz = 10^{6} Hertz

K = Kilo Hertz = 10^{3} Hertz

db = decibels

Pf = Pico Farrads = 10^{-12} Farrads

t = Tao

t_0 = Any Arbitrary Starting Time

CTD = Charge Transfer Device

SNR = Signal To Noise ratio

CZT = chirp-Z-transform

Transfer Function = V_{output}/V_{input}

ACKNOWLEDGEMENT

It is with great appreciation that this author acknowledges Dr. T. F. Tao for his guidance in this work. The technical discussions and suggestions from all members of the research group led by Dr. Tao proved to be valuable aids. Special appreciation is given to my wife, Peggy, for her assistance in typing this thesis and to she and my children, Frank, Joseph, and Elizabeth for their patience and understanding in my absence.

I. INTRODUCTION

A. GENERAL

One of the major considerations in system design is signal processing. For all types of systems, it is necessary to consider how the signal will be represented (analog, digital, or sampled analog), received and conditioned to minimize errors and noise; and finally, how the desired signal will be recognized and/or discriminated. All these factors must be considered whether the system under concern is a communication, radar, sonar, accoustical, optical, or some other type. Although the signal processing techniques vary greatly in all the previously mentioned systems, the operations performed have a great deal in common. The many processing operations can be grouped into four catagories:

Two types of filters:

1. Nonrecursive
    a. Convolvers
    b. Correlators
2. Recursive

Two types of spectral analysis:

1. Fourier type of transforms
2. Other types of transforms

This thesis is concerned with the sampled analog recursive filter. Specifically, the recursive comb filter is studied both experimentally and theoretically. The feasibility of this filter's application is also demonstrated.

B. RECURSIVE COMB FILTERS

A comb filter is a class of filters whose transfer function is periodic in the frequency domain. There are two classifications of comb filters: canceller or bandstop, and the integrator or bandpass. The canceller is characterized as having a very narrow but a high attenuation region between neighboring teeth and good transmission within the passband region. The integrator is the opposite of this in that the passband region exhibits good signal passage in periodically spaced narrow bands of frequencies and a relatively wide attenuation band in between neighboring teeth. Comb filters have been developed for both analog and digital filtering systems. The development of these circuits has been based on the feedforward, frequency sampling, fast Fourier transform, and recursion technique of implementation. The common feature of circuit implementation for all these devices is that they all require delay lines as the basis of their operation.

The delay devices which are used vary with the systems encountered. For example, shift registers are used in digital systems whereas sampled analog systems use the bucket brigade device (BBD), charge coupled device (CCD), or the serial analog delay (SAD) device. Due to the sampling technique of these sampled analog devices, they exhibit both sampled analog properties and some of the digital properties as well.

The comb filter was analyzed for a sampled analog filter to determine its frequency response characteristics. The technique used in designing this type of filter was the Bilinear Z transform which is discussed in Chapter 2. This filter was implemented as a recursive filter which is a filter that is characterized as a device whose output depends on the present input, past output, and its present output. It can also be implemented as a non-recursive feedforward filter and used for spectral analysis through the chirp-Z-transform (CZT).

C. PURPOSE OF THE STUDY

During the past two years, recursive comb filters have been studied at the Naval Postgraduate school. V. Iamsa-ad[10] first studied the use of charge transfer device delay lines for the implementation of sampled analog recursive filters. B. Fruend[7] studied the first order recursive filter and emphasized the comb feature. L. Saetre[8] extended the study to the second order recursive comb filter and demonstrated the application of the canceller type comb filter to MTI radar. S. Holmes[6] developed a computer aided design procedure for the recursive comb filters and studied their sensitivity to device errors and variations. The status of the recursive comb filter study before the beginning of this thesis can be summarized as follows:

-Theory-

The digital recursive filter theory was modified to analyze the sampled analog recursive comb filters. While the

modified theory accounted for the comb feature of the filter, it was not able to explain three major features of sampled analog recursive comb filters which are different from an ideal comb filter.

*The peak of the frequency characteristics do not remain constant as in an ideal comb filter. They become frequency dependent in the sampled analog implementation.

*The frequency characteristics do not remain zero between neighboring teeth as in the ideal case. Deterioration of these nulls generally increases with frequency.

*The shape of the comb teeth do not remain constant as in the ideal comb filter. These also change with frequency.

-experimental study and Application-

Only the canceller type comb filter was experimentally studied in detail and its application to MTI radar was demonstrated. The Integrator comb filter was not studied thoroughly.

Therefore, there are three objectives for this thesis:

1. Improve the theoretical analysis.

2. Experimentally study the integrator comb filter and demonstrate its applications.

3.Demonstrate other applications of the canceller comb filter and discuss some of its applications.

D. OUTLINE

Chapter 1 presents the background and purpose of this thesis. Chapter 2 summarizes the basic ideas about digital

filters together with a discussion of the mapping transforms (H(s) into H(z)) which are used for the design of recursive comb filters. In Chapter 3, the design procedures for both the canceller type and the integrator type recursive comb filters are discussed. The experimental results with comb filters are presented and compared with the theoretical analysis in Chapter 4. Chapters 5, 6, and 7 present applications of comb filters. Chapter 5 specifically demonstrates the use of the integrator comb filter as a means to improve signal-to-noise ratio of a pulse train signal which has been contaminated with white Gaussian noise. The integrator comb filter is used as a pulse train sorter to select a particular pulse train from among varied frequency pulse trains. A third application of the comb filter is presented for a canceller comb filter in Chapter 7 where the device is used to eliminate sinusoidal interference from a second, desired sinusoid. Finally, Chapter 8 summarizes the results and offers suggestions for further studies.

II. THEORY

A. INTRODUCTION

The theory of digital recursive filters has been well developed in several text books and published papers as well as some past theses written here at the Naval Postgraduate School(i.e. see references 6,7,and 8). For this reason the theory of recursive filters will not be covered in detail, although a general overview of sampled analog theory will be presented beginning with the transform theory. This will lead into a discussion of the transforms which are used for designing both digital and sampled analog filters.

B. BASIC TRANSFORM THEORY

The analysis of analog circuits is highly dependent on the Laplace Transform to ease the computations which are involved as well as to simplify the circuit synthesis of the desired equations. For these same reasons transforms have been developed for use in digital circuits. It has been found that these same transforms can be used in sampled analog circuits. The Z Transforms which have been developed can be considered as steppingstones from either the Laplace S-plane domain, the discrete time domain (t=nT), or the continuous time domain into the Z-plane domain (see figure 2.1).

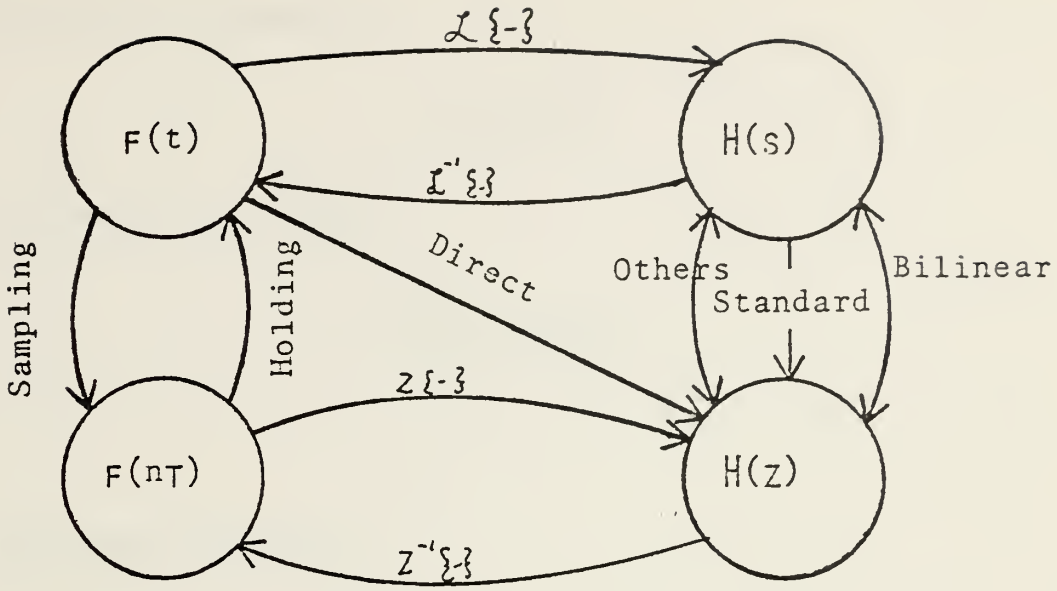

Figure 2.1 Transform Steppingstones

C. TRANSFORMS

There are a number of transforms which can be used to change a transfer function in the S-domain to a transfer function in the Z domain:

1. Impulse Invariant Transformation (Standard Z)
2. Bilinear Z Transformation
3. Mapping of Differentials
4. Matched Z Transform
5. Others

The most popular of these are the Impulse Invariant and the Bilinear Z transforms shown in figure 2.1. These mapping functions are given below:

The Standard Z Transform:

$$Z=\exp(sT)$$

The Bilinear Z Transform:

$$S = \frac{2(1 - Z^{-1})}{T(1 + Z^{-1})}$$

D. TRANSFORM PROPERTIES

The inherent properties of these types of transforms are similar although they do have some pronounced differences which make one technique more desirable than the other for some applications. These properties of both transforms are shown in Tables 1 and 2.

This thesis utilizes the Bilinear Z Transform technique because it maps the entire left half S-plane into the entire unit circle and there is no aliasing effect. These were the two major reasons for using this transform, other reasons are shown in Tables 1 and 2.

TABLE 1

TRANSFORM	PROPERTIES
Bilinear Z	1. Simple algebraic mapping between continuous and digital filters. 2. Maps entire jw axis in the S-plane to the unit circle in the Z plane. 3. Realizable, stable continuous circuits map into realizable, stable digital systems. 4. Wideband sharp cutoff continuous filter can be mapped into wideband sharp cutoff digital filter without aliasing. 5. There is a non-linear relation between the analog and digital frequencies resulting in frequency warping. 6. The amplitude response of the analog systems being transformed must be piece-wise constant, otherwise the digital frequency response will be warped. (See ref. 3, pg. 222-223) 7. Neither the impulse nor the phase response of the analog filter is retained in a digital filter.

TABLE 2

TRANSFORM	PROPERTIES
Standard Z	1. Encounters an inherent aliasing problem unless the sampling frequency is high. 2. The input signal must be band limited between -PI/T Hz and PI/T Hz for the frequency responses of the analog filter and its digital filter design equivalent to correspond. 3. The impulse response of the digital filter is a sampled version of its analog counterpart. 4. To use this transformation, the order of the numerator must be less than the order of the denominator of the analog filter to avoid intolerable aliasing problems in the digital filter.

E. PHYSICAL SIGNIFICANCE OF Z^{-1}

The operation of Z^{-1} is an important property in designing a sampled data circuit. Mathematically, Z^{-1} is simply a complex variable; but, physically, it represents a unit of delay for a sampled data circuit. How then can such a function be implemented? There are two techniques which are used to implement this delay physically. A digital circuit uses a shift register or memory. For sampled analog circuits the family of Charge Transfer Devices (CTD) delay lines are used.

F. DIGITAL FILTERS VERSUS SAMPLED-ANALOG FILTERS

There are major differences between digital filters and sampled-analog filters. However, much of the digital filter design theory is carried over into sampled analog filters. A digital filter receives an analog signal, quantizes it (i.e. represents the signal amplitude by a series of pulses which make up a coded binary number corresponding to the analog amplitude) and then performs its filtering action. This quantizing action is accomplished by an analog-to-digital (A-D) converter. It is generally an operation which introduces errors and extraneous electrical noise into the filter system. A sampled-analog filter eliminates this A-D conversion by sampling the signal's amplitude and storing a quantity of charge proportional to the signal amplitude. The storage (or delay action) is accomplished by the charge transfer devices for analog

filters and by shift registers for digital filters.

The relationship between digital filters and sampled-analog filters that are interchangeable is seen in the design techniques. The well developed digital filter design theory is applicable to sampled- analog design as well with some modification.

G. THE UNIT CIRCLE

When mapping from the S-plane to the Z-plane, it is important to consider which regions in the S-plane and Z-plane will correspond. This knowledge is important to consider the stability of the filter designed according to a transfer function in the Z domain.

For the Bilinear Z transform, the entire left half S-plane maps into the unit circle in the Z-plane, shown in figure 2.2, whereas the right half S-plane maps outside the unit circle.

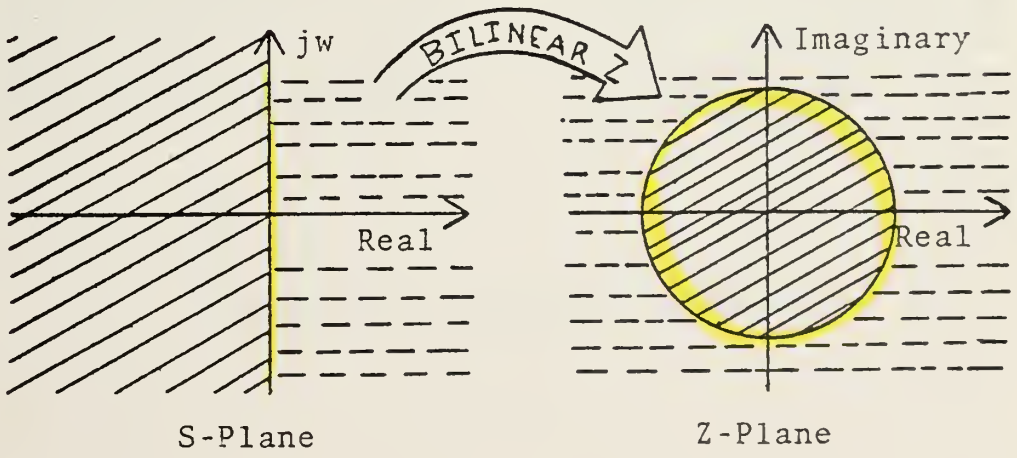

FIGURE 2.2 Bilinear Z Mapping

This is an important result, since the mapping of the entire jw axis onto the perimeter of a unit circle preserves the frequency selective properties of the analog system. The mapping of the left half S-plane inside the unit circle in the Z-plane ensures that stable analog filters will map into stable discrete time filters.

The desirable mapping characteristics described above are not inherent with the Standard Z transform, shown in figure 2.3. The Standard Z transform only maps periodic strips of the left half S-plane into the unit circle in the Z plane. The right half of the same strip maps outside of the unit circle. This is the reason for the possibility of aliasing at improper sampling frequencies. These strips are 2PI/T Hz in width and the first desirable mapping strip is between -jPI/T and jPI/T radians in the S-plane.

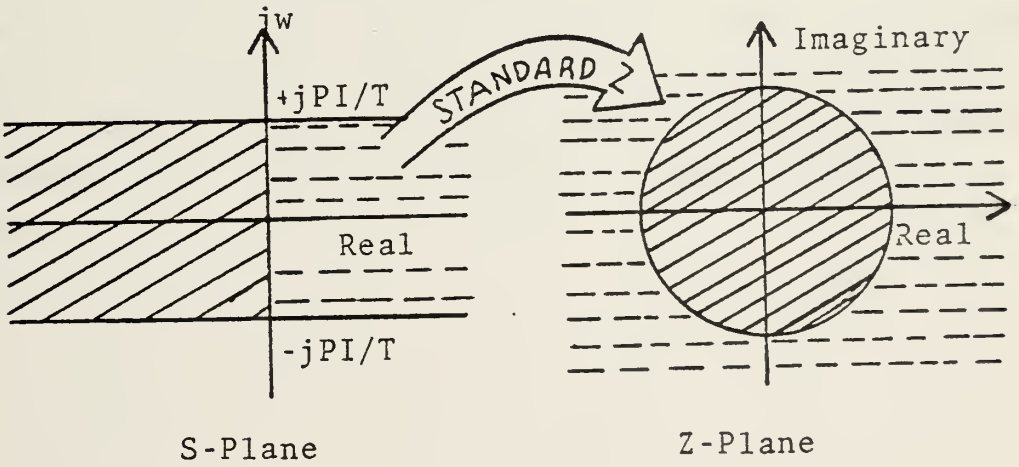

Figure 2.3 Standard Z Mapping

III. FILTER DESIGN

A. SAMPLED ANALOG FILTER DESIGN

1. Introduction

The design and implementation of a filter can be approached from many aspects. Basically, the numerous techniques which are used fall into one of two catagories; the Direct Method or the Indirect Method. Rabiner and Gold[3] in their excellent textbook have discussed these methods in detail. The procedures used in this thesis were a version of the indirect method using the previously discussed transforms. Figure 3.1 shows the procedural flow of these design techniques. In this section, the design and characteristics of the recursive comb filter will be covered.

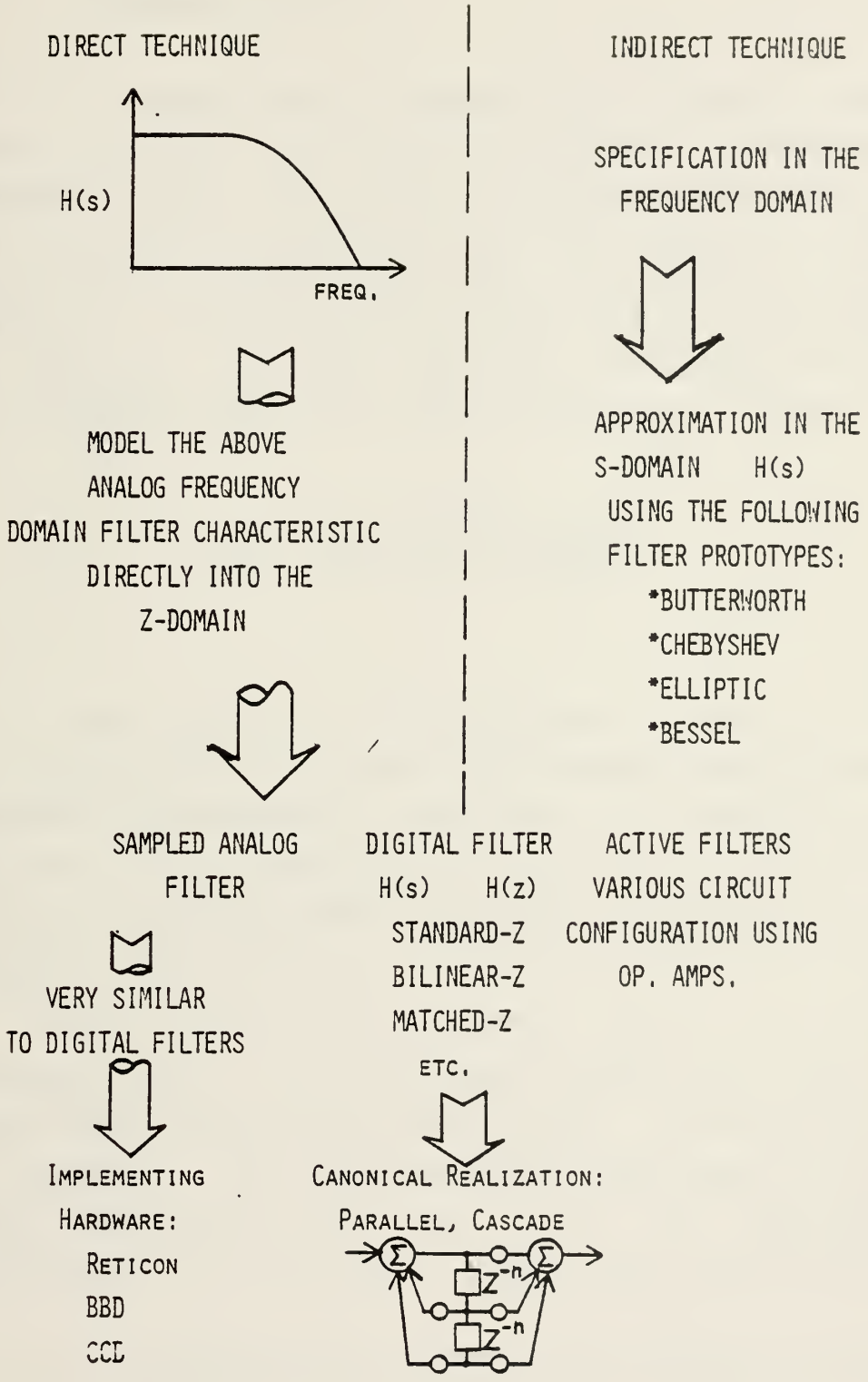

Figure 3.1 Design Methods

2. Recursive Filters

A filter which depends on its present input, past output, and also its present output is defined as a Recursive Filter. This definition implies that there are at least two operations which must be performed to synthesize such a device; feedback and delay. In addition to these two operations, a Recursive Filter also includes multiplication and addition. All these operations are evident by studying the Z transfer function as seen in equation 1 below:

$$H(z) = \frac{a_o + a_1 Z^{-1} + a_2 Z^{-2}}{1 + b_1 Z^{-1} + b_2 Z^{-2}} \qquad 1$$

This equation is developed from either the analog low pass or the analog high pass transfer function using the Bilinear Z transformation technique. The derivation of this equation is a common one and is found in most text books. However, for completeness the reader is encouraged to read Appendix B of reference 7 pages 99 through 120. Freund, B. R.[7] in his thesis has derived, using the Bilinear Z transform method, the transfer function for the first and second order low and high pass filter. Since the derivation of equation 1 has been thoroughly explained by Fruend the design techniques here were used to determine the coefficients for the proper response that was desired.

The relationship between the numerator coefficients is an important one since the numerator polynomial determines the location of the zeros of the transfer response. In the derivation of H(z) the normalized transfer

function showed that the relationship between a_0, a_1, and a_2 is 1, 2, 1, respectively. As shown below, this gives a double zero on the unit circle either at $Z=1+j0$ or $Z=1-j0$ depending upon the sign of the a_1 coefficient.

For $a_1=+2$:

$$1+2Z^{-1}+Z^{-2} = 0$$

Multiply by Z^2

$$Z^2+2Z+1 = 0$$

or

$$(Z_1+1)(Z_2+1) = 0$$

therefore

$$Z_1 = -1, \; Z_2 = -1$$

Similarily for $a_1=-2$

$$Z^2-2Z+1 = 0$$

$$(Z-1)(Z-1) = 0$$

$$Z_1 = 1, \; Z_2 = 1$$

Plotting these values of Z on the unit circle reveals that there is a double zero at Z= +1 or at Z = -1. This indicates that either a low or high pass filter is

determined simply by the sign of a_1 (plus for low pass and minus for high pass). See figure 3.2. Other numerical relationships between a_0, a_1, and a_2 will result in the zeros becoming complex, and/or shifting to either inside or outside the unit circle resulting in deterioration of the transfer function stop bands.

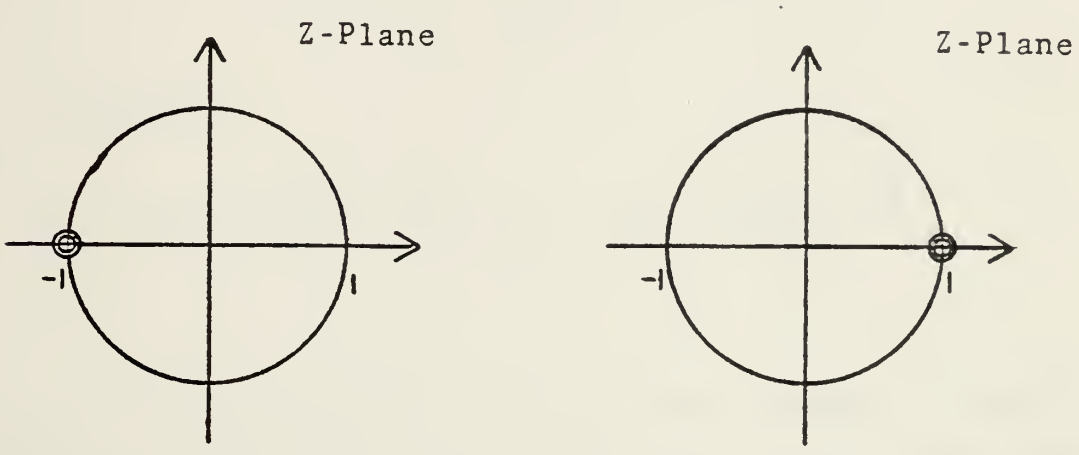

a. Low Pass Filter
$a_1 = +2.0$
$z_1 = z_2 = -1$

b. High Pass Filter
$a_1 = -2.0$
$z_1 = z_2 = +1$

FIGURE 3.2 Zero location for low or high pass filter.

The "b" coefficients also effect the transfer characteristics, although much more differently than the a" coefficients. The denominator coefficients affect the shape of the pass band region width. By either increasing or decreasing the pass band, the 3db cutoff frequency is also changed. This change in the pass band shape is accomplished by the shifting of the pole locations within the unit circle as seen by the calculation below:

Denominator equation

$$1+b_1 Z^{-1}+b_2 Z^{-2} = 0$$

Multiplying through by Z^{+2}

$$Z^2+b_1 Z+b_2 =0$$

Factoring

$$(Z_1 + \frac{b_1 + j\sqrt{4b_2 - b_1^2}}{2})(Z_2 + \frac{b_1 - j\sqrt{4b_2 - b_1^2}}{2}) \qquad 2$$

Thus the problem of the filter design becomes a problem of selecting the proper value of the denominator coefficients in the Z transfer function.

3. Estimation of the B Coefficients

Insight in determining what the coefficients should be for a particular response can be obtained from the comparison of the unit circle pole-zero plot and the desired frequency response of the filter. This is done by first placing the zeros on the unit circle at the appropriate frequency. Usually the zeros are desired on the unit circle to afford as nearly as perfect a stop band as possible. The poles are placed inside the unit circle at the proper frequency and their distance from the center determines the sharpness (quality factor) of the peaks (or pass bands). Figure 3.3a below shows a desired low pass frequency response, However, when some insight concerning the pole and

zero location is desired, the procedure is as follows:

1. Place the zeros at the proper position on the unit circle for either the high or low pass filter characteristic.
2. Locate poles inside the unit circle at the frequency at which they occur on the frequency response.

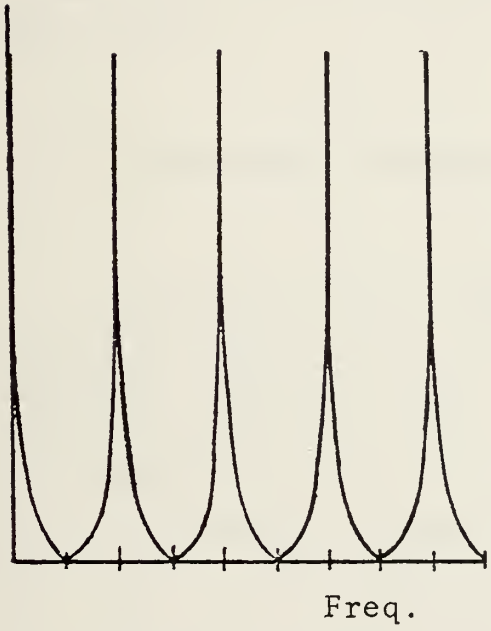

a. Desired Response

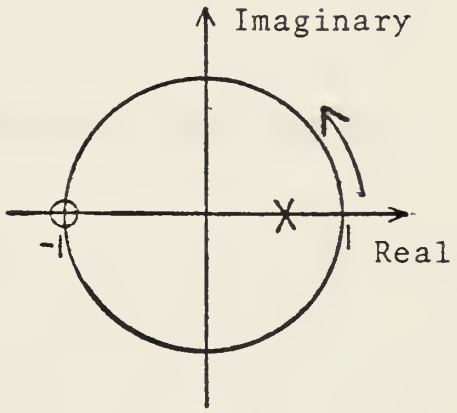

b. Estimating the Pole and Zero Locations.

FIGURE 3.3 Graphically Estimating Pole Zero Locations

This procedure can be performed in reverse also. For example,if the poles-zero locations are known, the frequency response can be estimated by moving counter-clockwise around the circle starting at Z= 1+j0. The amplitude is increased as a pole is approached and decreased as a zero is approached. Midway between the poles and zeros, an arbitrary median amplitude value is maintained. If the pole is closer to the perimeter of the circle the peaks are sharp (high Q) and if they are closer to the center of the circle the peaks are not sharp but wider (low Q).

4. Integrator and Canceller Recursive Comb Filters

The Recursive Comb filter can be configured as either an integrator or a canceller type of filter. The difference between these types of filters is simply in the relationship between their stop band and pass band widths. The integrator is characterized as having a very narrow pass band (thus implying a very high Q circuit) and a very wide stop band. The canceller is the opposite of this with a very wide pass band and a narrow stop band. These characteristic responses are shown in figure 3.4.

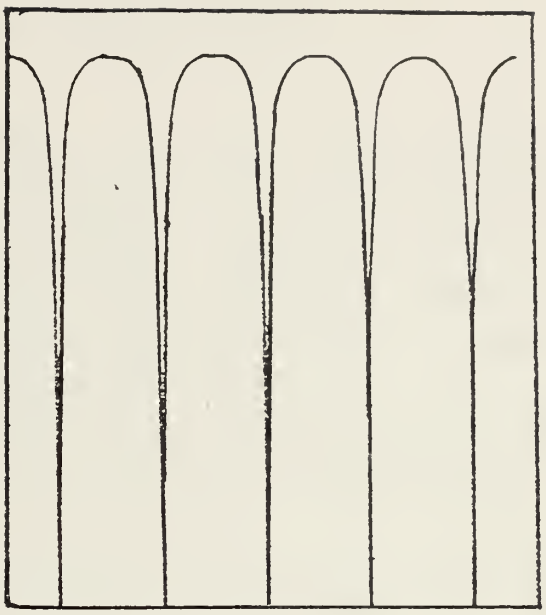

Canceller

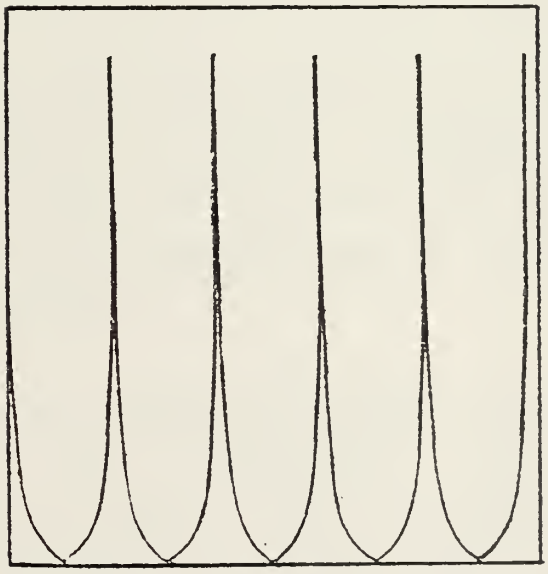

Integrator

Figure 3.4 Recursive Comb Filter Types

5. Coefficient Determination

One portion of this thesis deals with Integrator Recursive Comb Filters, and the demonstration of their use as a device to improve signal-to-noise ratio of a pulse train signal added to white Gaussian noise. The Z transfer function is given by equation 1 (given in Chapter 2) and the numerator coefficients are known (1, 2, 1 respectively). The design of the filter as discussed earlier is a problem of determining the denominator coefficients b_1 and b_2. This is not a trivial problem since there are very many possible combinations of b_1 and b_2 each between ±1 and ±2. Where then does one begin searching for the proper coefficients that will give an integrator Comb filter response and also have a very narrow pass band? Due to the massive amount of calculations required to plot a frequency response of equation 1 the problem lended itself well to to a computer iteration. The fortran program shown in Appendix B is a programing of equation 1.

To obtain the frequency response from equation 1, $Z=\cos(wT)+j\sin(wT)$ was substituted into the transfer function resulting in $H(jw)$. This was then programed and the only inputs that were required were the numerator and denominator coefficients. The output is a plot of the frequency response on a linear graph and the amplitude is normalized to the maximum amplitude encountered throughout the frequency range of interest. This program will automatically plot the results on the textronix terminal of the CP/CMS time sharing system.

As noted earlier equation 1 is the transfer

characteristic of a digital filter design technique. This equation applies equally well to the Sampled-Analog filter design technique, although a slight modification must be made to account for the sample and hold circuitry which is used in the filter to reproduce the filtered signal at the output. In the frequency domain the sample and hold characteristic is a SinX/X function which affects the filter response in a multiplicative manner. This characteristic has been included in the fortran program. One other characteristic which was necessary to model the Sampled-analog filter was the adjustment of the frequency of the sin and cos arguements to give the proper number of comb teeth, corresponding to the number of delays which were used in each stage of the filter. A second order filter was designed with 96 delays per stage. This resulted in a comb response with 96 teeth between D.C. and the sampling frequency. The 96 teeth are a result of the repetitive nature of the bilinear design technique. This characteristic was also modeled into the fortran program which is shown in Appendix B.

6. Filter Design

The computer program of Appendix B will give the frequency response of the desired Z transfer function, but as previously mentioned the coefficients are required input data. Thus, a method is needed to determine where to start searching for the proper coefficients. This problem was answered by the result of a thesis by Stacy V. Holmes[6]. In his research he derived a means to analize Sampled-Analog filters based on the coefficients b_1 and b_2. In his

dissertation he introduced a b-plane triangle of stability (shown here in figure 3.5[6]). From this graph a rough estimation of the denominator coefficients can be obtained. Although the coefficients which are obtained in this manner are very rough figures it does provide a starting point to use the previously discussed computer model. Several "b" coefficients can be used in the program until the desired frequency response is obtained, prior to building the filter. Since this study is of recursive Comb Integrators and Cancellers, from the graph the b_1 coefficients are limited to values of approximatly +0.2 to -2.0 where as the b_2 coefficient can very from +1.0 to -1.0. This technique is ,needless to say, time consuming and tedious; however, the b-plane triangle of stability decreases the coefficient search immensely.

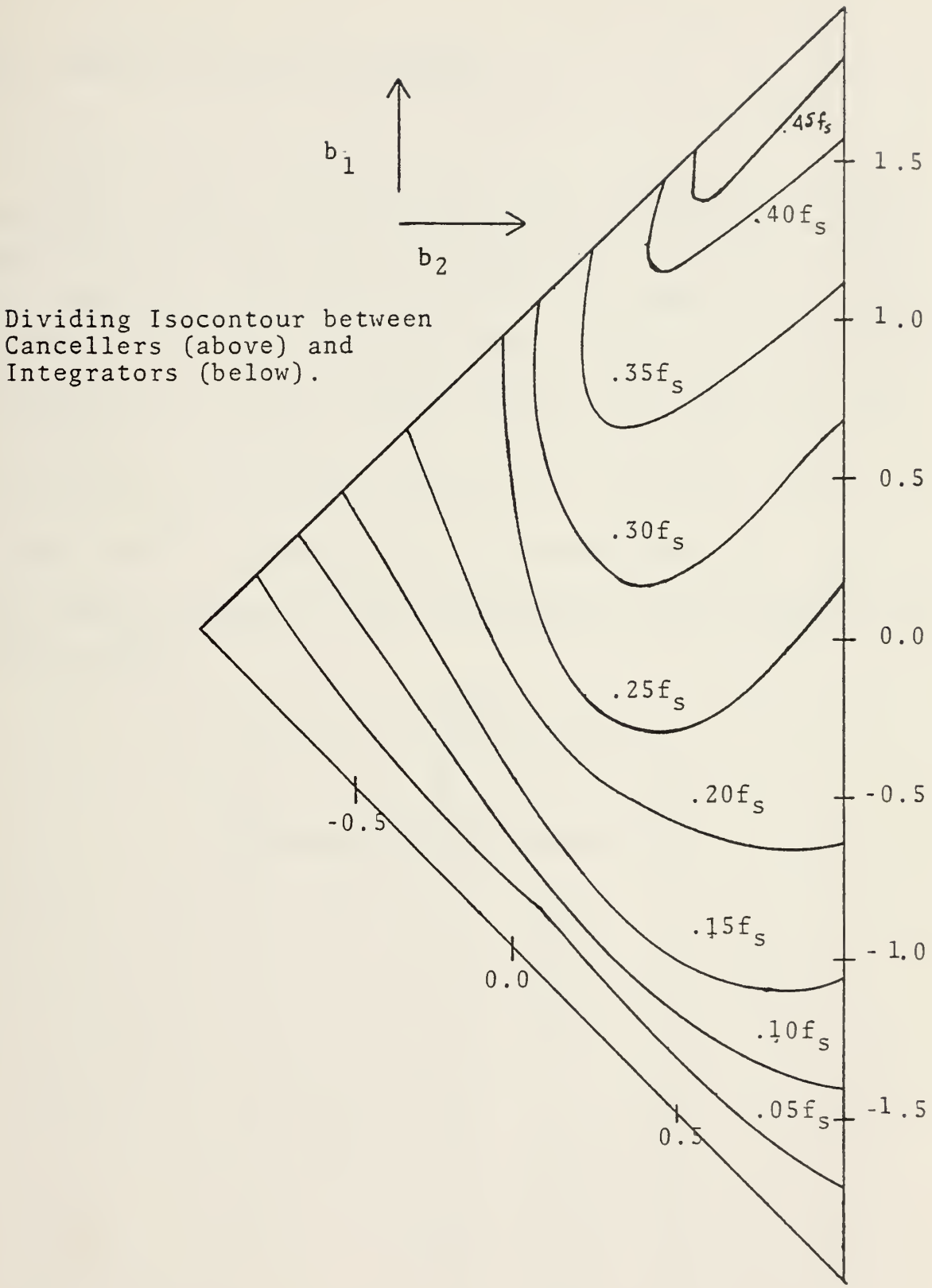

Figure 3.5[6] b-Plane Triangle of Stability

B. COMPUTER AIDED FILTER DESIGN

One of the intentions in this study is to design a Recursive Integrator Comb filter with a very narrow passband and a broad stop band and demonstrate its use as a device for improving Signal-to-Noise ratio of a pulse train input signal (a topic of a later chapter). Suffice it to say that the type of filter design desired can be found with coefficients that are located in the region below the $.05f_s$ isocontour on the b-plane triangle of stability shown in figure 3.5[6]. Several values of coefficients were tried in the computer program. these coefficients are as shown in the table below:

TABLE 3

b_1	b_2
+0.2	±0.2 ±0.4 ±0.6 ±0.8 ±1.0
-0.2	±0.2 ±0.4 ±0.6 ±0.8 ±1.0

Figures 3.6 through 3.25 show the computer results for the coefficients listed above. These plots give an indication of the results which can be expected experimentally from a filter with these coefficients and this number of delays.

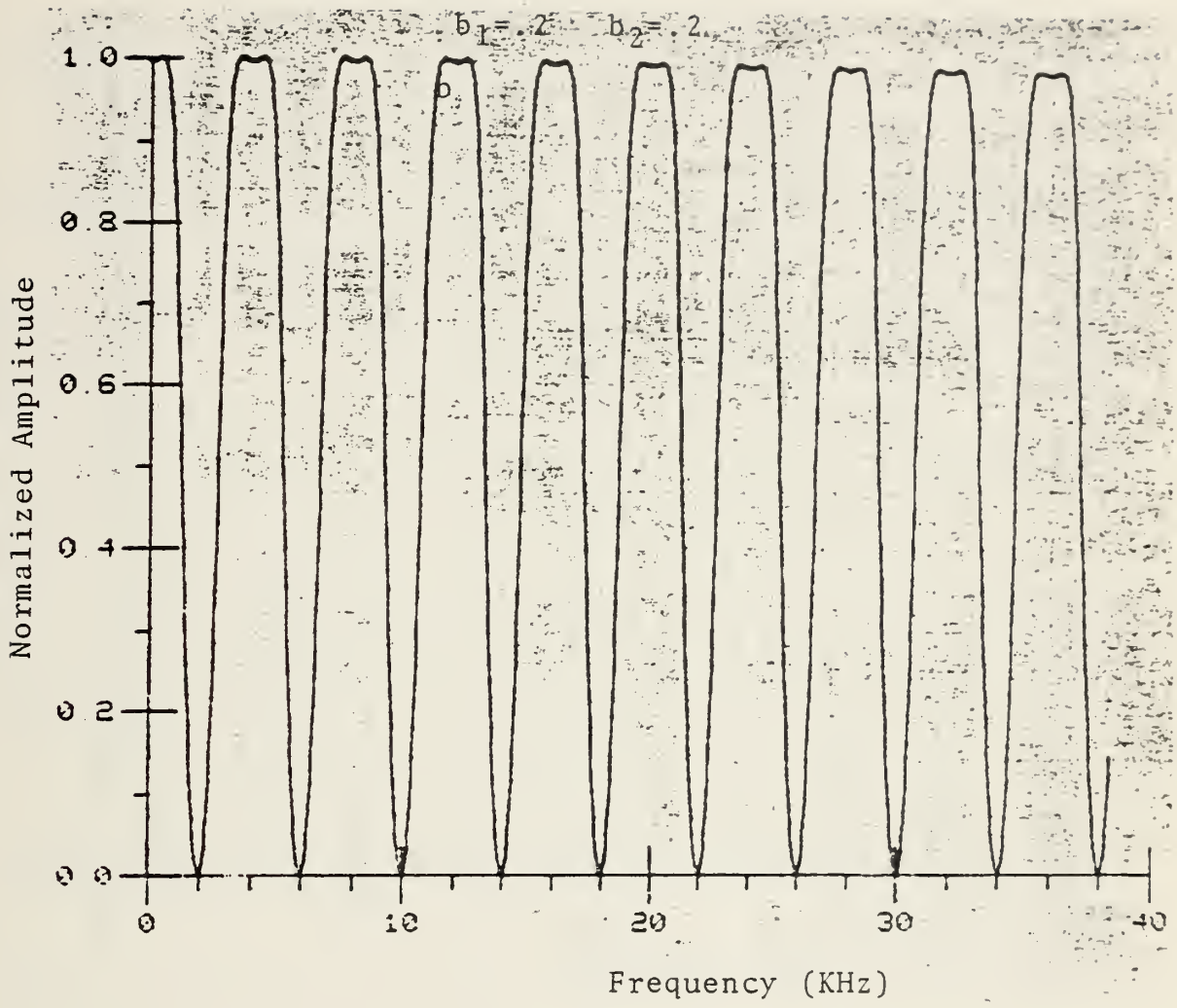

Figure 3.6 Comb Frequency Spectrum (Theoretical)

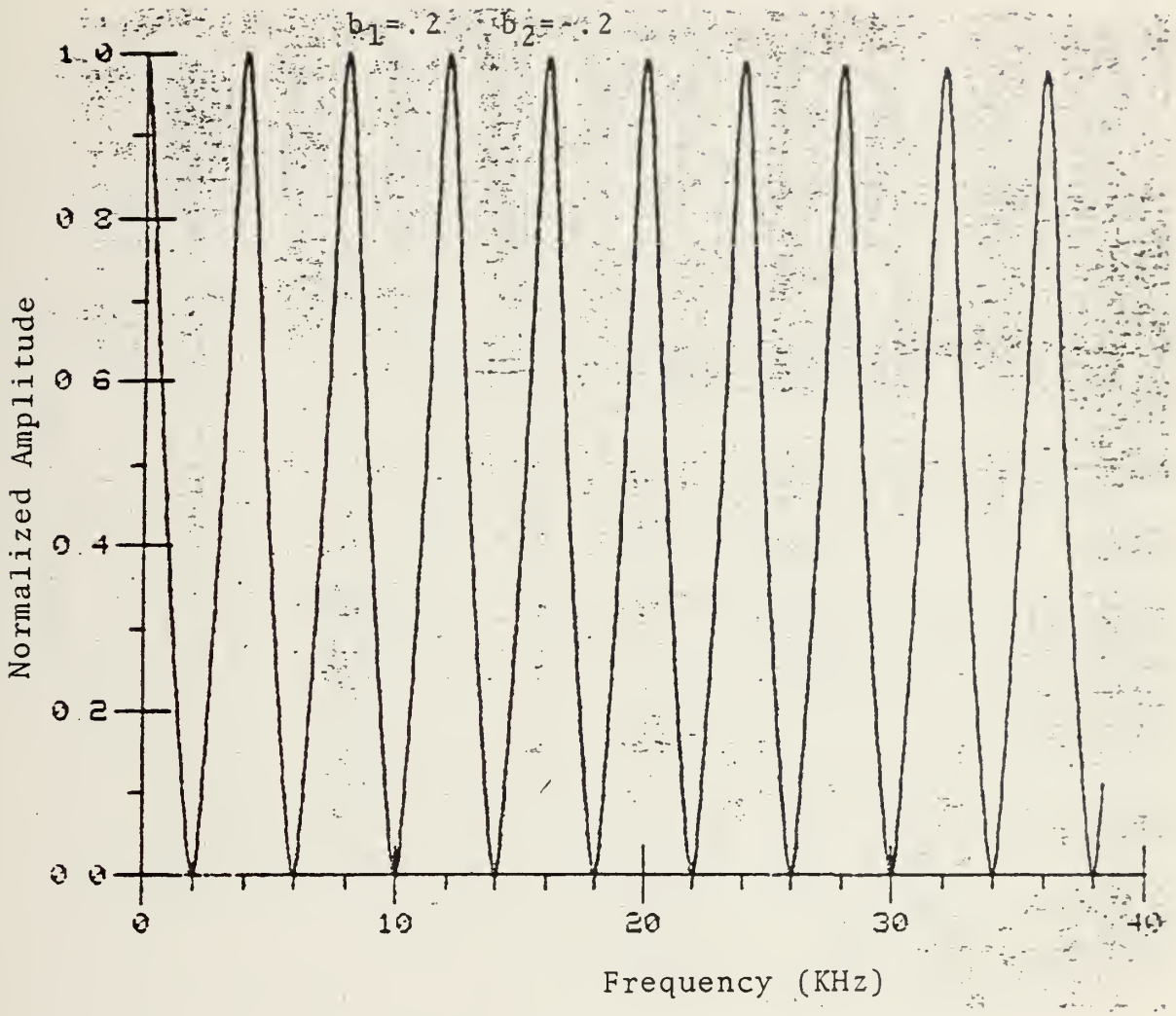

Figure 3.7 Comb Frequency Spectrum (Theoretical)

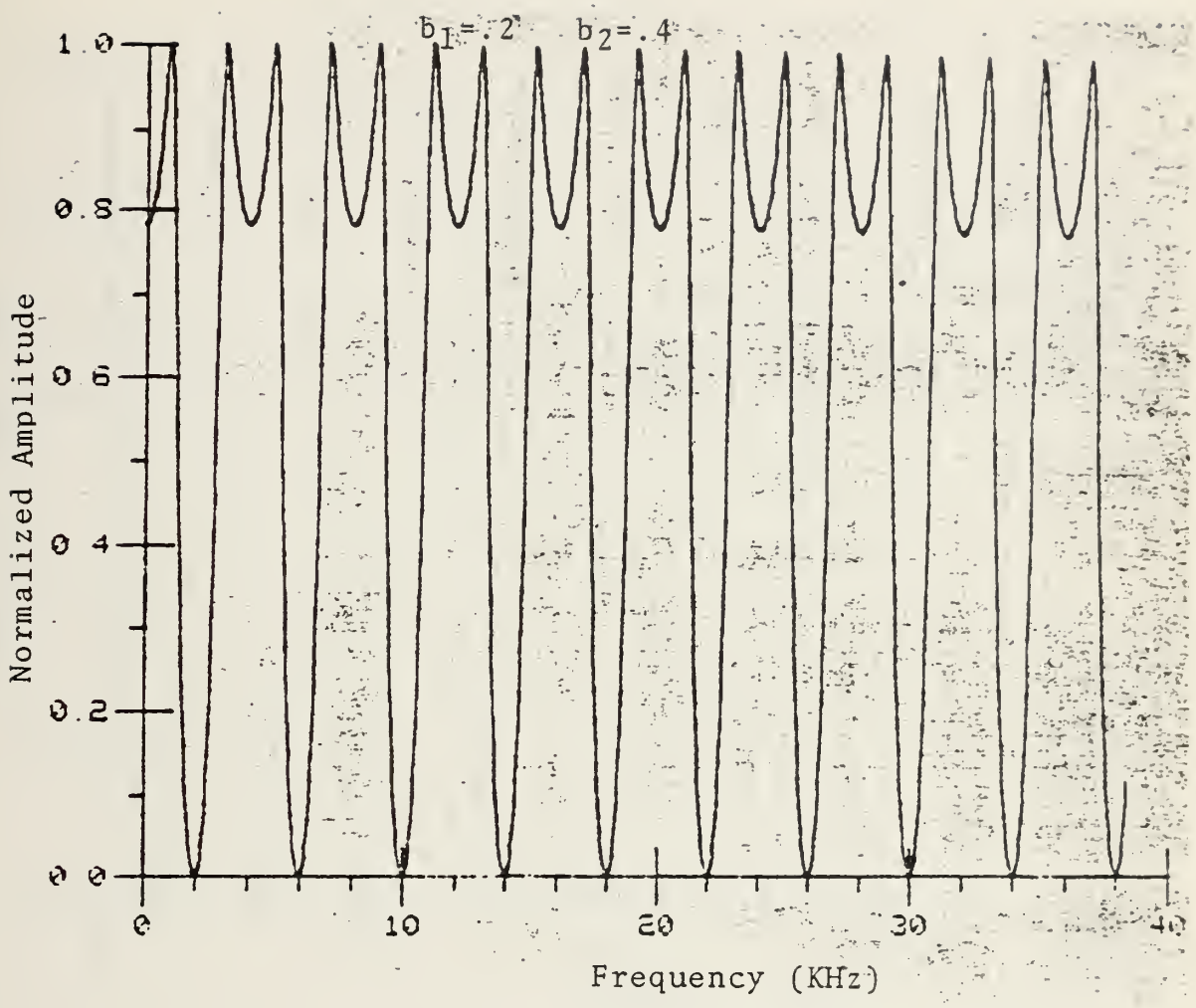

Figure 3.8 Comb Frequency Spectrum (Theoretical)

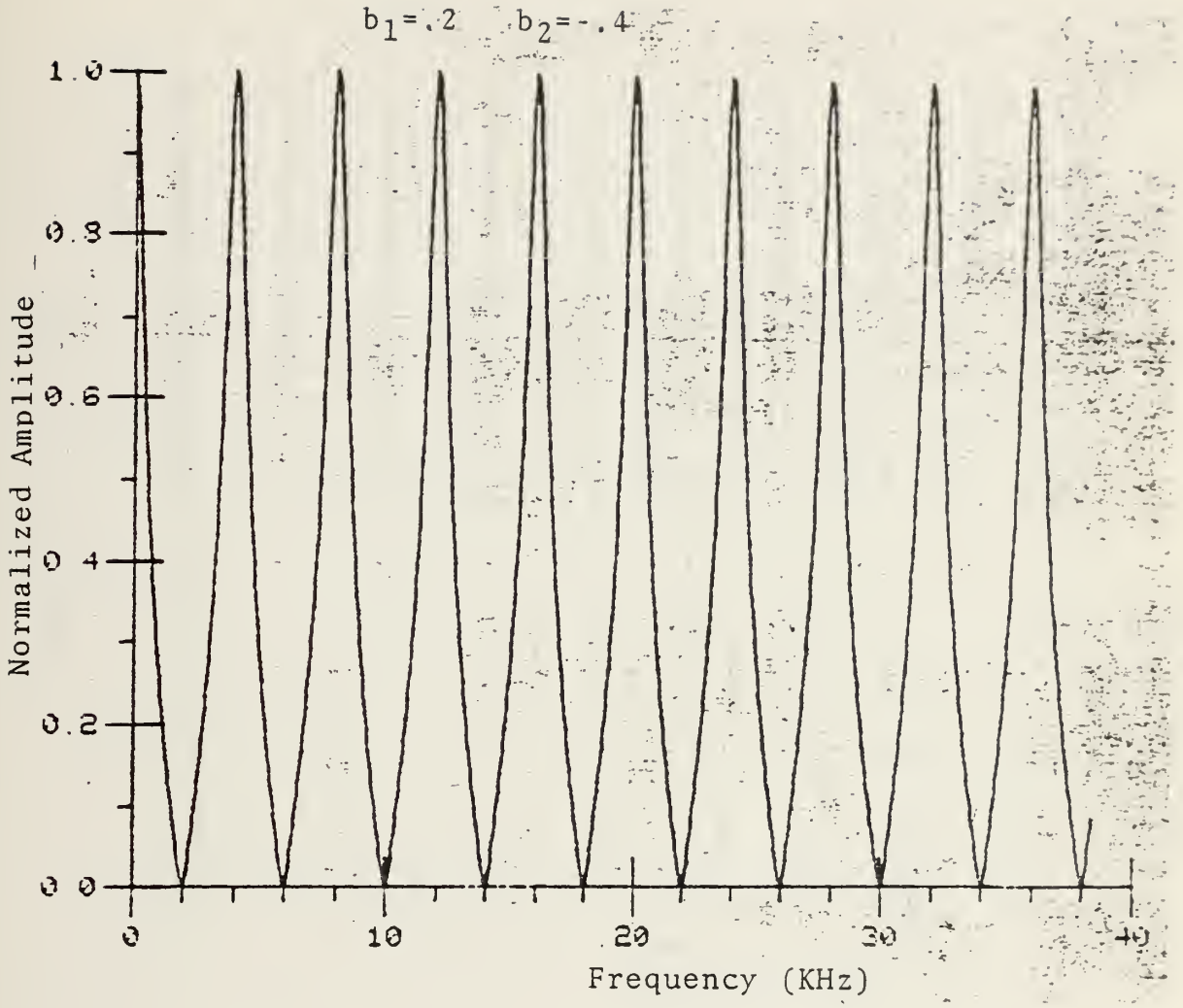

Figure 3.9 Comb Frequency Spectrum (Theoretical)

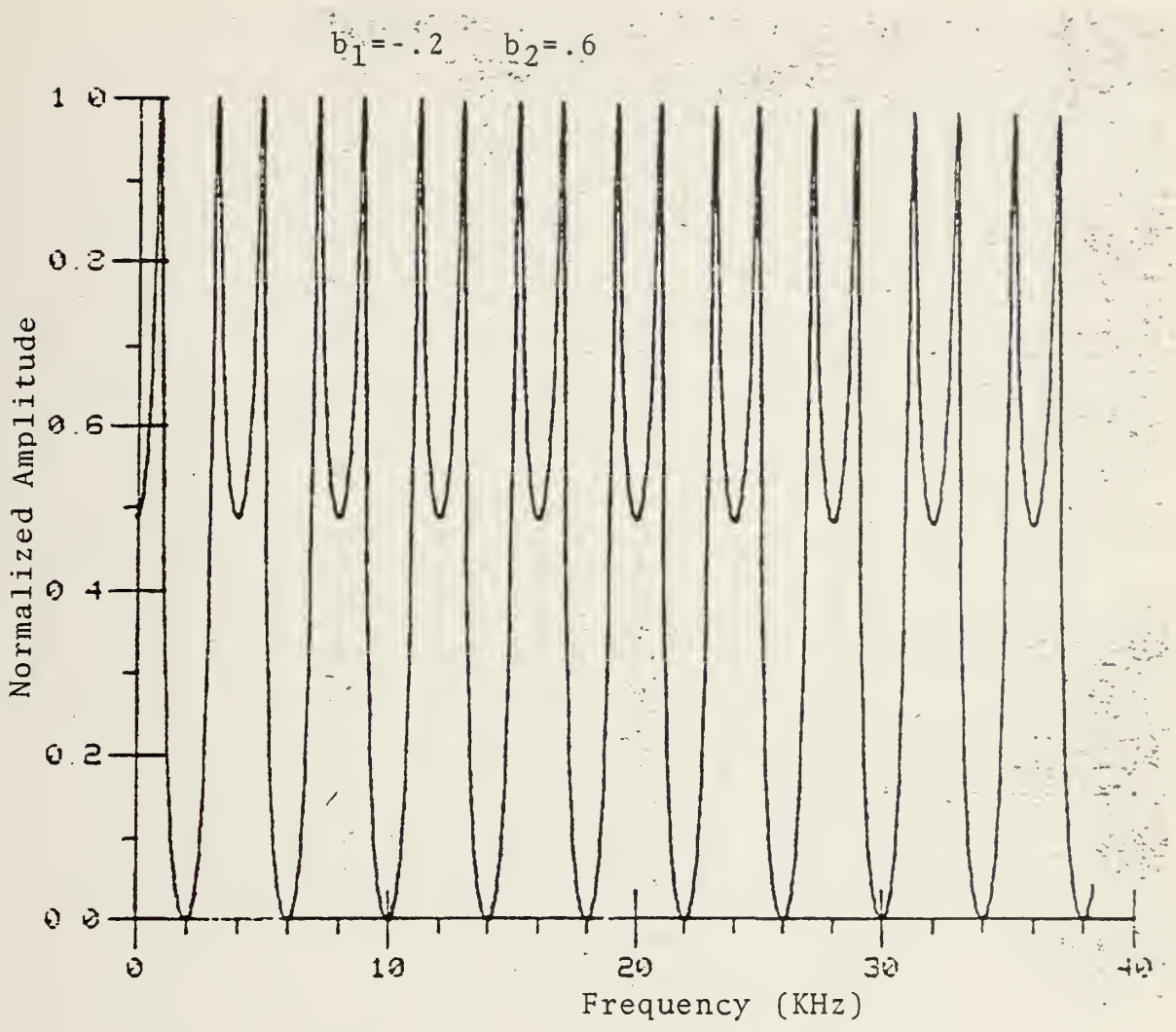

Figure 3.10 Comb Frequency Spectrum (Theoretical)

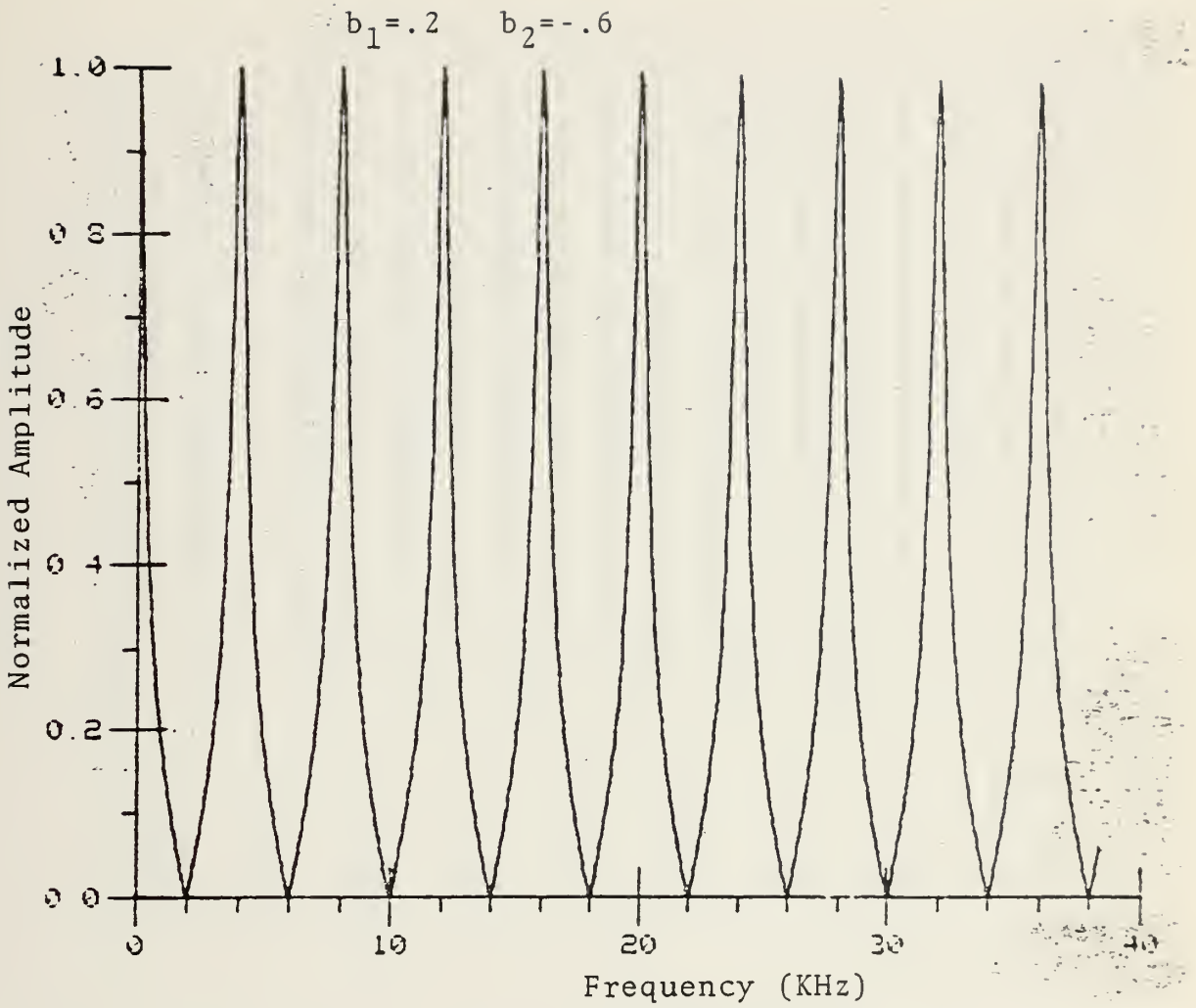

Figure 3.11 Comb Frequency Spectrum (Theoretical)

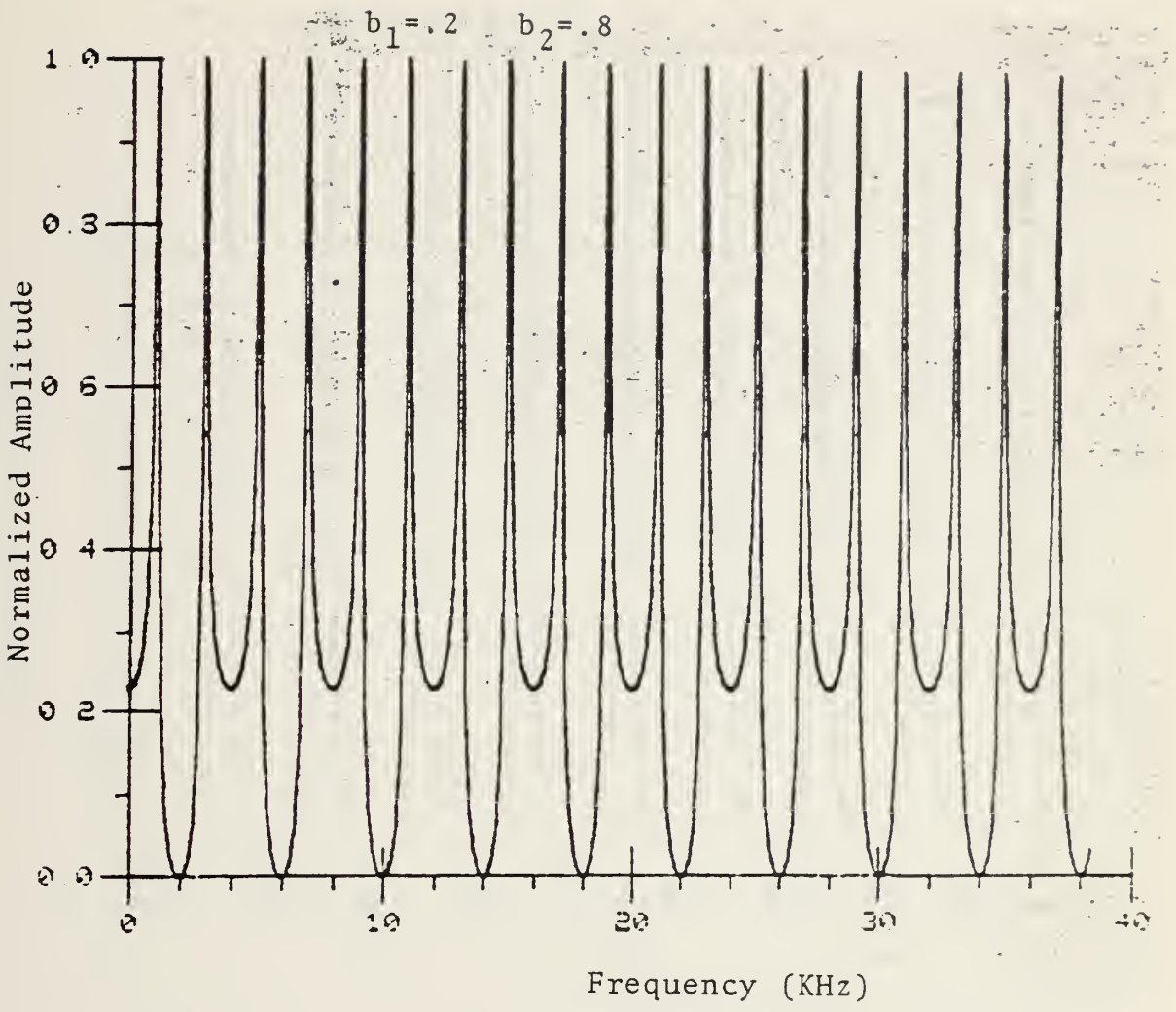

Figure 3.12 Comb Frequency Spectrum (Theoretical)

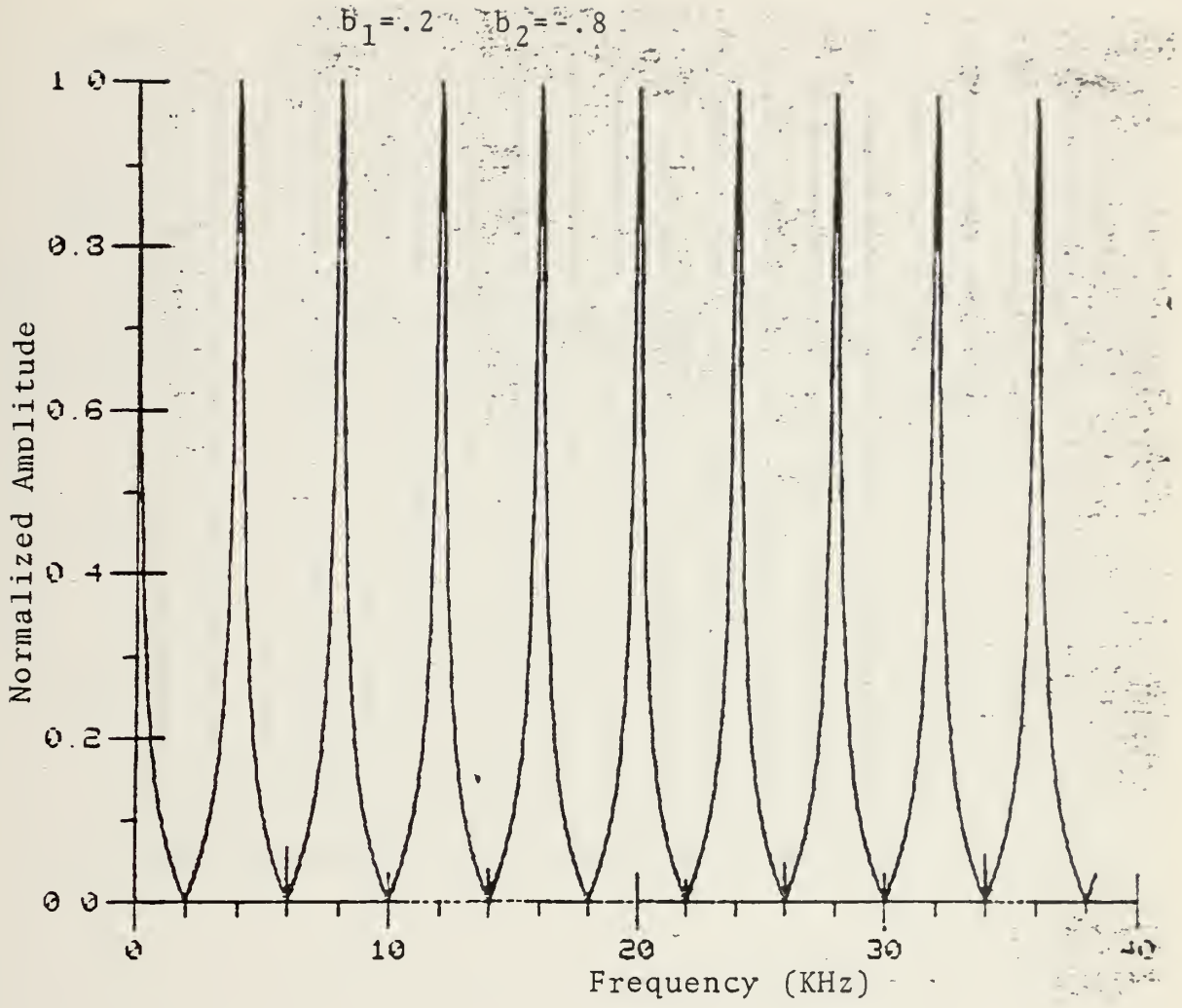

Figure 3.13 Comb Frequency Spectrum (Theoretical)

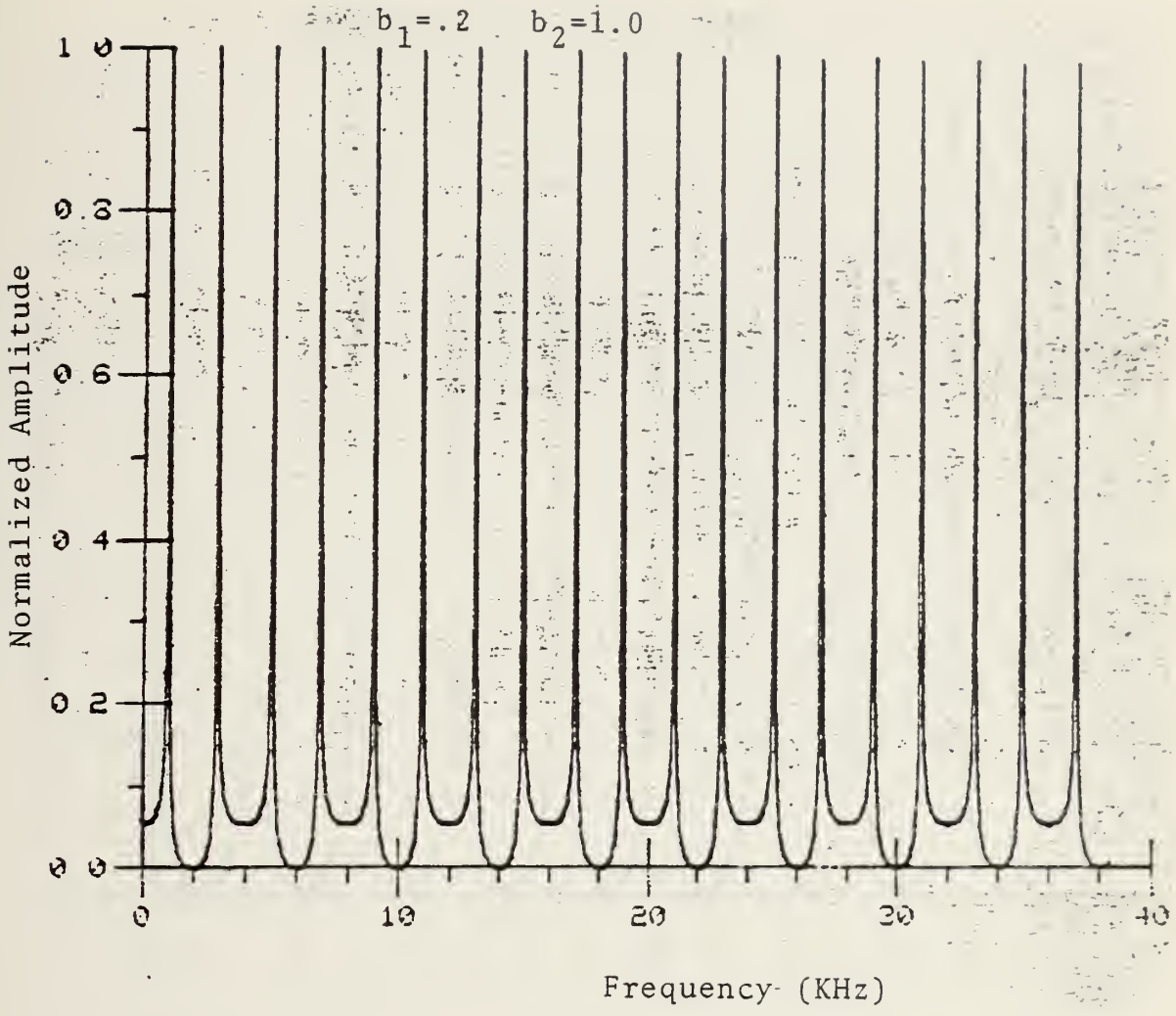

Figure 3.14 Comb Frequency Spectrum (Theoretical)

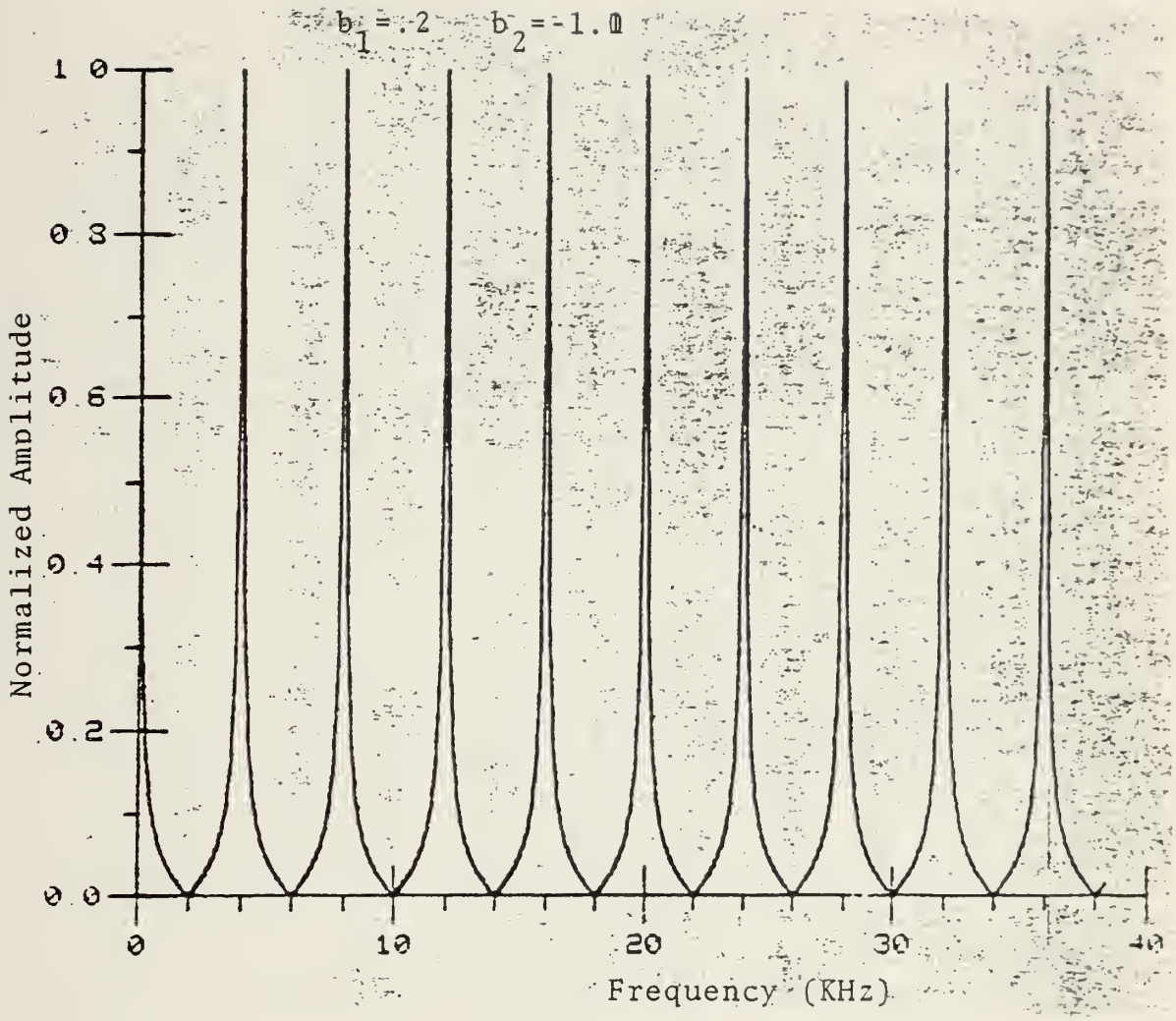

Figure 3.15 Comb Frequency Spectrum (Theoretical)

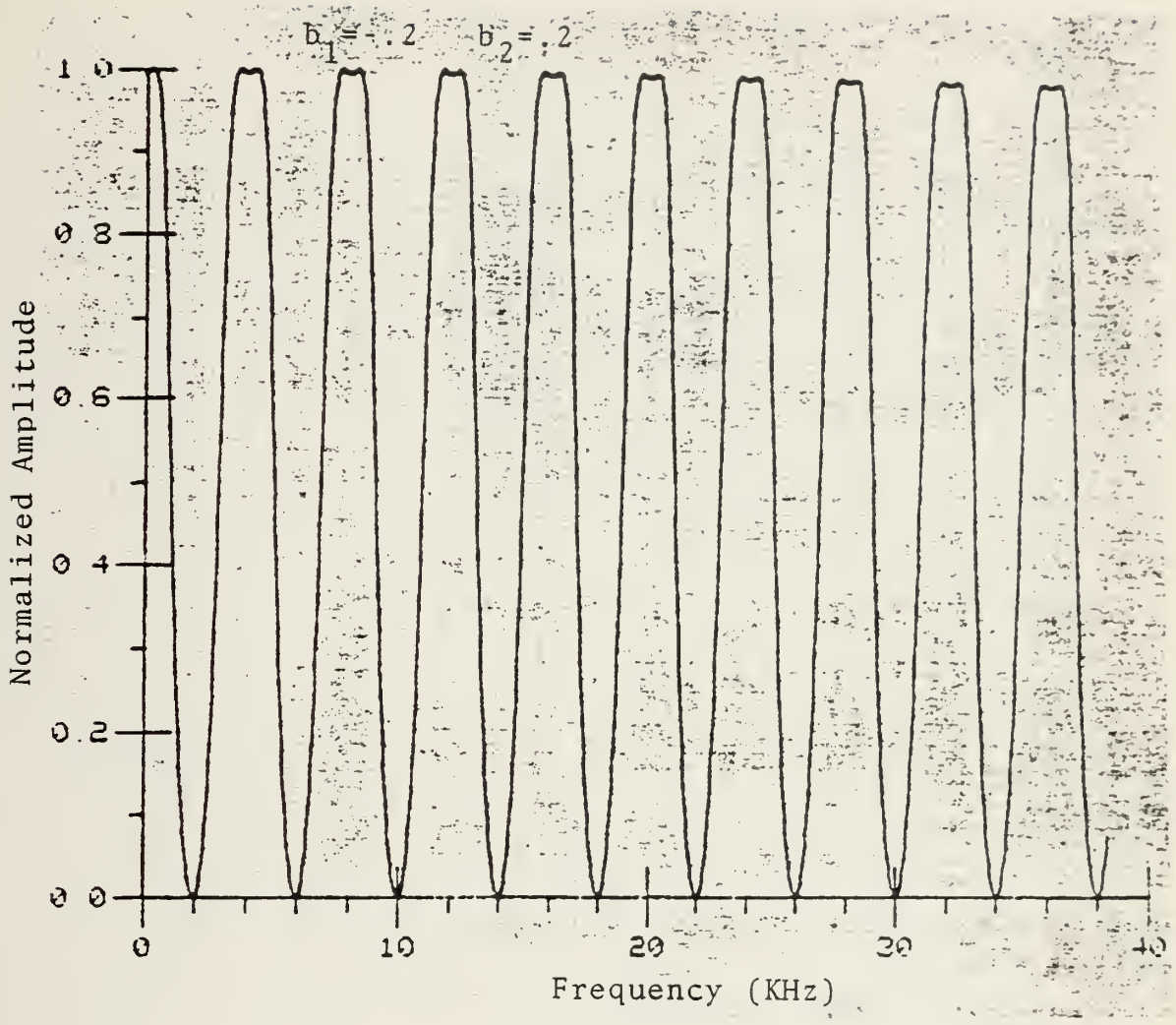

Figure 3.16 Comb Frequency Spectrum (Theoretical)

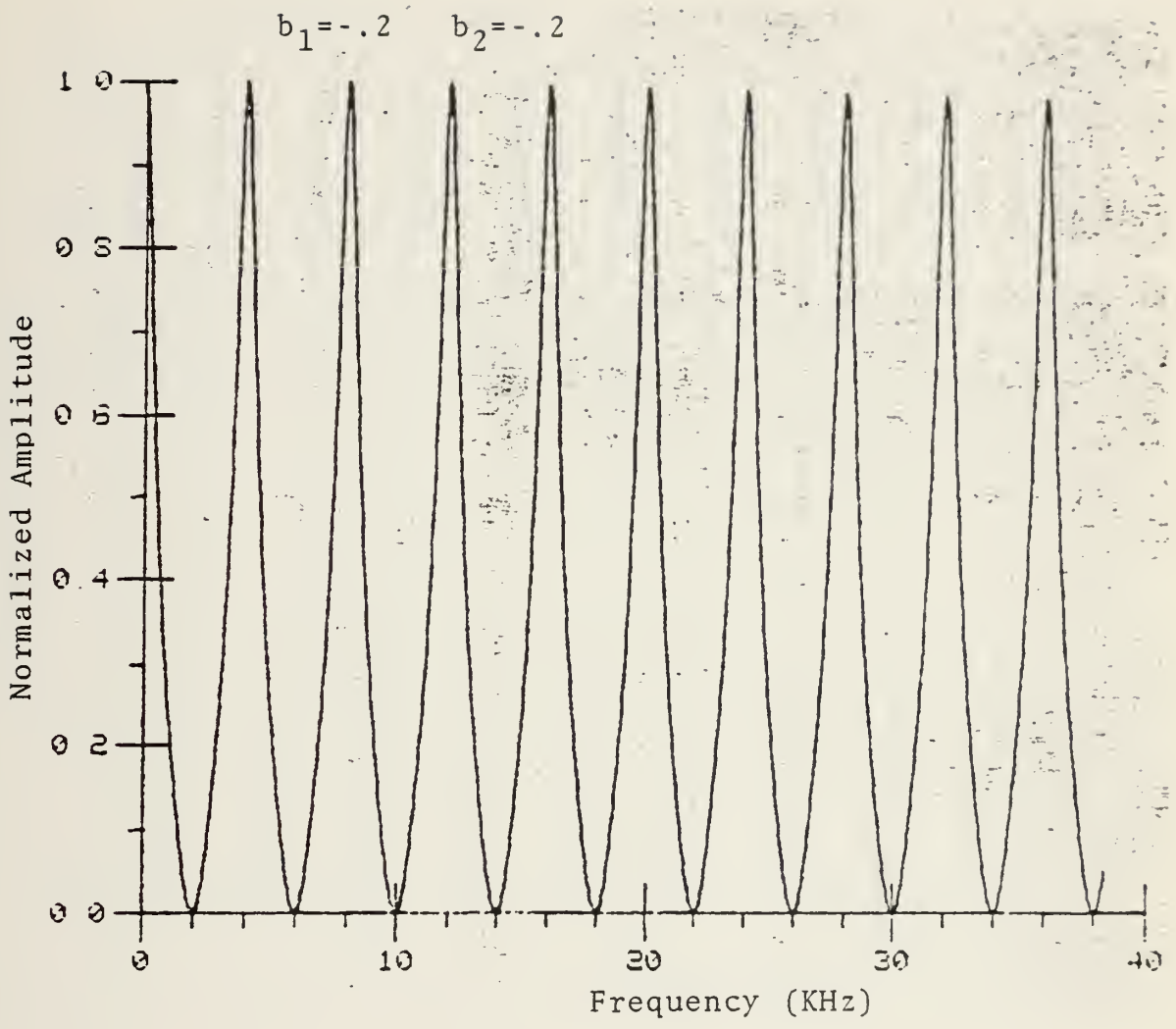

Figure 3.17 Comb Frequency Spectrum (Theoretical)

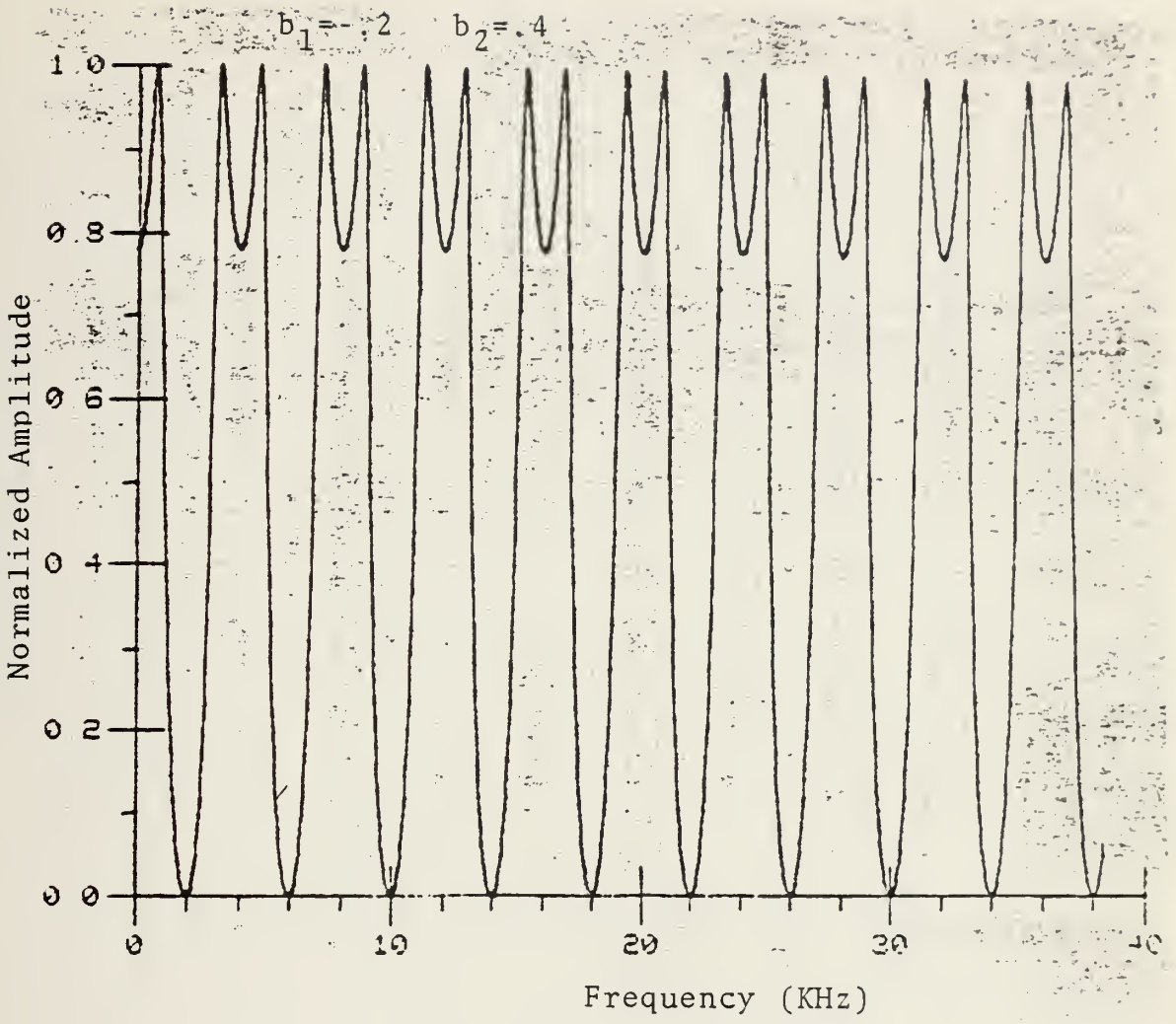

Figure 3.18 Comb Frequency Spectrum (Theoretical)

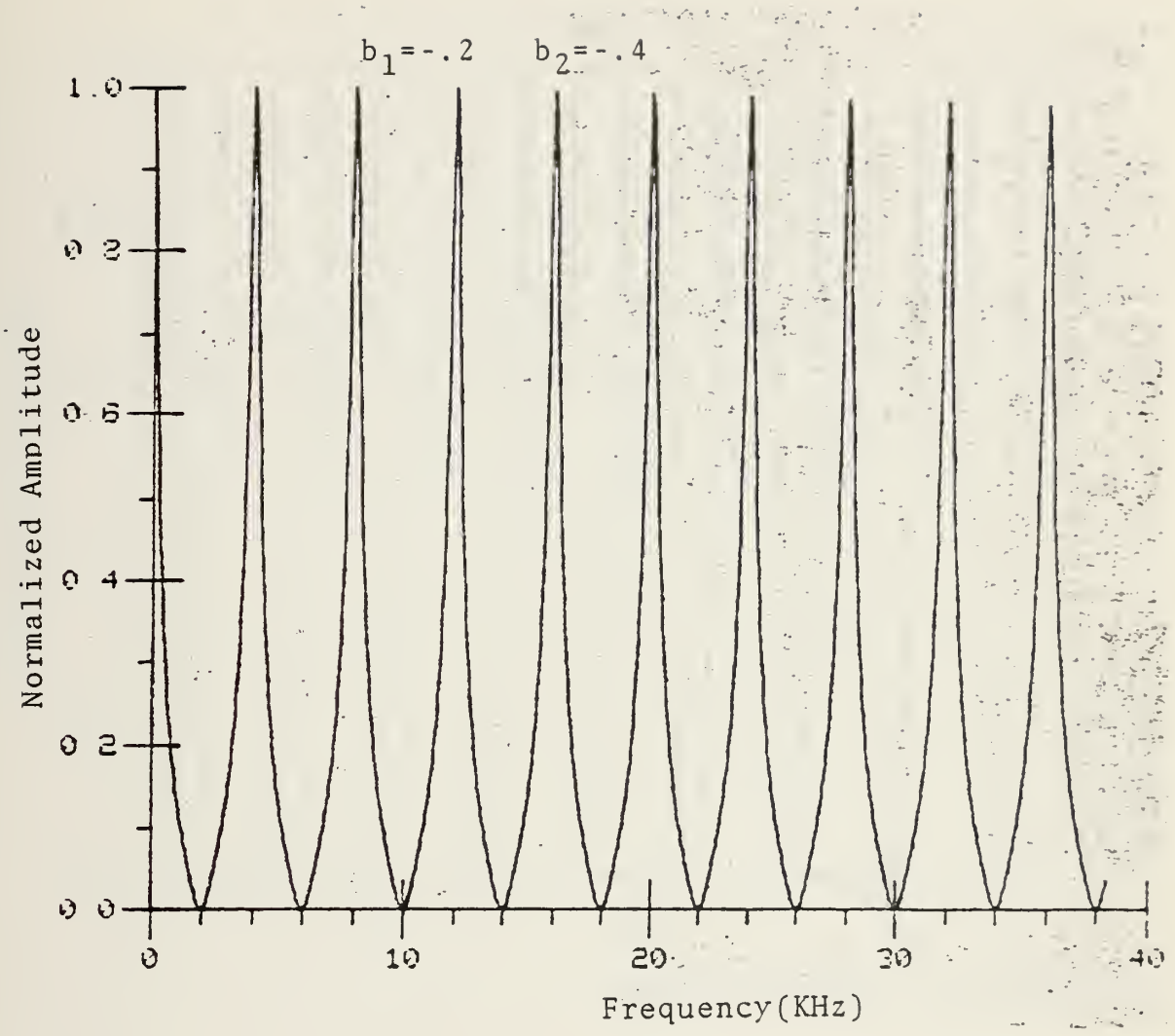

Figure 3.19 Comb Frequency Spectrum(Theoretical)

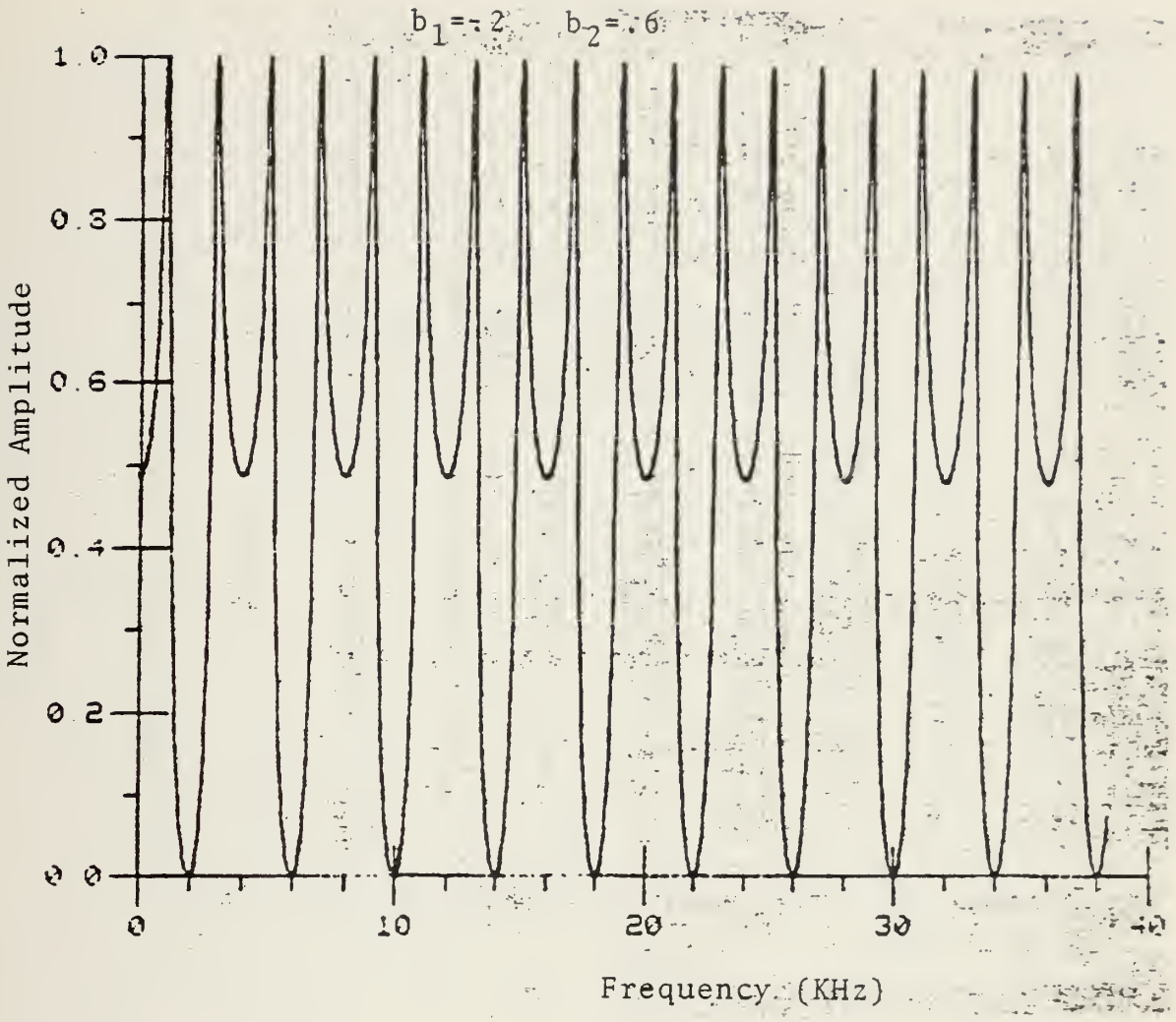

Figure 3.20 Comb Frequency Spectrum (Theoretical)

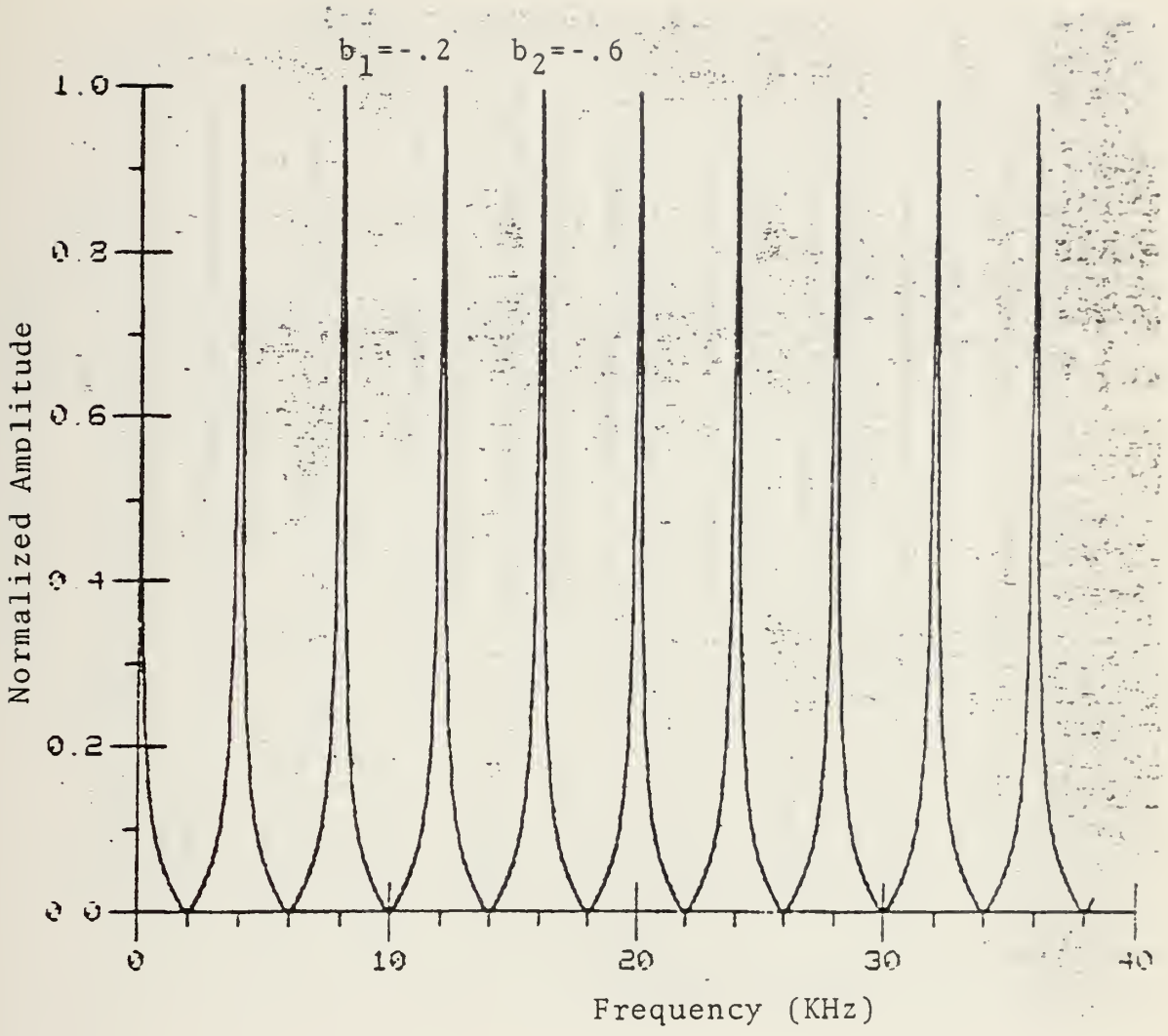

Figure 3.21 Comb Frequency Spectrum (Theoretical)

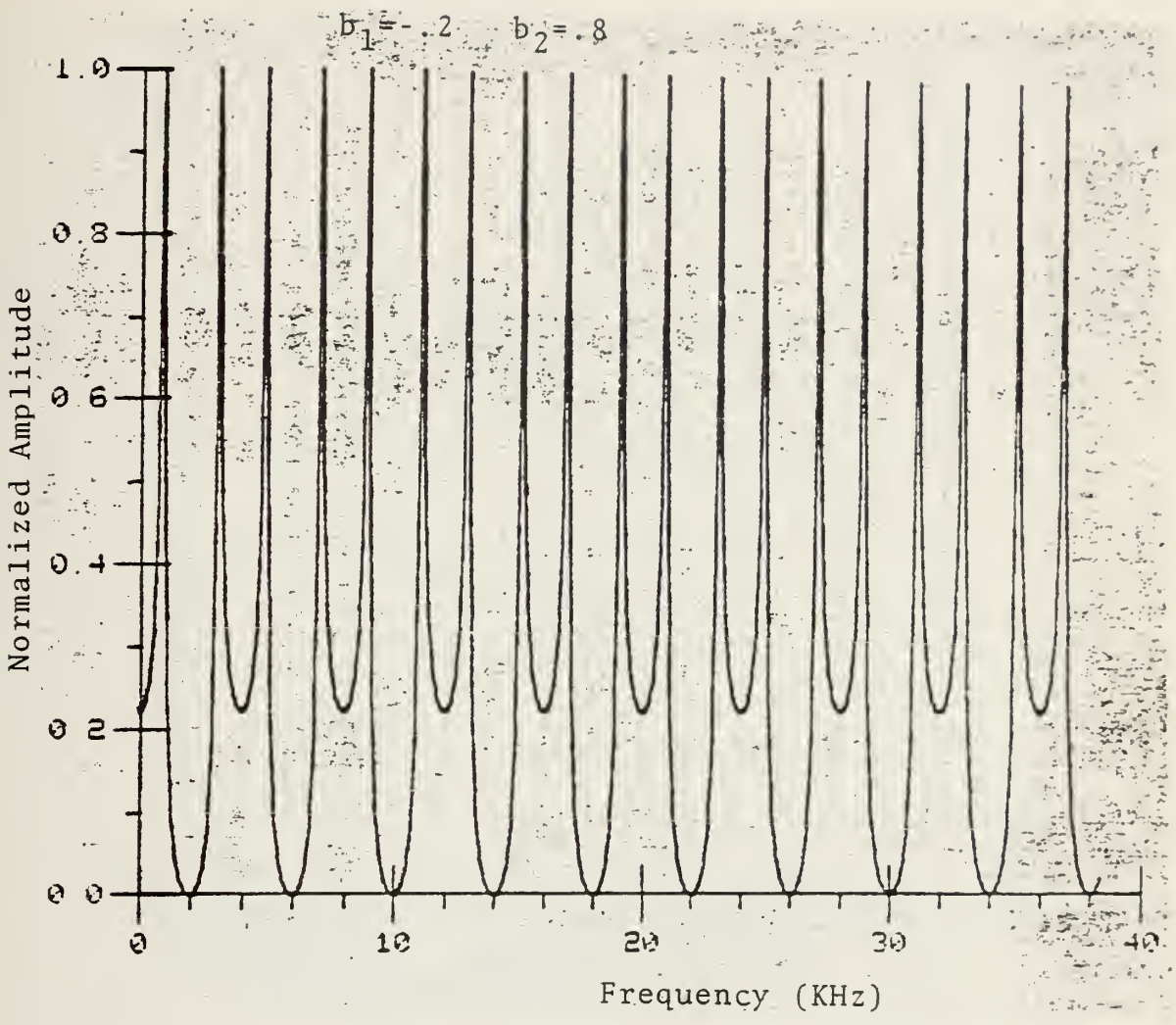

Figure 3.22 Comb Frequency Spectrum (Theoretical)

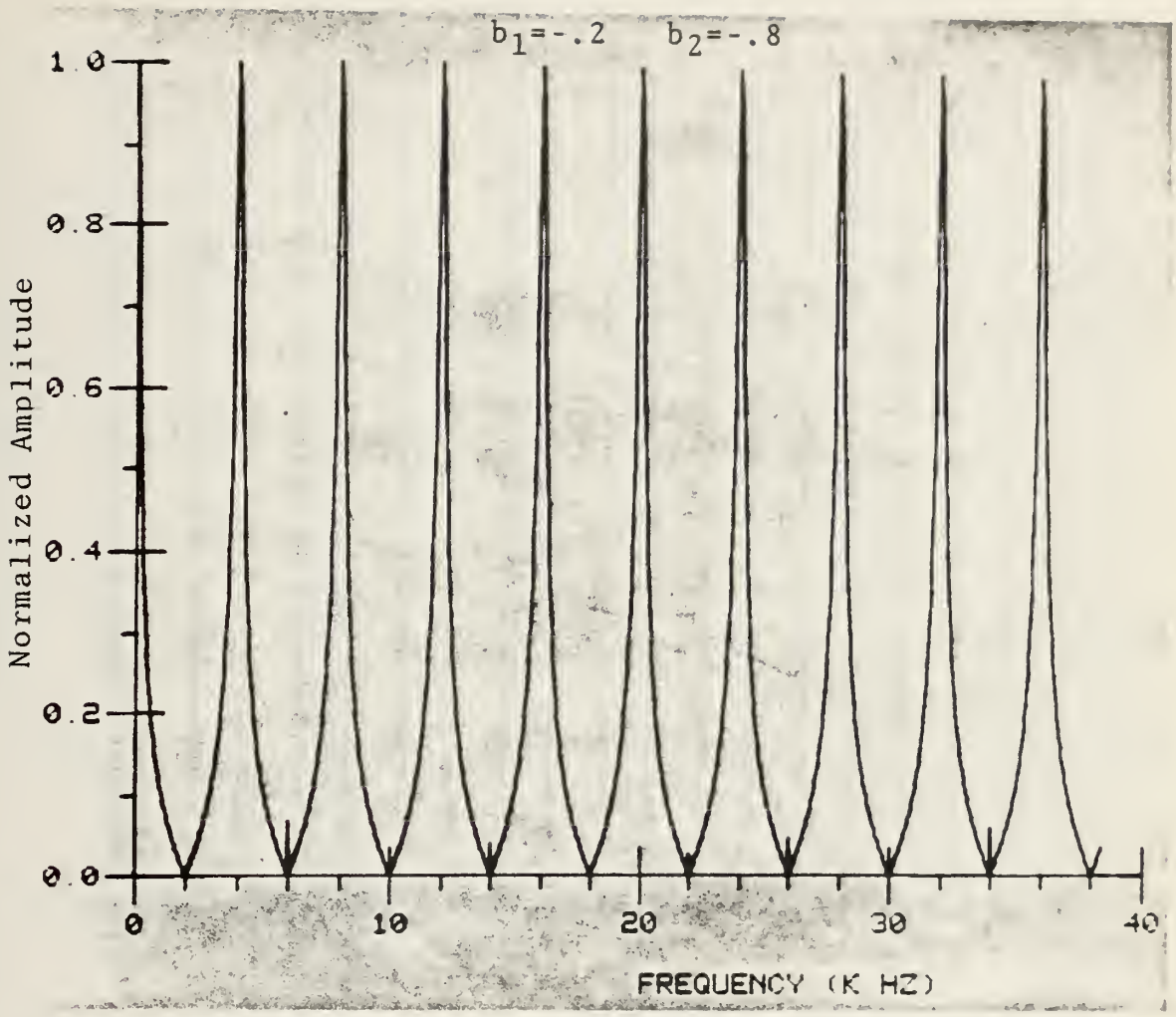

Figure 3.23 Comb Frequency Spectrum (Theoretical)

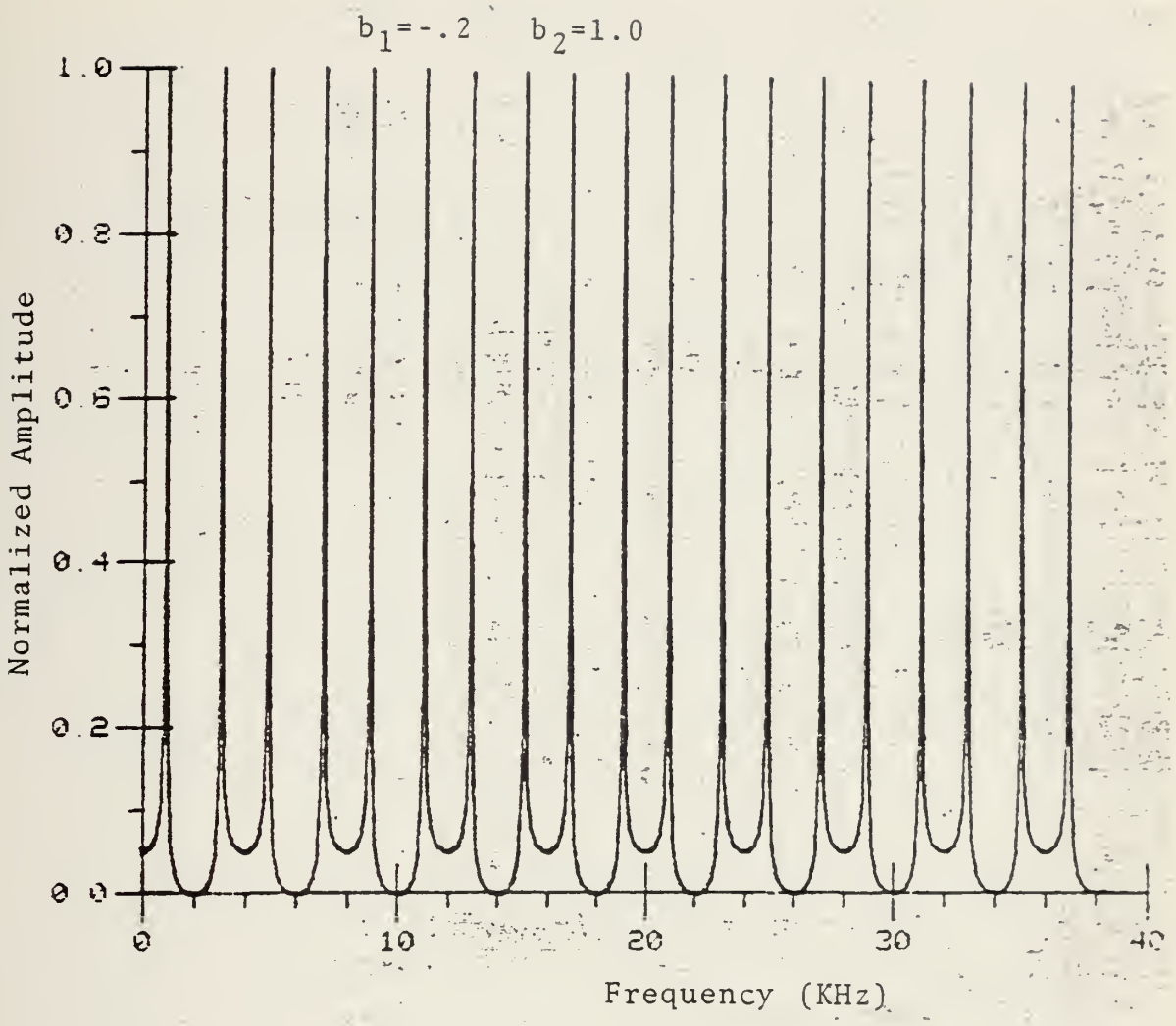

Figure 3.24 Comb Frequency Spectrum (Theoretical)

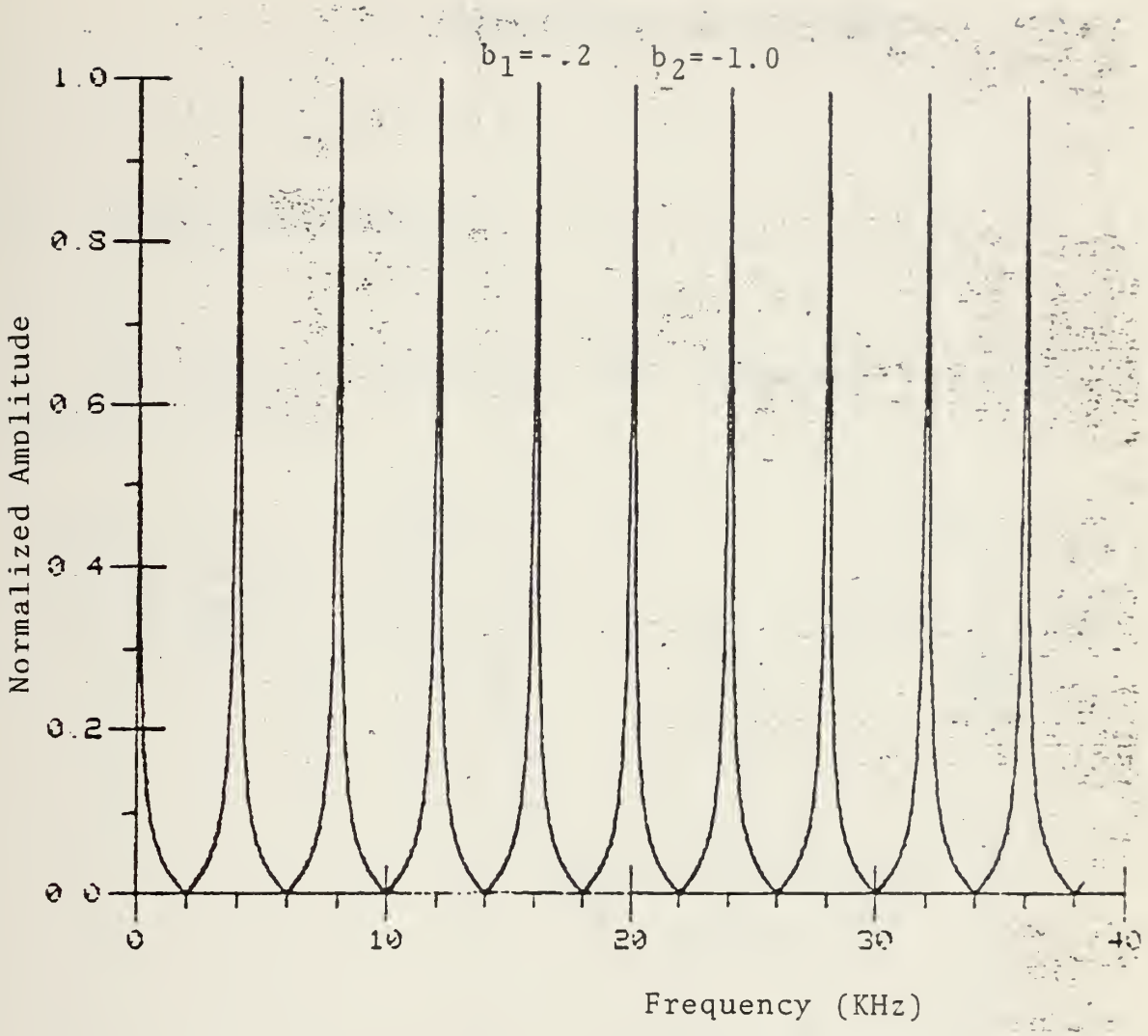

Figure 3.25 Comb Frequency Spectrum (Theoretical)

IV. EXPERIMENTAL FILTER STUDY

A. CIRCUIT CONFIGURATION

The Recursive Comb filter was connected as shown in Figure 4.1 below.

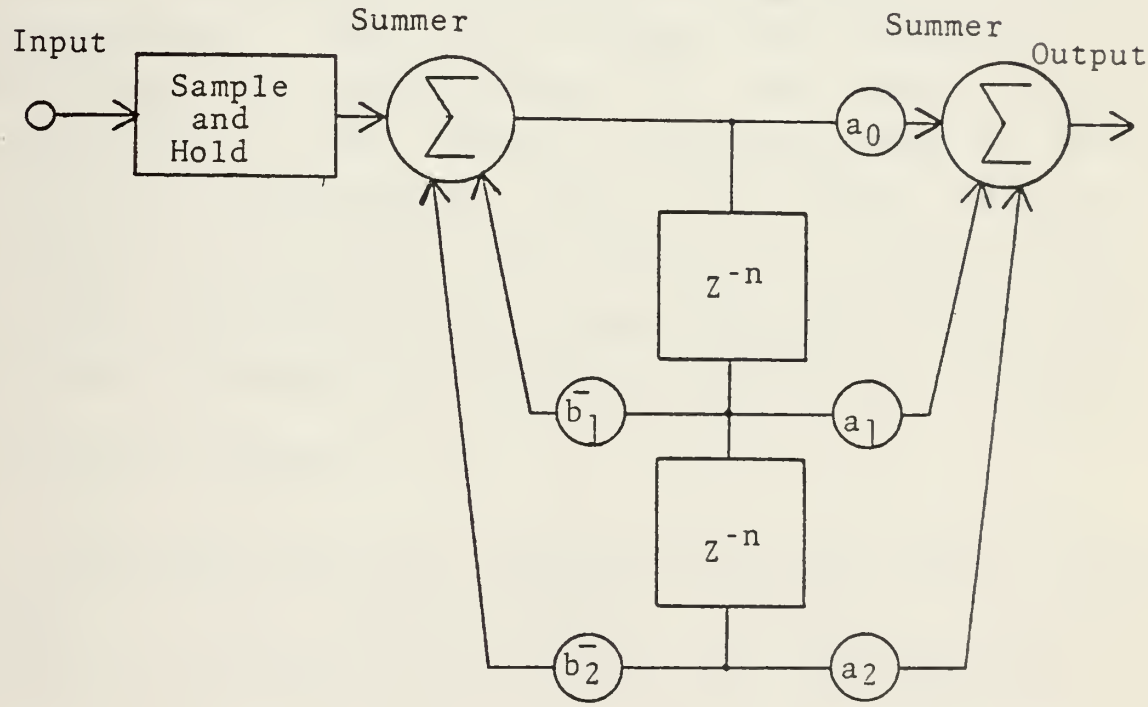

Figure 4.1 Filter Circuit Configuration

This circuit configuration is the conical circuit realization; using the Bilinear Z transform of either the high or low pass S-Plane analog filter transfer function. The sample and hold circuit was necessary to give better nulls in the frequency response characteristics of the filter. If this circuit had not been used, the sumation of

the signals at the operational amplifier summer would be the addition of a strict analog signal and a sampled analog signal. This introduces errors and rapidly deteriorates the nulls of the frequency response. With the sample and hold circuit, two similar signals are added in the operational amplifier. To further reduce errors, the clock frequency of the sample and hold circuit was adjusted to be the same as the sampling frequency of the delay elements. The coefficients were composed of carbon resistors with five percent tolerences. The resistors were arranged as voltage divider networks where the values were adjusted by combining resistors in series and measuring the tap voltage (which was a portion of the entire voltage across the series resistance combinations). The tap voltage was determined by multiplying the total voltage on the entire series combinations by the desired coefficient value; and after this value was measured at one of the tops, the entire combination was placed into the circuit. It was necessary to obtain the coefficients in this manner, instead of using variable potentiometers for coefficients, since these latter devices were found to be frequency dependent (as determined in earlier studies[6,7]).

The delay device was the Reticon SAD-100 serial analog delay. In the circuit diagram of Figure 4.1, the total delay is represented as Z^{-n}. Since the Reticon SAD-100 has ninety -six bits of delay, the value of n in this circuit is ninety-six clock periods for each delay stage.

B. EXPERIMENTAL DATA

The circuit which has been described above was studied

to determine its frequency response characteristics and the dependence of these responses on the denominator coefficients. The numerator coefficients were of no interest here since it was determined in Chapter Two that their relationship must be fixed to give the comb response; and, that changing the sign of a_1 defines either a high or low pass filter (+ for low pass and - for high pass filter) characteristic. Therefore, for all data presented here, a low pass filter was used.

The data plan is the same as the plan used for the computer design section (table 3). This was done to compare the results of the computer program. Table 3 has been repeated here for convenience.

TABLE 3

b_1	b_2
+0.2	±0.2 ±0.4 ±0.6 ±0.8 ±1.0
-0.2	±0.2 ±0.4 ±0.6 ±0.8 ±1.0

The experimental data is shown on the following pages in Figures 4.2 through 4.17. The two sets of curves for b_2 =

±1 were not taken since the device was unstable with these coefficients. Accompanying each frequency plot is a plot of the poles and zeros of the transfer function for the coefficients used in the respective response. This was included to obtain a better understanding of the reason for the shape of the filter teeth. The Z plane plot starts at D.C. at Z = 1 + jo and one counterclockwise revolution, around the circle, increases the frequency to fs/96 , or one complete cycle of the frequency response that it accompanies. The clock frequency for the following figures was 400 K Hz.

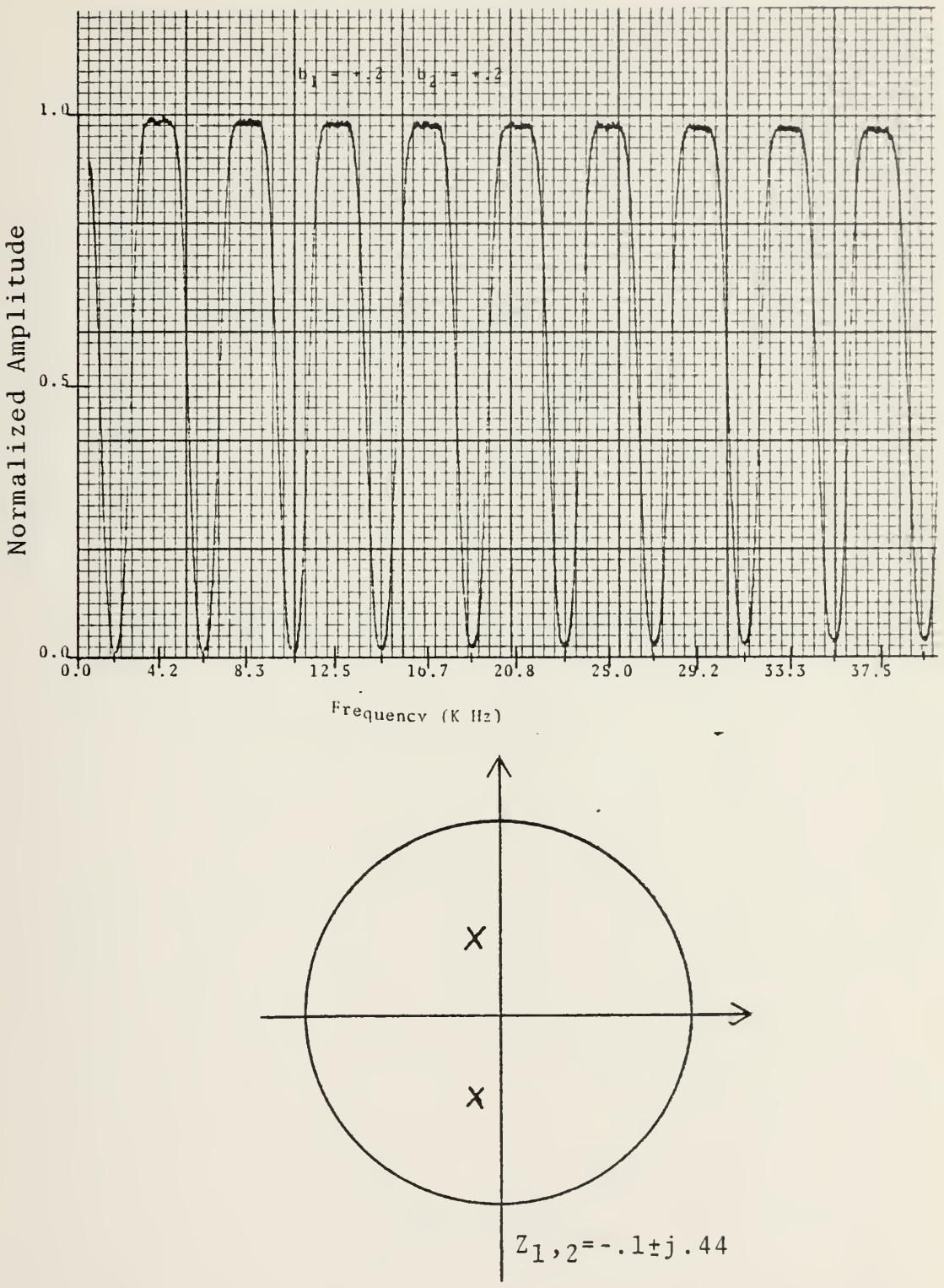

Figure 4.2 Comb Frequency Spectrum (Experimental) and Pole Location

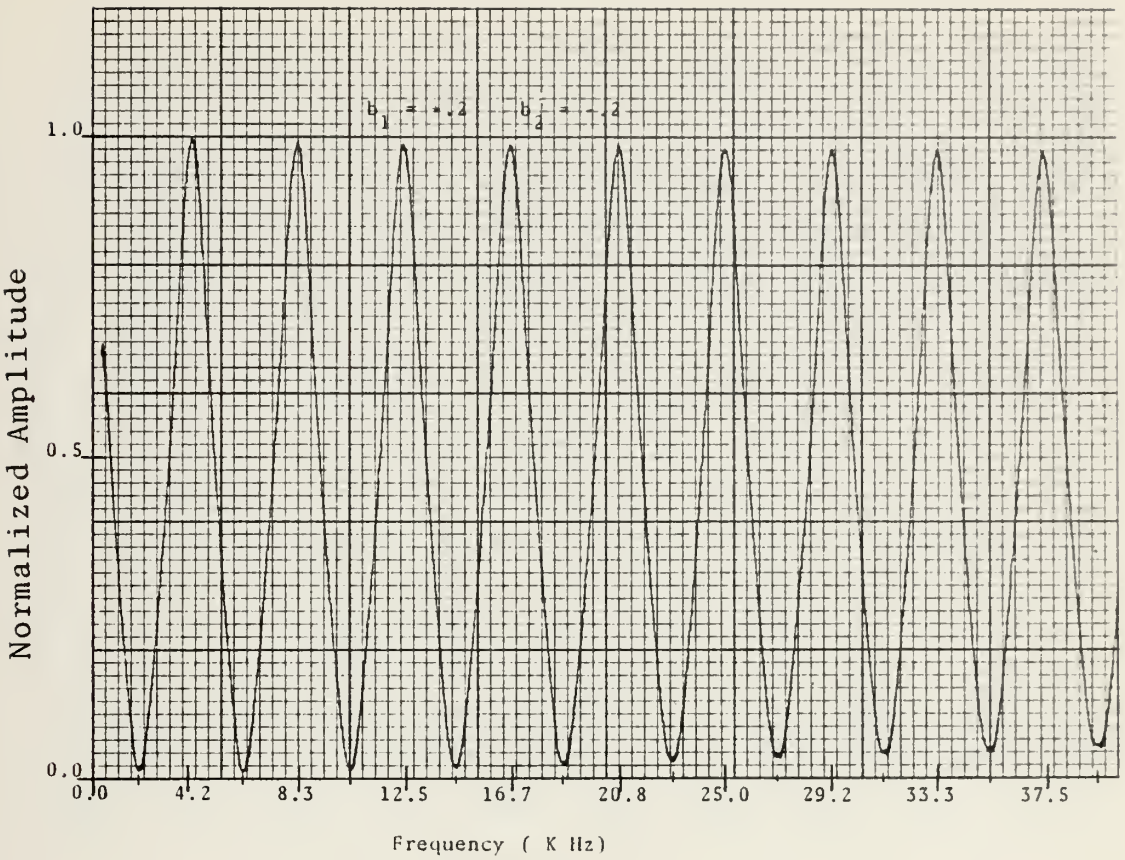

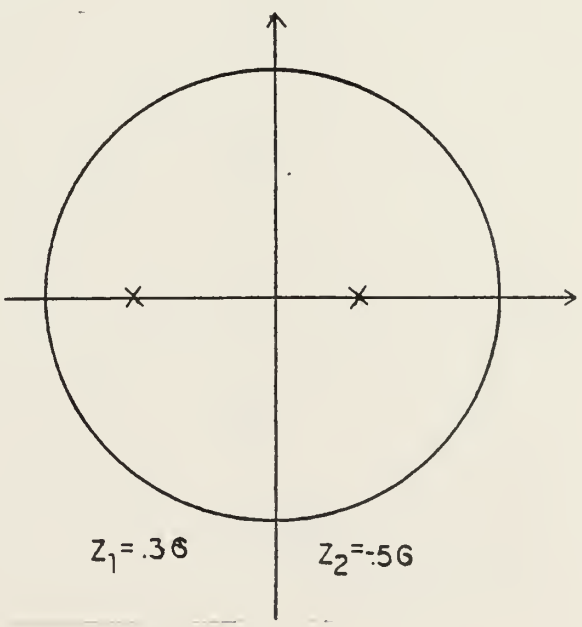

Figure 4.3 Comb Frequency Spectrum (Experimental)

and Pole Location

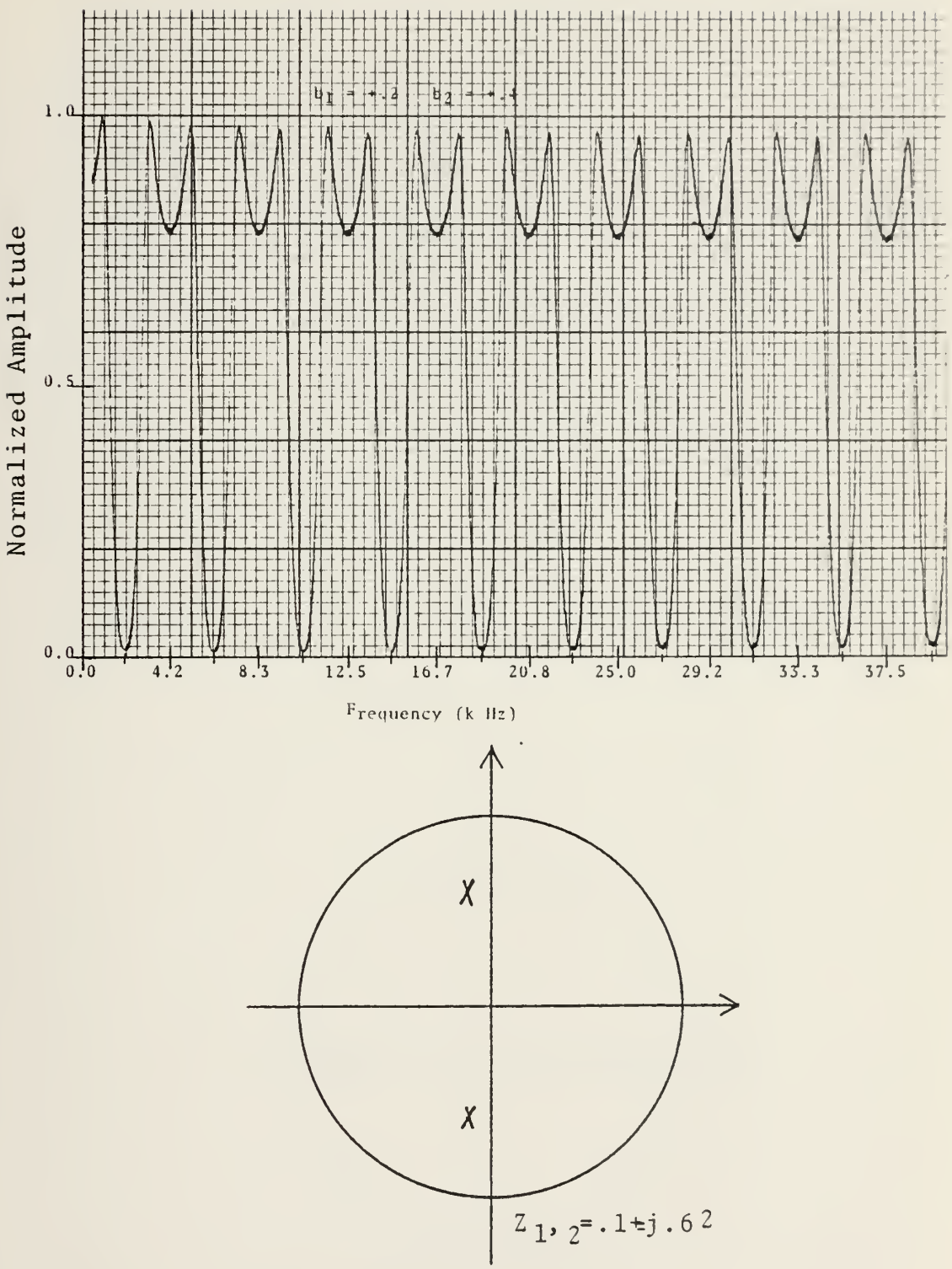

Figure 4.4 Comb Frequency Spectrum (Experimental)

and Pole Location

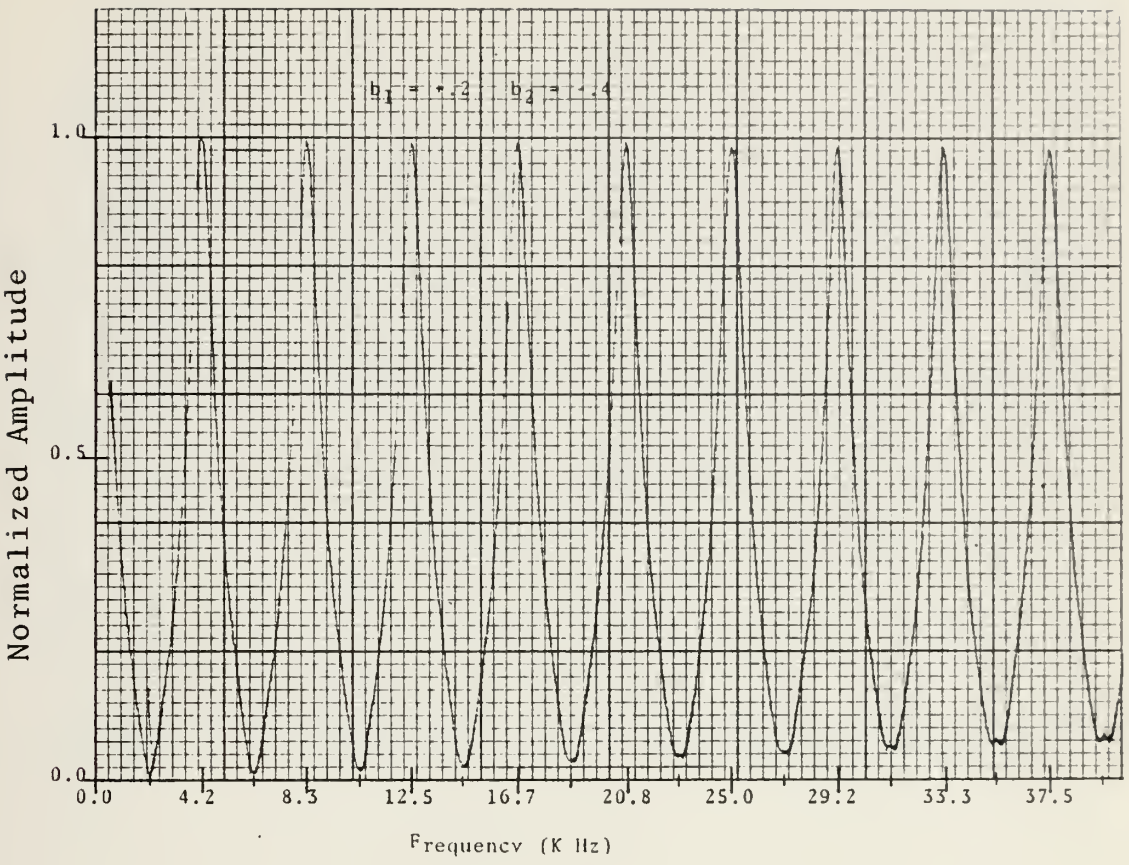

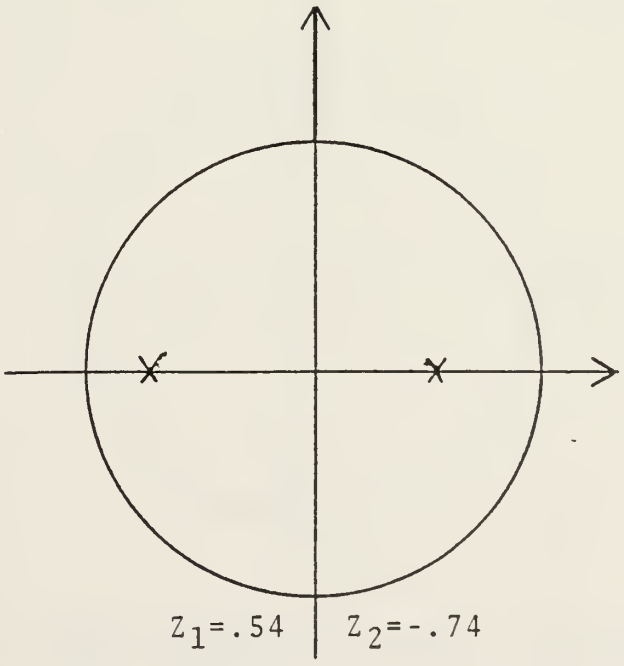

Figure 4.5 Comb Frequency Spectrum (Experimental) and Pole Location

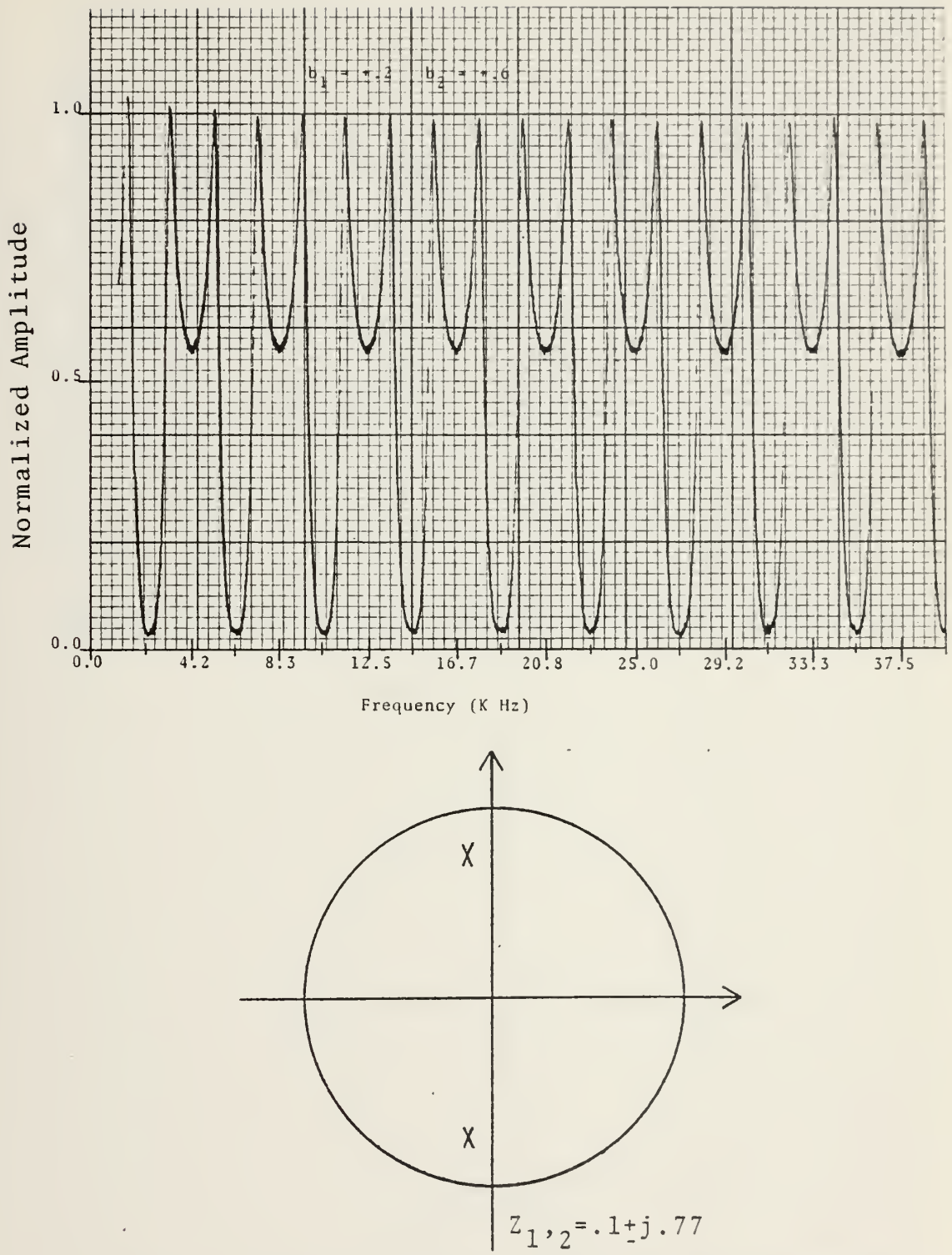

Figure 4.6 Comb Frequency Spectrum (Experimental)

and Pole Location

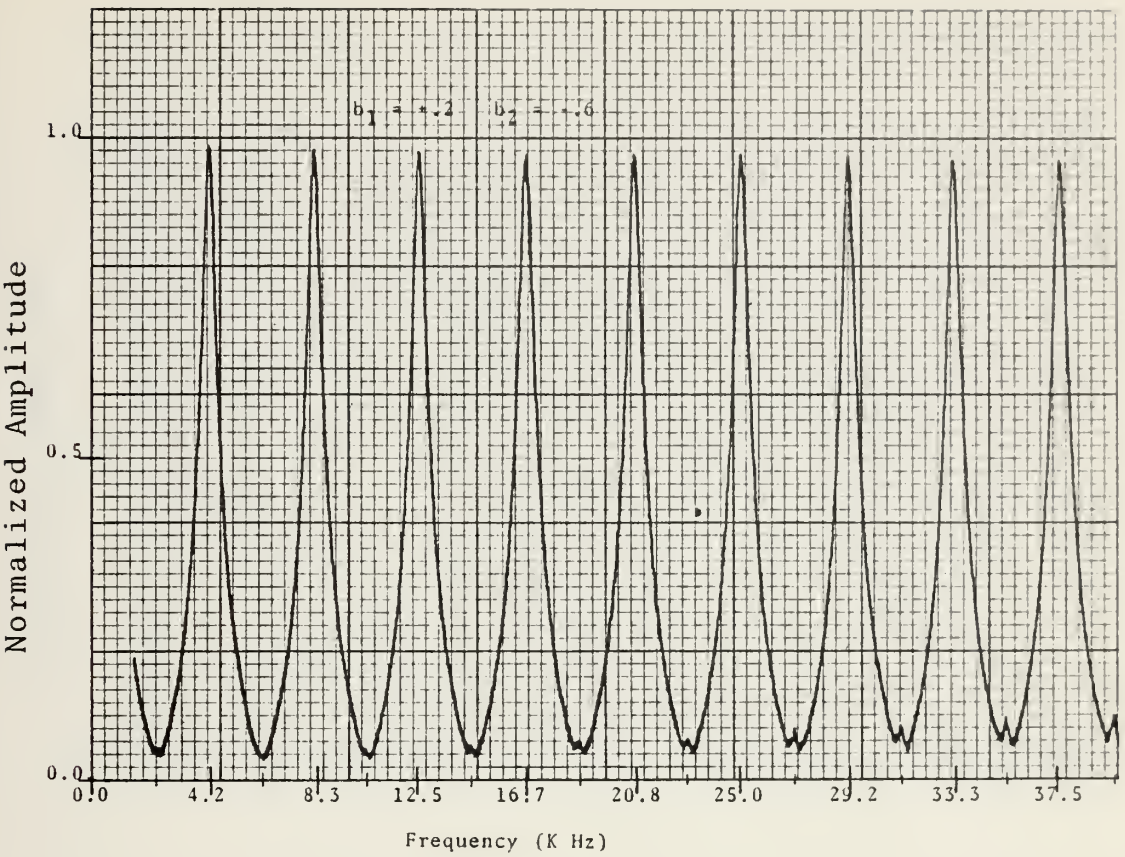

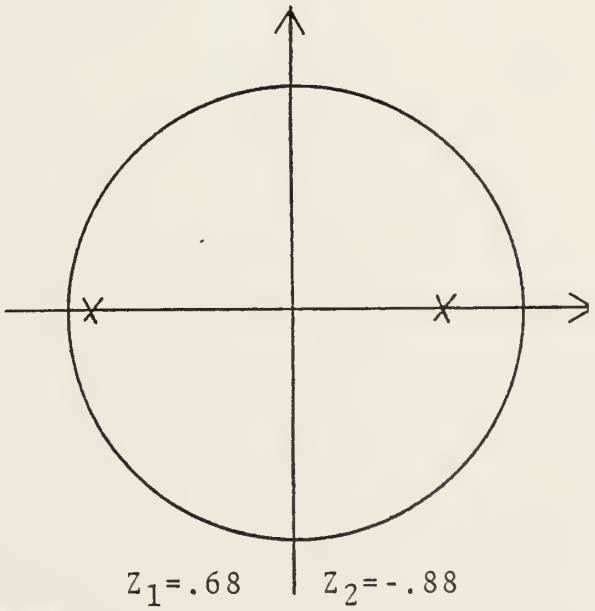

Figure 4.7 Comb Frequency Spectrum (Experimental) and Pole Location

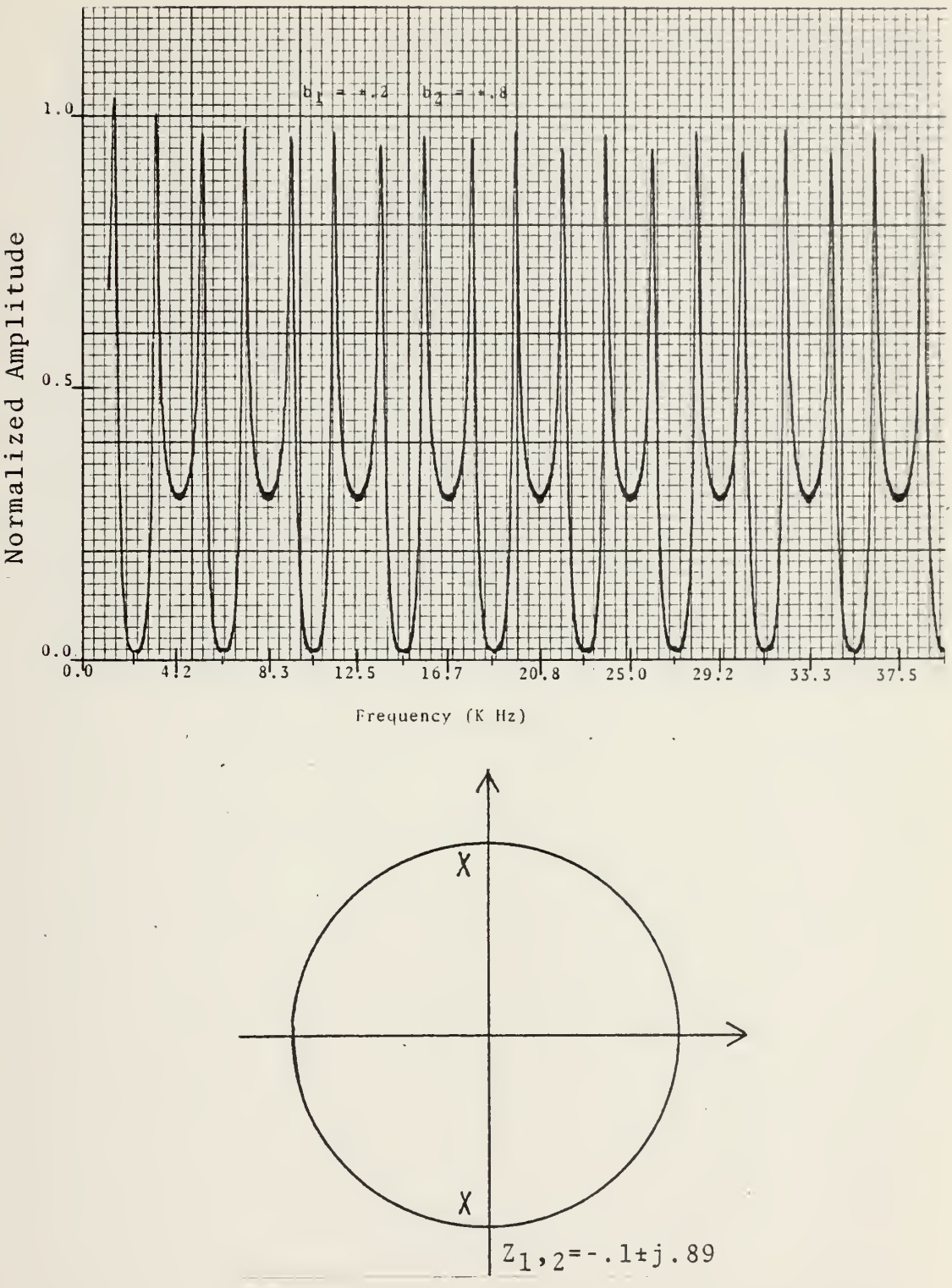

Figure 4.8 Comb Frequency Spectrum (Experimental) and Pole Location

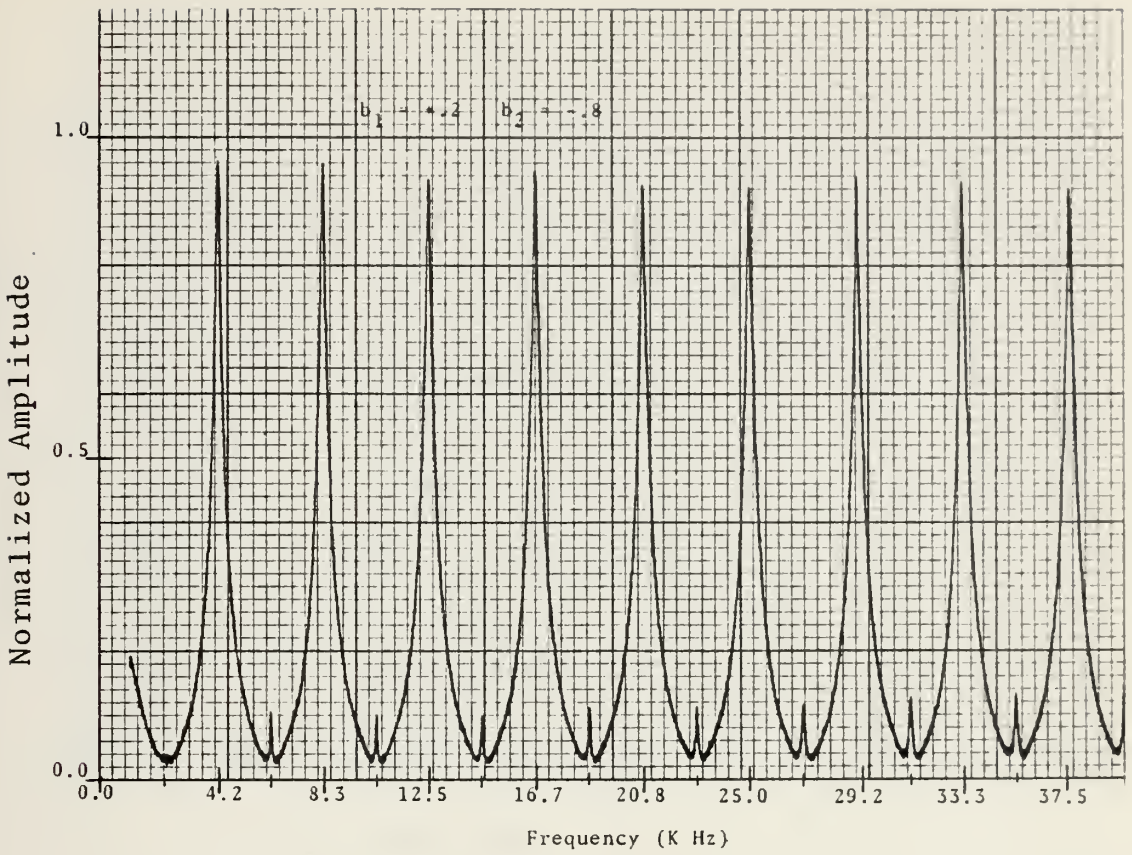

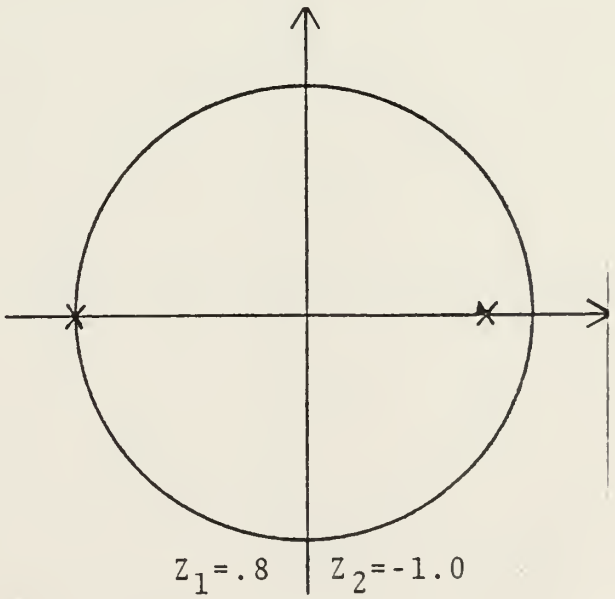

Figure 4.9 Comb Frequency Spectrum (Experimental) and Pole Location

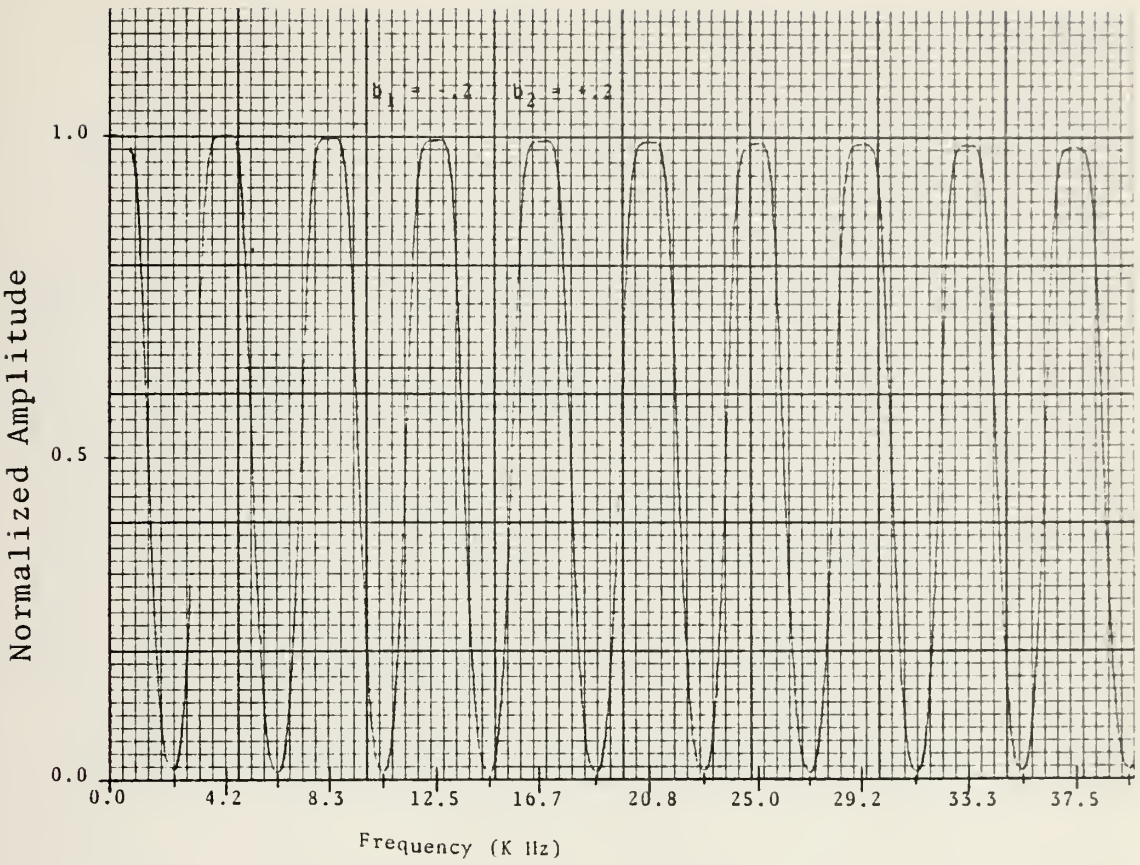

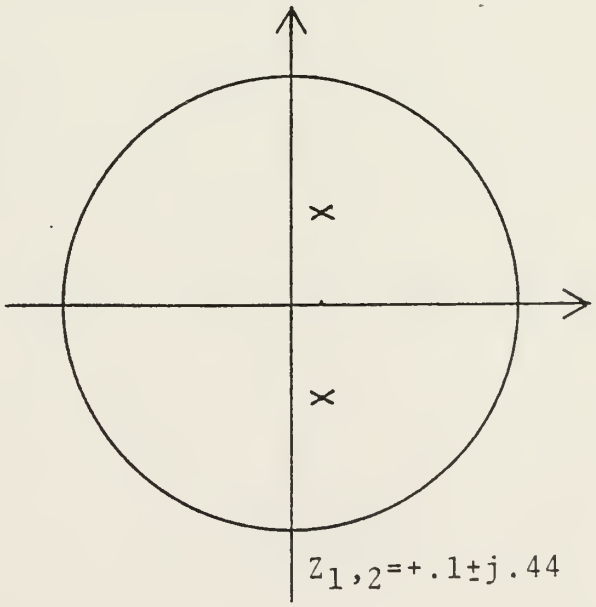

Figure 4.10 Comb Frequency Spectrum (Experimental) and Pole Location

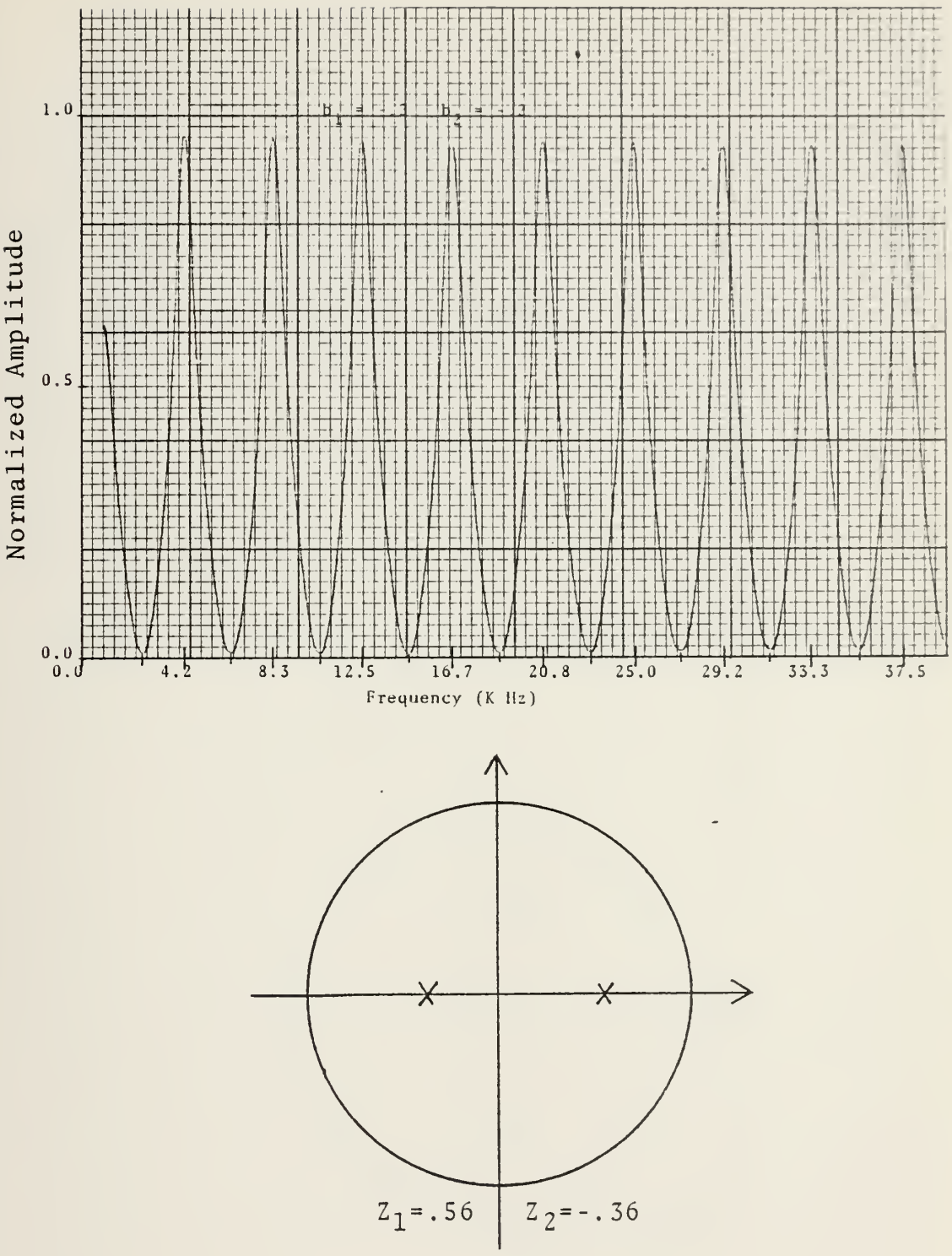

Figure 4.11 Comb Frequency Spectrum (Experimental)

and Pole Location

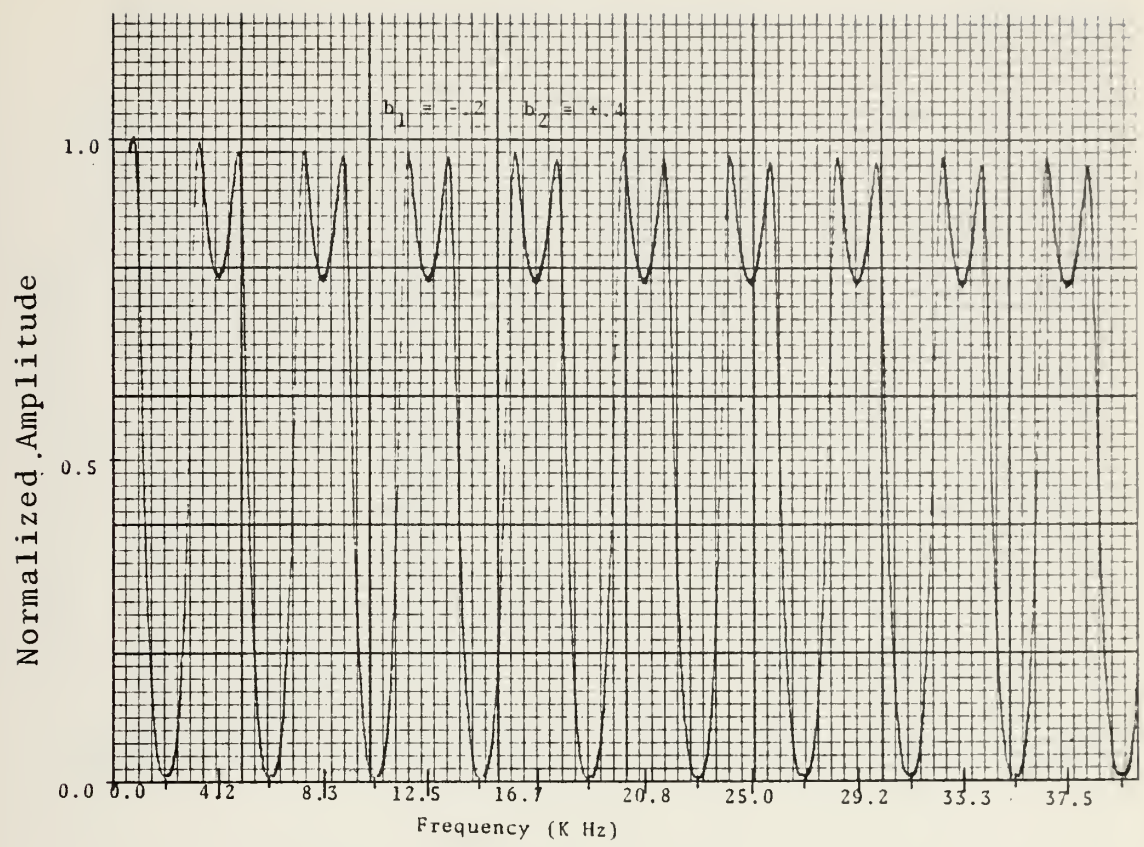

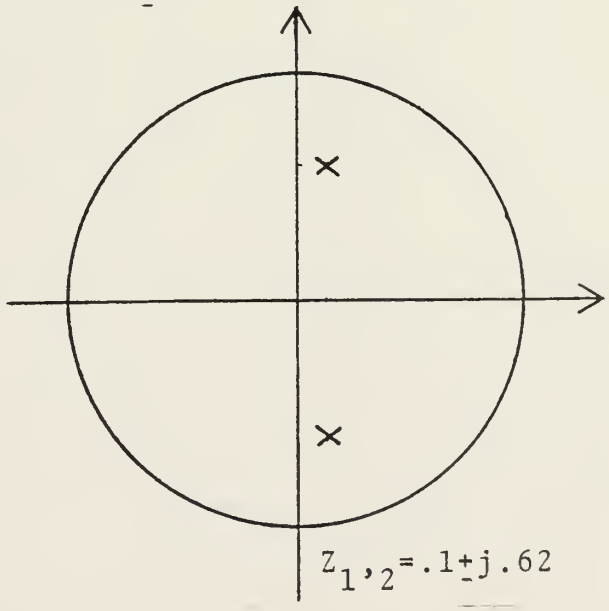

Figure 4.12 Comb Frequency Spectrum (Experimental)

and Pole Location

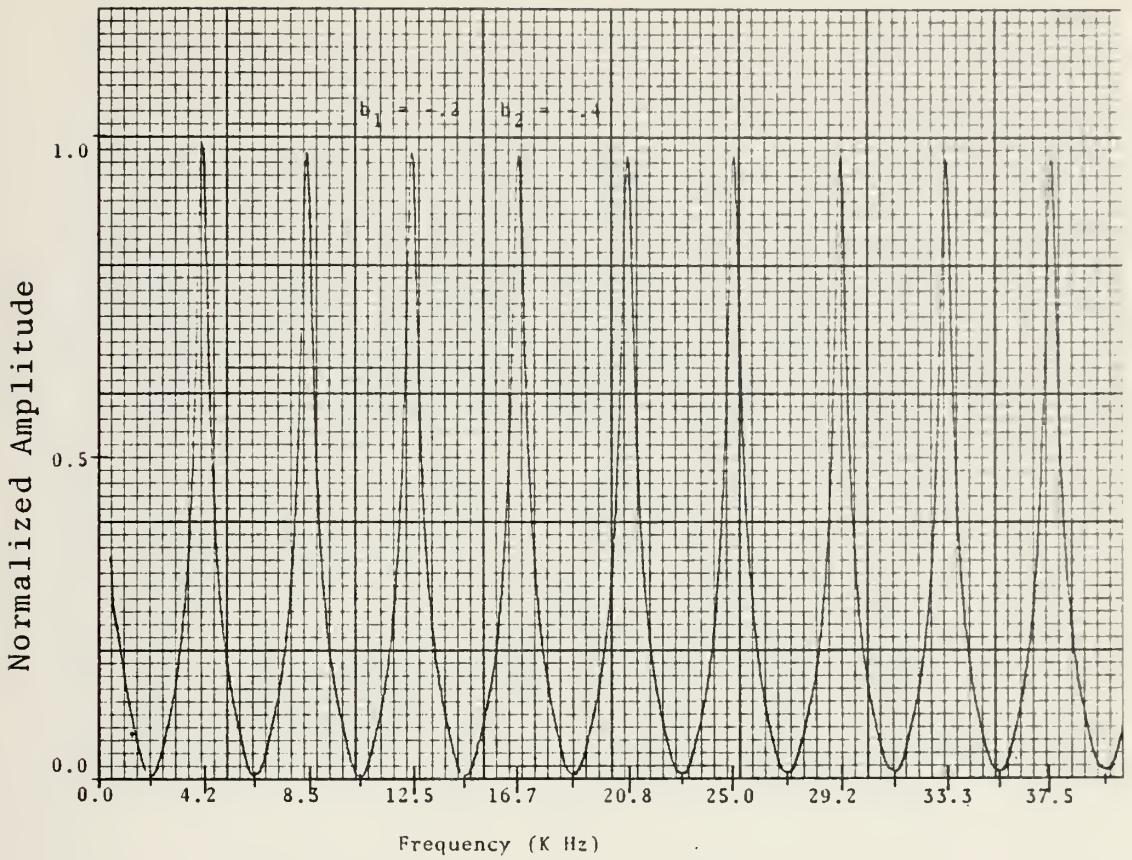

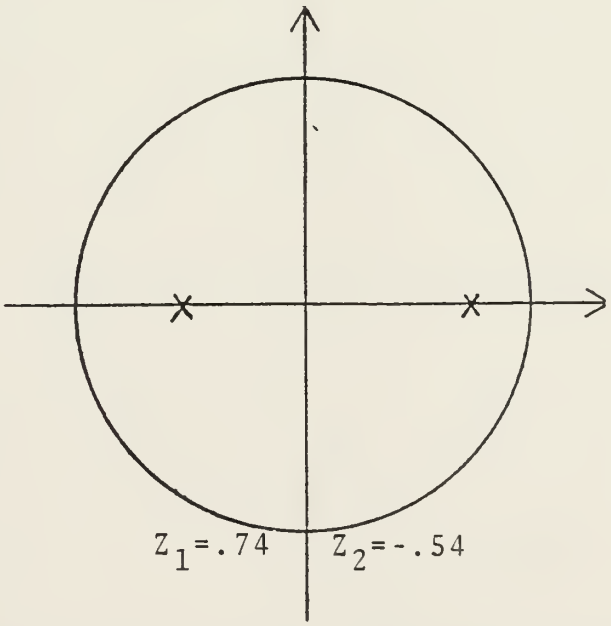

Figure 4.13 Comb Frequency Spectrum (Experimental)

and Pole Location

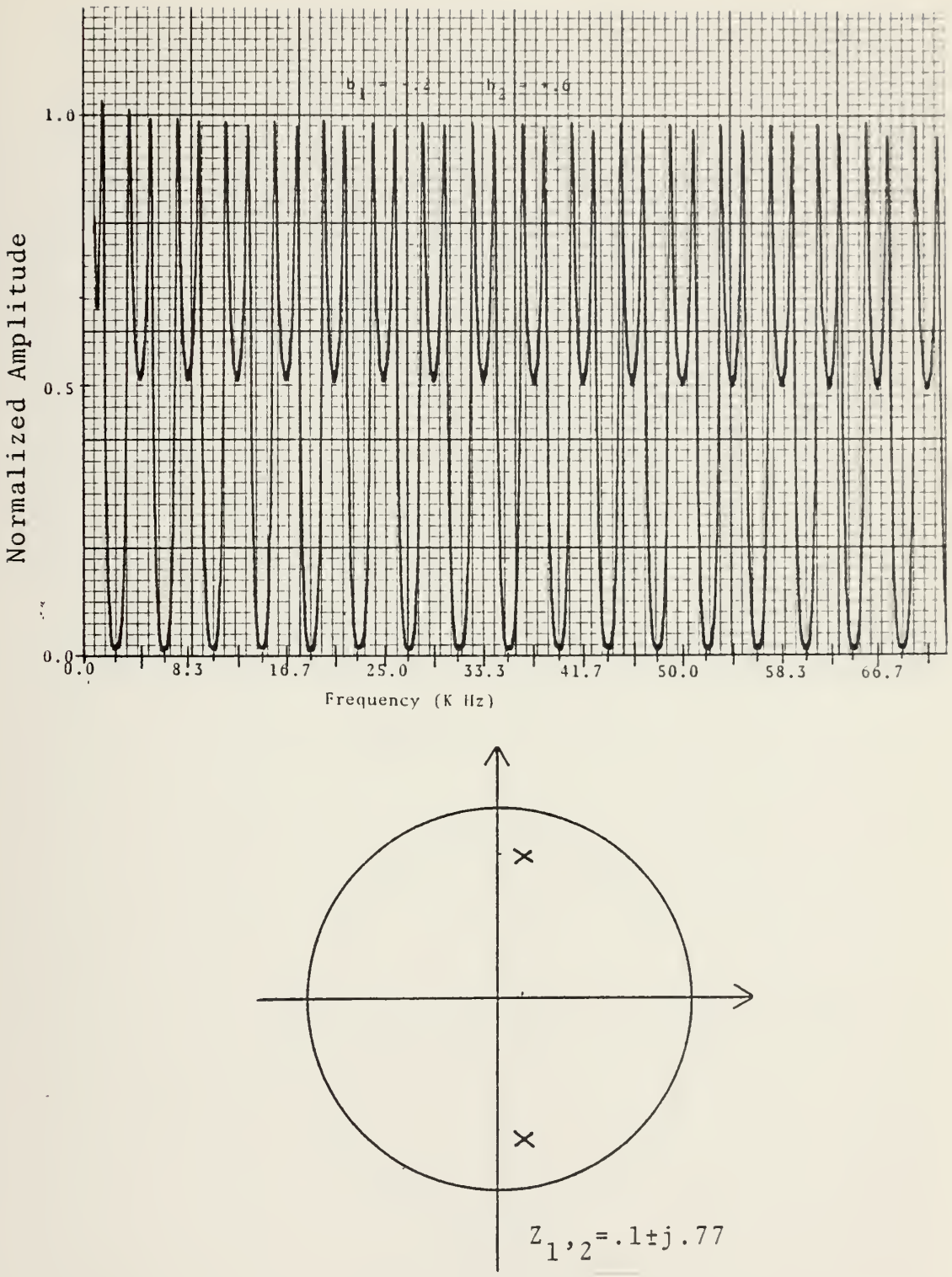

Figure 4.14 Comb Frequency Spectrum (Experimental)

and Pole Location

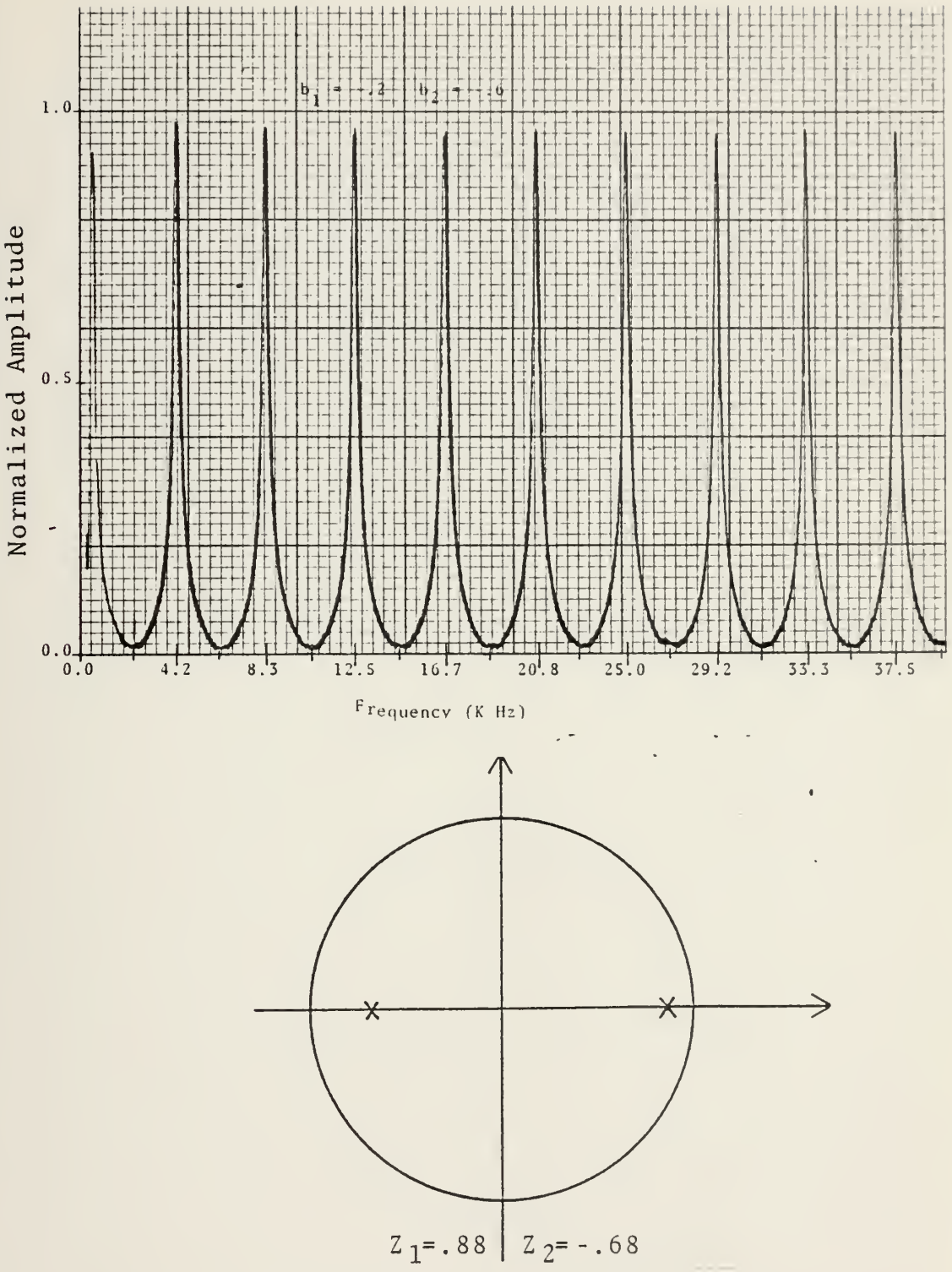

Figure 4.15 Comb Frequency Spectrum (Experimental) and Pole Location

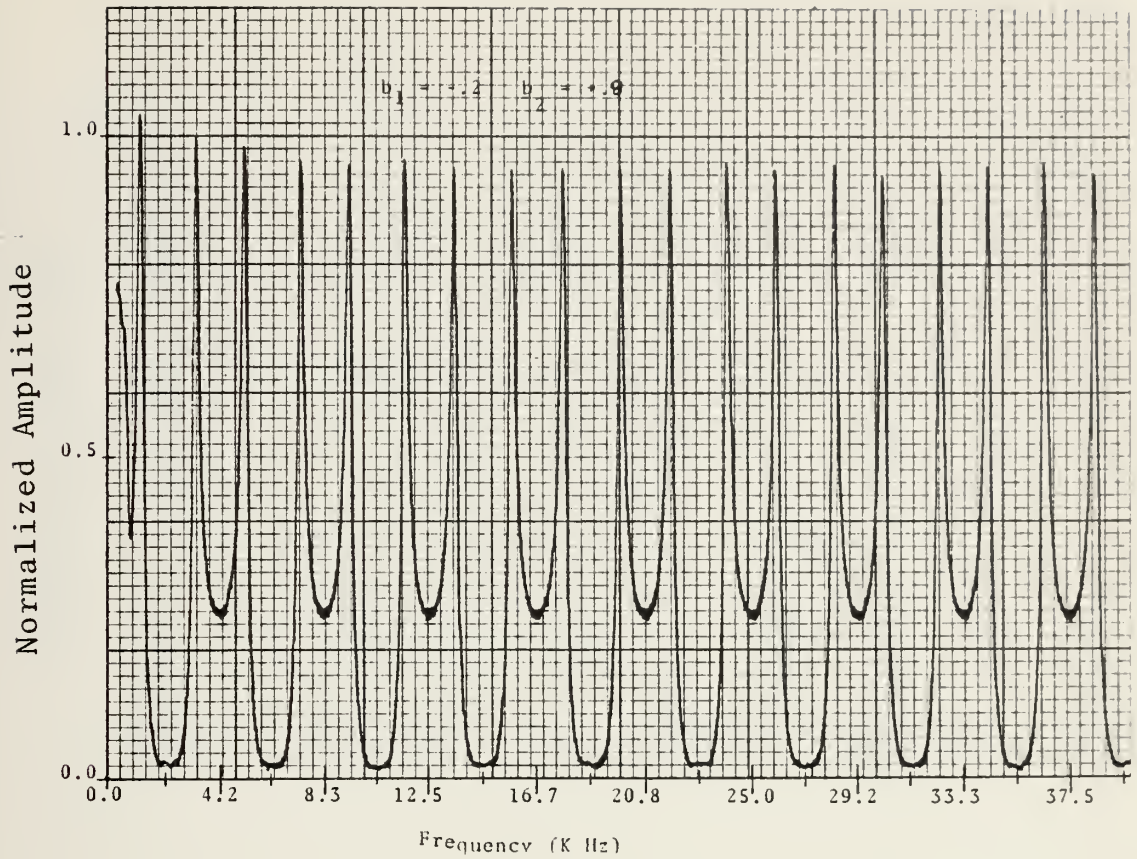

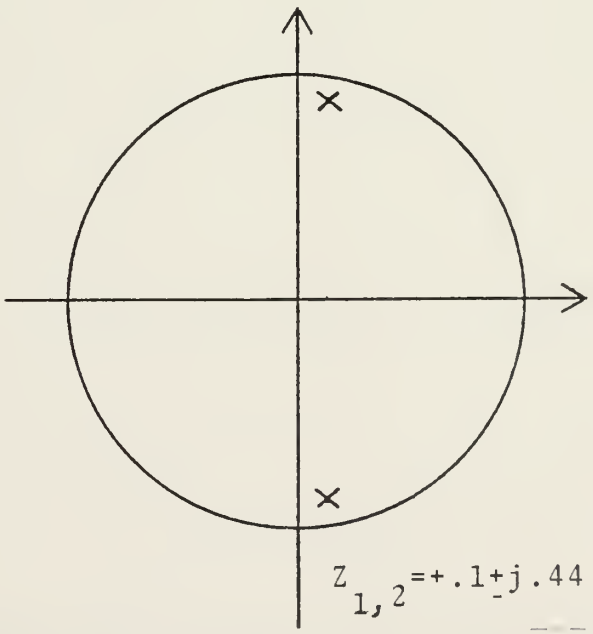

Figure 4.16 Comb Frequency Spectrum (Experimental) and Pole Location

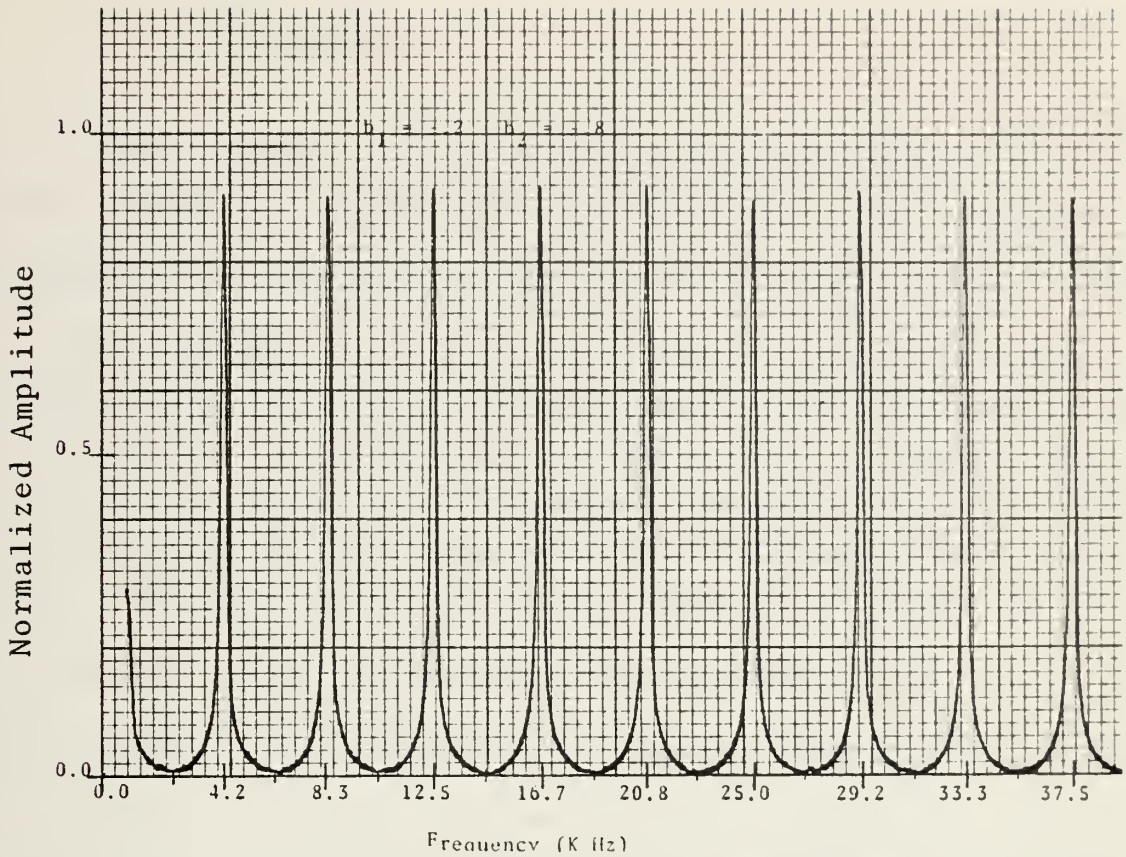

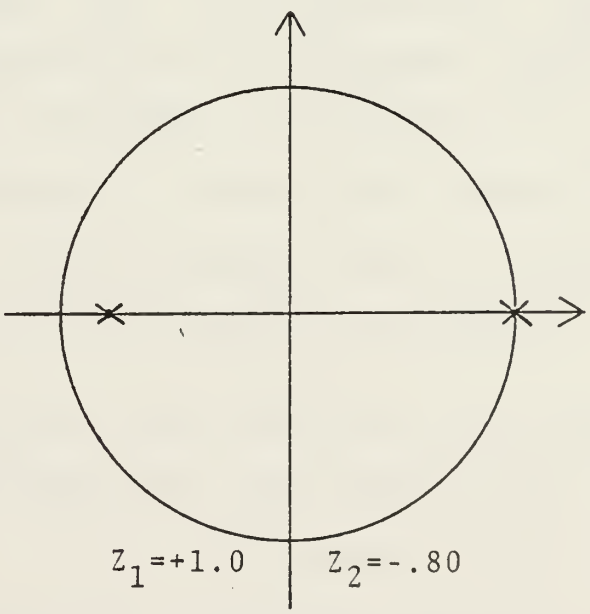

Figure 4.17 Comb Frequency Spectrum (Experimental)

and Pole Location

1. Data Analyses

It appears , from the data in the previous figures, that changing the sign of b_2 causes the filter response to change from a canceller to an integrator type filter. This is not completely true. The reason that the filter is changing back and forth between canceller and integrator can be explained by referring to Figure 3.5 of Chapter 3. In this figure, there is an isocontour denumerated .25fs which distinguishes between the two types of filters under concern here. The fact that b_1 is held numerically close to this isocontour causes the filter characteristic to jump back and forth across this isocontour. However, when $b_1 = 0.2$ and b_2 is greater than 0.6 in absolute value, the filter response remains as an integrator since these coefficients fall below (integrator side) the .25fs isocontour. There is a large difference in the shape of the frequency response teeth just described. The changing of the sign of b_2 from minus to plus causes the poles to change from being real(minus b_2 coefficients) to being imaginary (plus b_2 coefficients) even though both curves are integrator responses.

Another point which was noted was, that as the value of b_2 decreases negatively, the slopes of the curve skirts become steeper. This was expected, since, as the b-plane triangle of stability indicates, when b_2 becomes more negative,(holding b_1 constant) the value of the isocontour

ratio becomes smaller. This indicates that the three decibel cutoff frequency is decreasing (f_s was held constant throughout the experiment). This, in effect, causes the pass band to decrease, bringing about a sharper response curve. This can be seen by comparing Figures 4.3, 4.4, 4.6, and 4.8 and their counterparts which are plotted with b_2 plus.

Figures 4.14 and 4.16 show the nulls beginning to deteriorate quite rapidly. This is due to the shifting of the zeros around the unit circle from the Z = ±1 + jo point. Since there is a real pole relatively close to the perimeter of the unit circle in these two figures, the pole immediately becomes effective; allowing some of the signals at these frequencies to pass through. However, as the frequency was increased still further, the second zero is encountered and a second null obtained. The deterioration became increasingly apparent as the frequency was increased. An example of this deterioration is shown in Figure 4.18. This figure shows the entire spectrum of the filter response from DC to fs = 400 K hertz. Also shown in Figure 4.18 is the deterioration of the nulls due to the shifting of the zeros and some inefficiency of the Reticon filter.

The shifting of the zeros may have been due to stray capacitances caused by the connecting leads of the circuit. This would cause the coefficients of both the transfer function numerator and denominator to vary and, in the case of the numerator coefficients, cause the zero locations to shift off the real axis. This results in an imaginary term in the value of Z, causing a shift around the unit circle.

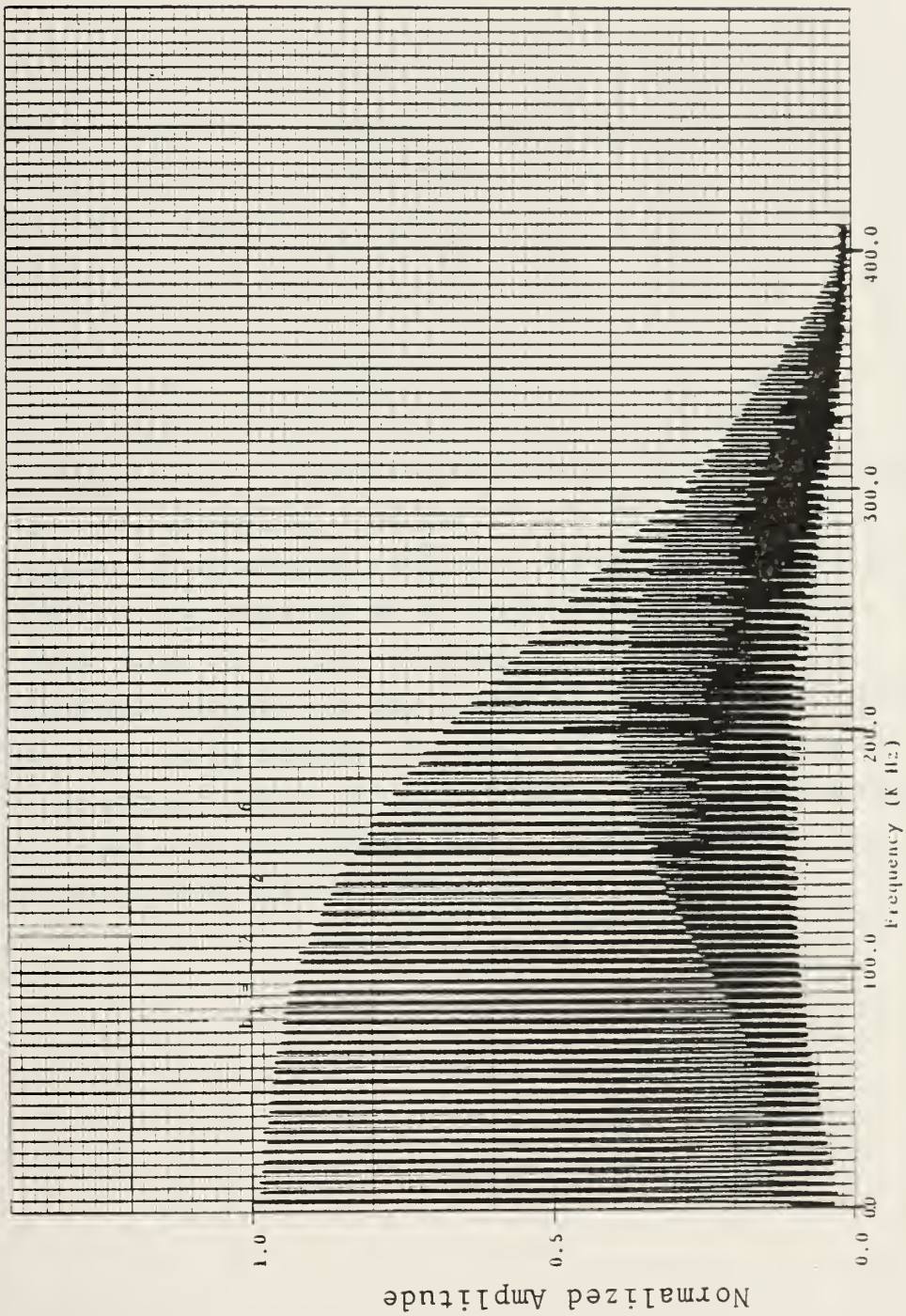

Figure 4.18 Comb Frequency Spectrum (0-400 KHz)

C. FILTER SELECTION

As will be discussed in the following chapter, an integrator recursive comb filter is desired with very narrow pass band teeth to demonstrate the Signal-to-Noise ratio improvement ability of the comb filter. The type of response chosen was the filter with $b_1 = -0.2$ and $b_2 = -0.6$. This filter has a very narrow three decibel pass band (approximately 417 hertz wide) and a wide stop band (approximately 3.91 K hertz wide). This is shown in Figure 4.6. Figure 4.19 shows the entire frequency response from DC to 400 K Hertz. The zeros are relatively unaffected at the higher frequencies although the amplitudes of the teeth are increasing between 80 K hertz and 110 K hertz. This was possibly due to the frequency dependence of the b coefficients since, as explained earlier, these coefficients affect the teeth shape. However, for the purposes of the next chapter, this was acceptable. The discrepency in the teeth amplitude at approximately 200 K hertz is due to instrumentation errors only.

Figure 4.19 Comb Frequency Spectrum (0-400 KHz)

V. APPLICATIONS OF THE INTEGRATOR TYPE RECURSIVE COMB FILTERS 1: SIGNAL-TO-NOISE RATIO IMPROVEMENT

A. INTRODUCTION

Signal-to-Noise ratio (SNR) improvement is a major concern in radar and communication design problems. In this section an attempt has been made to use a Charge Transfer Device (CTD) to improve the SNR. The input signal that was chosen was a pulse train. A pulse train was chosen since it is commonly used in radar applications as well as the fact that it has a discrete frequency spectrum with many frequency components. This latter fact demonstrates the intent of this section more explicitly, as will be seen later.

B. FOURIER ANALYSIS AND FILTER CONSIDERATIONS

The result of a Fourier analysis of a pulse train is given by equation (1) below and its development is shown in Appendix A.

$$C_k = \frac{Vt}{T}\left(e^{-jkw_o(t_o + t/2)}\right)\left(\frac{\mathrm{Sin}kw_o t/2}{kw_o t/2}\right) \qquad 1$$

where:

t =pulse width

T= pulse repition frequency (PRF)

V= pulse amplitude

w= 2PI/T

The line spectrum is shown in Figure 5.1. Note that the amplitude is a function of the familiar SinX/X curve (where X = kwt/2 for this explanation) and that all the even and odd harmonics are present since the pulse train in this situation is neither an even nor an odd function of time. Further note that the value of C_k is directly related to the pulse width (t) and inversely proportional to the pulse period T. If the pulse period (T) increases, the band width of the spectrum (band width is from 0 hertz to 1/T) does not change, but the number of spectral lines between freq.= 0 and freq.= 1/T increases. If this pulse train were transmitted through a very noisy environment it would be most difficult, if not impossible, to detect it unless special filtering techniques were employed. However, if the frequency spectrum of the pulse train could be matched with the frequency spectrum of a filter which will attenuate all other frequency components in between the desired signal components, then the system noise will have minimum effect on the transmitted/received signal. The problem then is to find a filter which has the same frequency spectrum characteristics as that of Figure 5.1. A filter with this type of spectrum is the Integrator Recursive Comb filter. This filter is periodic in the frequency domain and is capable of nearly perfect attenuation within the stop band. Since the spectrum of the pulse train has discrete frequency components over a very wide frequency range a very narrow comb filter pass band response is desired to capture the signal's spectral components and at the same time attenuate as much of the undesired spectral components as possible. The characteristic response of the Integrator Comb filter is such a response. The characteristic response of the

Integrator Comb filter is shown in Figure 5.2. This response can be produced very easily using sampled analog techniques. Sampled analog techniques are highly desirable since there is no analog-to-digital or digital-to-analog conversion required. Also, the frequency spectrum of the comb filter can be shifted without changing the relative amplitude of the pass band, simply by changing the sampling frequency f_s. Since the comb filter frequency response has a finite band width per tooth, some of the noise spectral components will pass through the device with the signal's spectral components. The major portion of the noise should be attenuated since the pass band widths are much narrower than the stop band widths of the filter response.

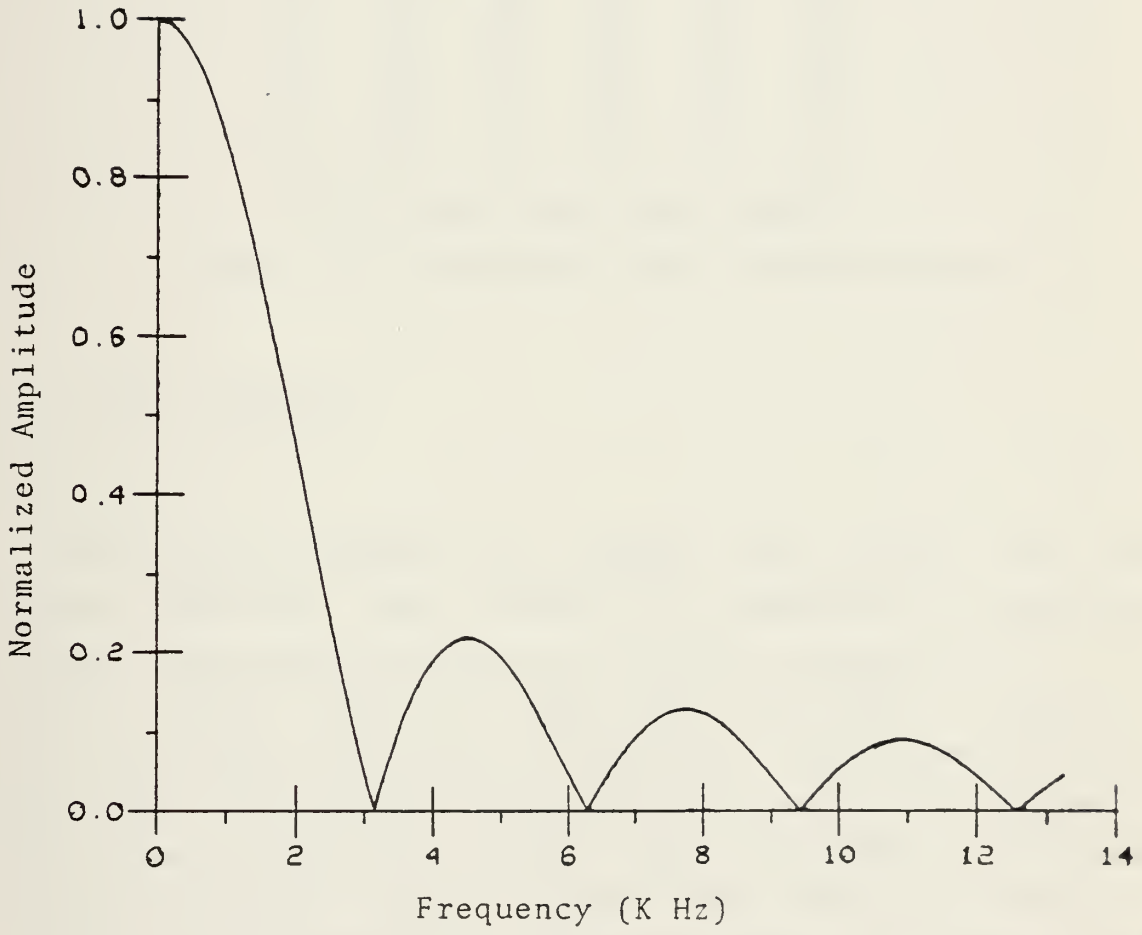

Figure 5.1 Pulse Train Frequency Spectrum

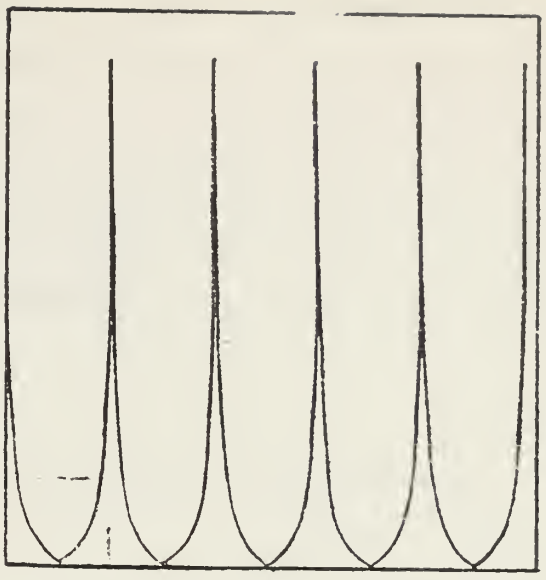

Figure 5.2 Integrator Comb Filter Response

C. DEVICE SELECTED

The device selected to compose the filter was the Reticon SAD-100. This device is a monolithic integrated circuit which provides storage of analog information. The device has 96 bits of delay and provides a first-in, first-out storage for these 96 samples. The specification sheet on the SAD-100 indicates that there are 100 bits of delay, two of which are used for input and output junctions leaving 98 storage cells. Earlier work with this device had indicated that there were 96 storage cells. The data which was obtained throughout this study proved this to be accurate.

Some of the important characteristics of the SAD-100 are given below:

Maximum Delay at 4 KHz sampling rate..... 25 msec
Maximum Sampling Rate..... 12 MHz
Dynamic Range..... 70 db
Minimum Clock Frequency..... 2.0 KHz
Storage Cell Capacitance..... 1.2 pf
Input Capacitance..... 8.0 pf
Output Capacitance..... 8.0 pf

The coefficients which were used are:

$$a_0 = 1.0$$

$$a_1 = 2.0 \qquad b_1 = -0.2$$

$$a_2 = 1.0 \qquad b_2 = -0.6$$

These coefficients give the most desirable frequency response as shown in Figure 5.3. The stop bands are nearly perfect zeros and the pass bands very narrow with very sharp slopes on both sides of their respective center frequencies.

The filter was operated at a sampling frequency of 390 K hertz during the measurements. Thus, if the pulse train is to pass through the filter unattenuated and without distortion, the spectral components of the pulse train must fall directly on the pass bands of the filter response.

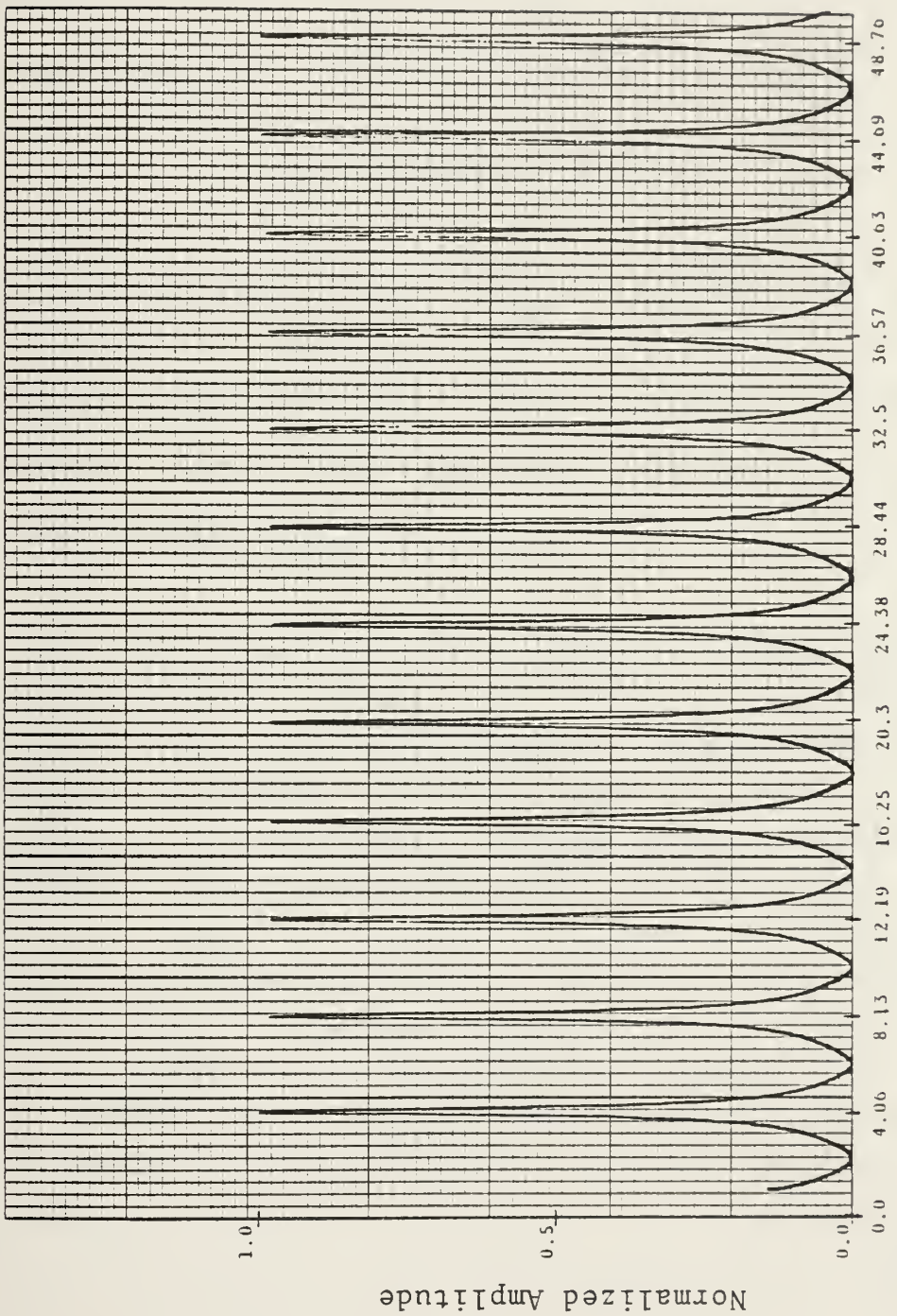

Figure 5.3 Comb Filter Frequency Spectrum (Experimental)

The pass bands of the Comb filter are periodic with respect to the sampling frequency (f_s) divided by the number of delays in the SAD - 100. The filter's first tooth center frequency is given by equation 2 below:

$$f_1 = f_s/\text{Number of Delays} \quad 2$$

This calculation gives a center frequency of the first tooth of the filter at f_1 =4063 hertz. Since the following teeth are repetitive with respect to this frequency, the following teeth center frequencies are given by $M*f_1$, where M is an integer equal to 1, 2, 3, ...

For the signal to pass through the filter, the spectral components of the signal and those of the filter must coincide. For the pulse train to coencide with the filter frequency spectrum, it must have a pulse repitition frequency of 4063 Hertz or some integer multiple of this frequency. The frequency selected was 4063 Hertz and its frequency spectrum is shown in Figure 5.4, Figure 5.5, and Figure 5.6. Figure 5.5 and 5.6 are an expanded scale of the input signal , whereas figure 5.6 is the entire spectrum from DC to 450 KHz. A comparison of figures 5.3 and 5.4 will reveal that the spectrums are matched perfectly. The time domain representation of both the input and output pulses are shown in Figure 5.7. In this figure only one input pulse is shown, and above it, one output pulse. The slight distortion in the output pulse is due to the loss of some of the higher frequencies resulting from an imperfect frequency match. This loss is caused by slight drifting of the pulse generator from the selected frequency, as well as

the zeros of the stop band at the higher frequencies rising above zero. Figure 5.8 shows a series of input and output pulses. Figure 5.9 demonstrates the signal attenuation when the input signal frequency spectrum is not matched to the filter spectrum. The input frequency in this case is a 3.56 K hertz pulse train (shown on the bottom of figure 5.9); note that the output signal is completly lost (shown in the top of figure 5.9).

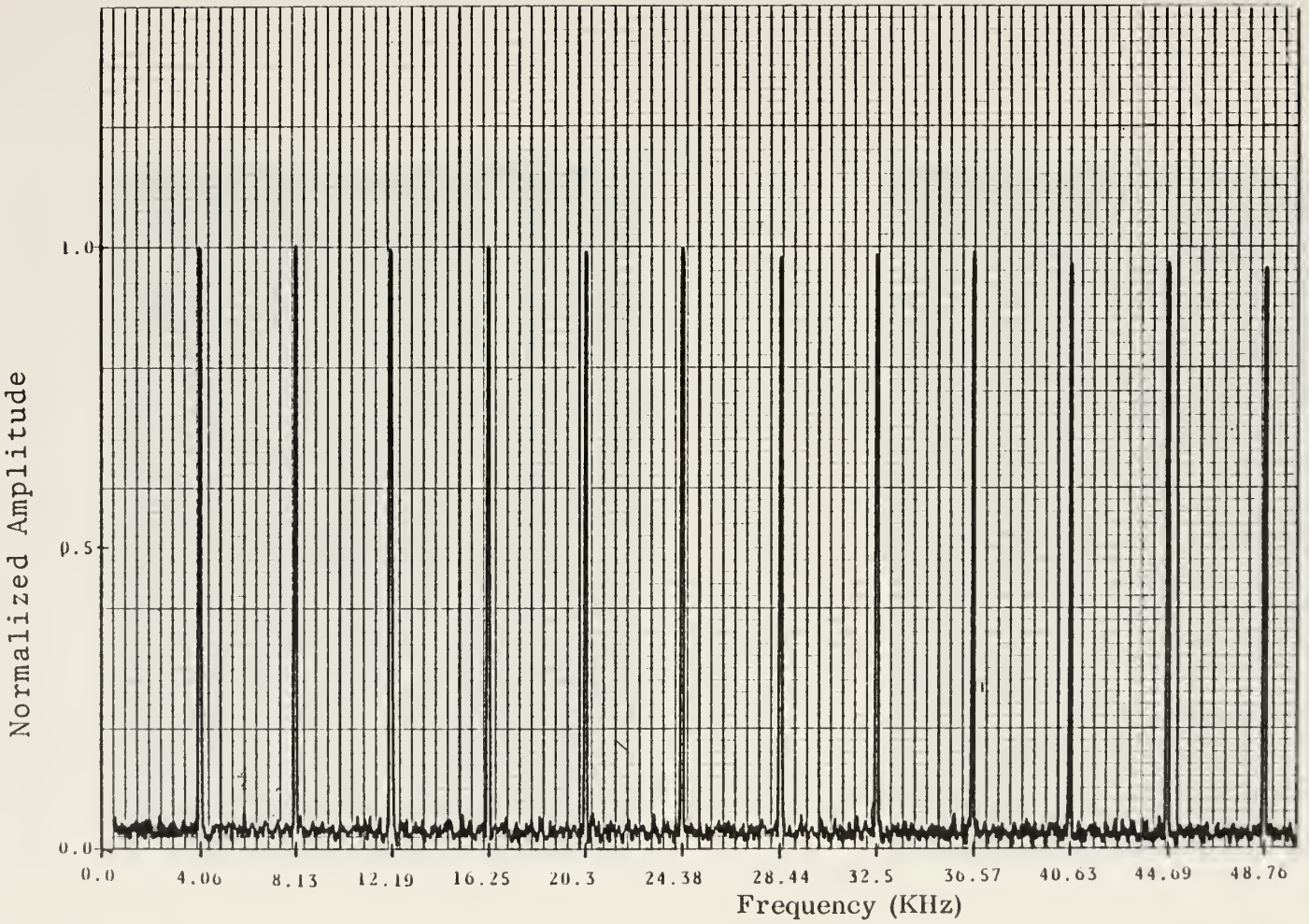

Figure 5.4 Pulse Train Frequency Spectrum (PRF=4063 Hz)

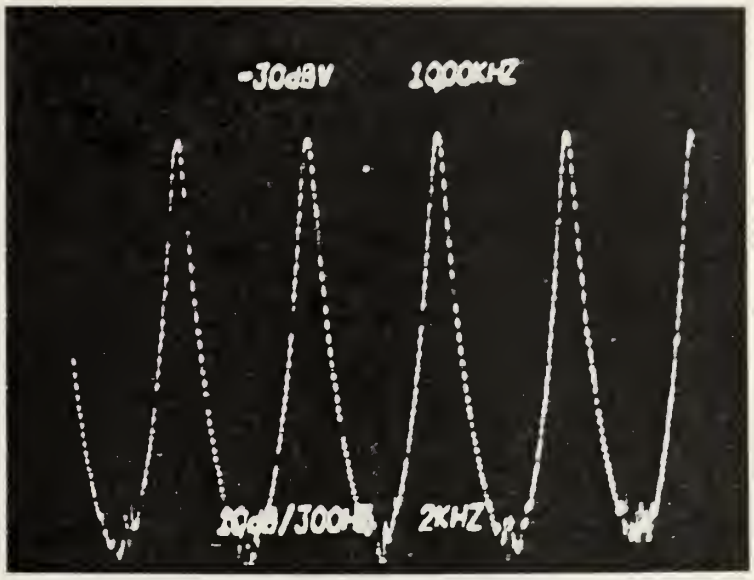

Figure 5.5 Input Pulse Train Frequency Spectrum (Experimental)

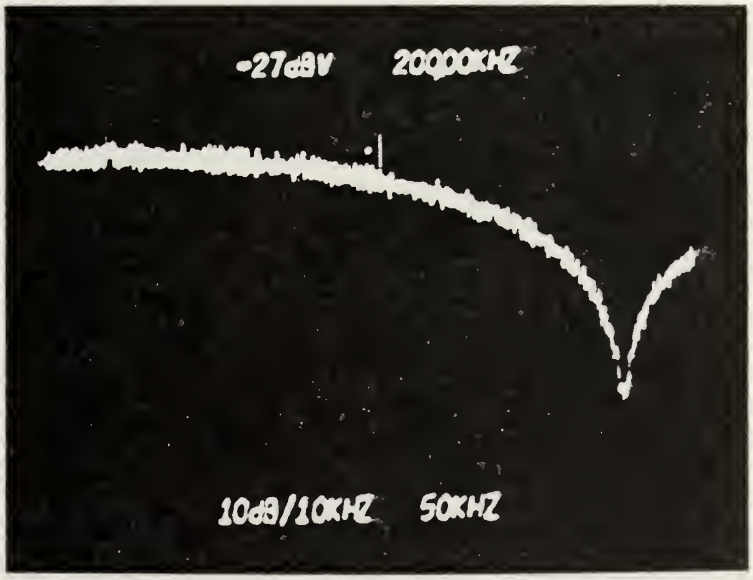

Figure 5.6 Input Pulse Train Frequency Spectrum (Experimental)

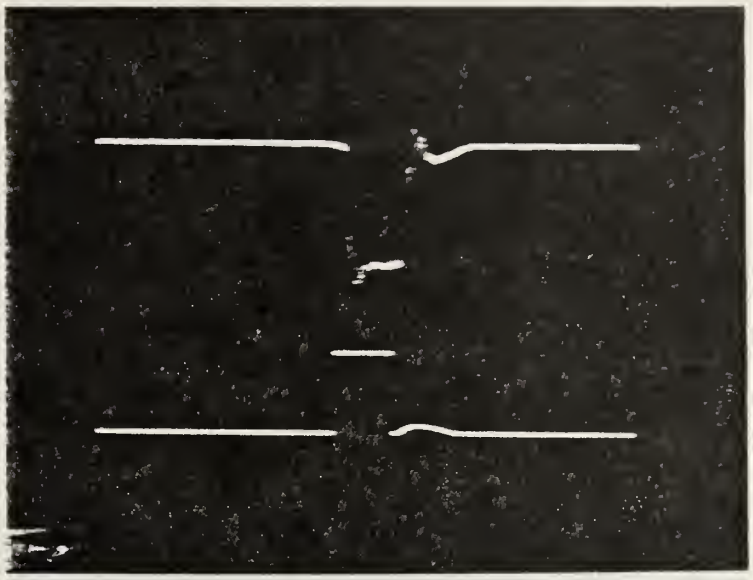

Figure 5.7 Input Pulse

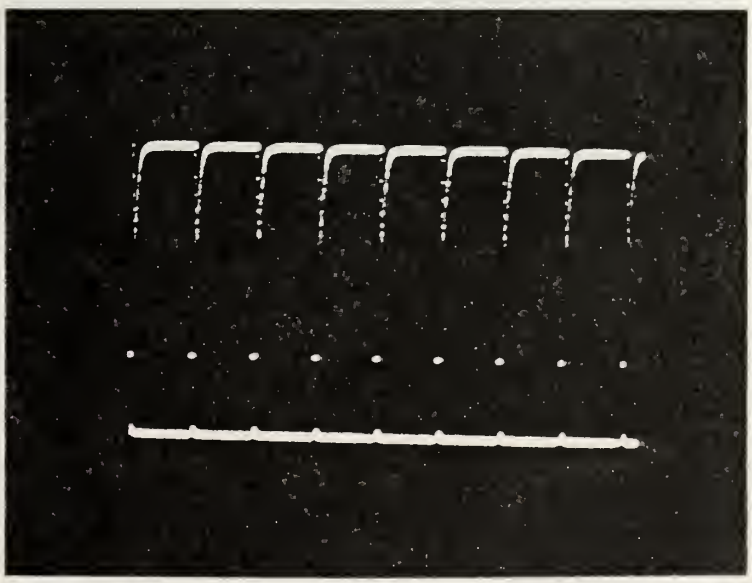

Figure 5.8 Filter Input and Output

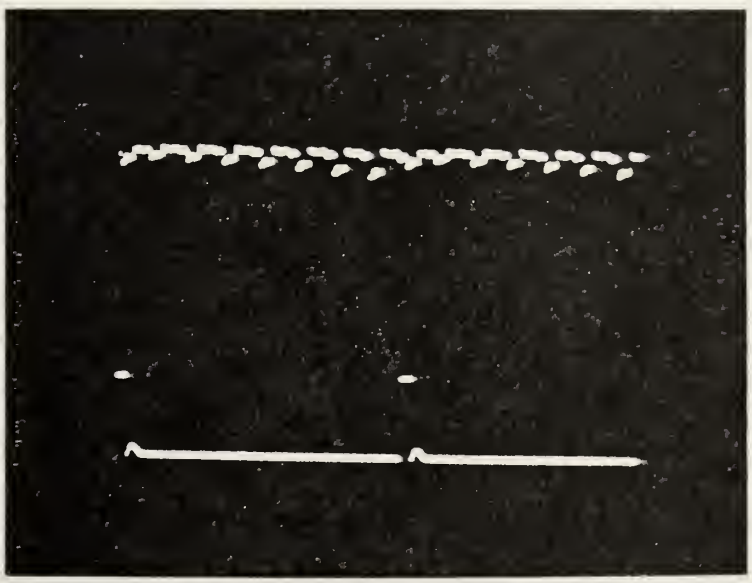

Figure 5.9 Cancellation of the Input Signal

The input noise which was used was produced by General Radio Company and was a type 1390-5 random noise generator. This device produces a white Gaussian noise over a frequency range of up to 5 M hertz. The frequency spectrum of the Gaussian noise was plotted on the X - Y recorder and is shown in Figure 5.10. This graph is plotted from zero hertz to 500K hertz. The slight dip from approximatly 100K hertz to 300K hertz is due to the noise generator characteristics.

The noise as seen in the frequency response of Figure 5.10 was passed through the Reticon integrator Comb filter. As to be expected, the filter frequency response should be similar to that of figure 5.3. The actual noise output frequency response of the filter is shown in Figure 5.11. This plot is from zero hertz to 50K hertz. A comparison of this and figure 2's response reveals that the base band has widened and that the peaks have become jagged. This is due to the noise having a very low input amplitude of 0.6 volts RMS. Thus, the product of the very low input signal and the filter pass band tooth on a normalized basis causes the small amplitude skirt portion of the pass band to remain approximatly the same as it was before but; the product of the very large center portion of the filter pass band with a very small input spectral components causes the large center frequency amplitude to decrease considerably giving the effect of widening the pass band of the filter on a normalized basis. However, this in effect is not the case. (Note that all of the actual curves plotted have been normalized to ease the comparisons which have been made.)

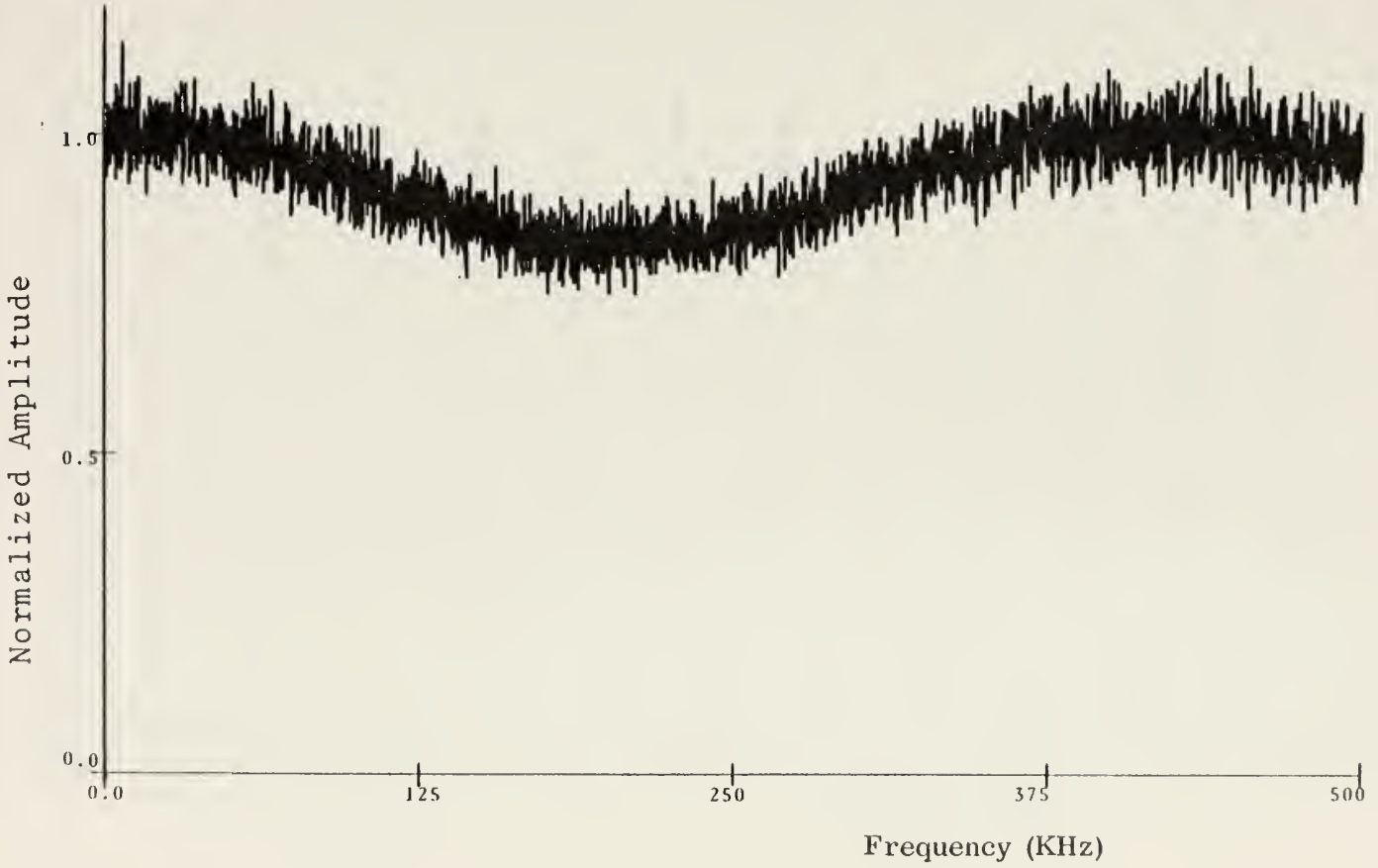

Figure 5.10 Input Noise Spectrum

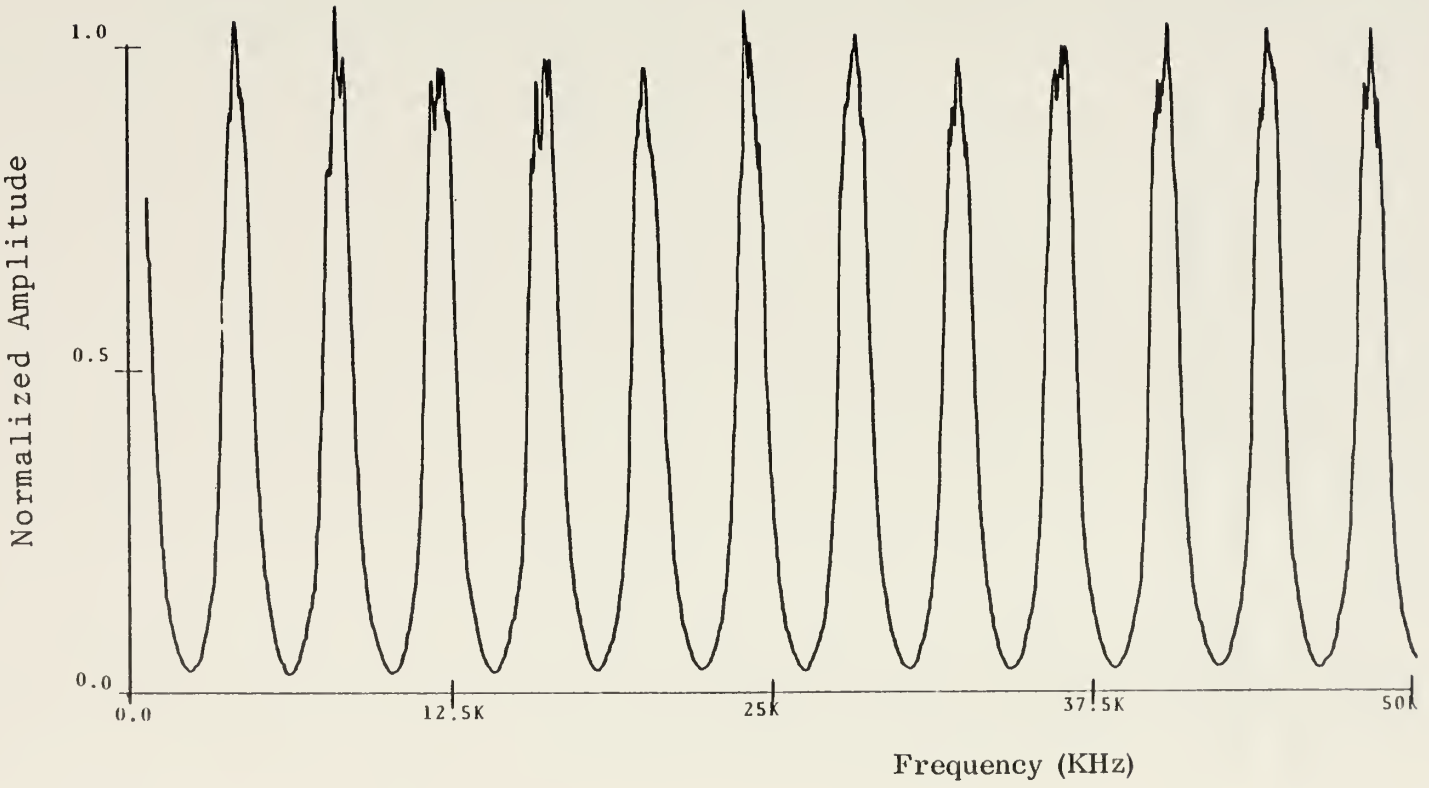

Figure 5.11 Output Noise Spectrum

Figure 5.12 graphically illustrates the attenuation of the noise signal with the input noise spectrum and output noise spectrum plotted on the same graph. The graph is plotted from zero to 50K hertz. The noise input spectrum is the top curve and the output spectrum is below it. This same input and output noise are shown in Figure 5.13 in the time domain. Note that although much of the noise is passed through the filter, much of it has been cancelled out. In Figure 5.13, the bottom is the input noise and the top, the output noise.

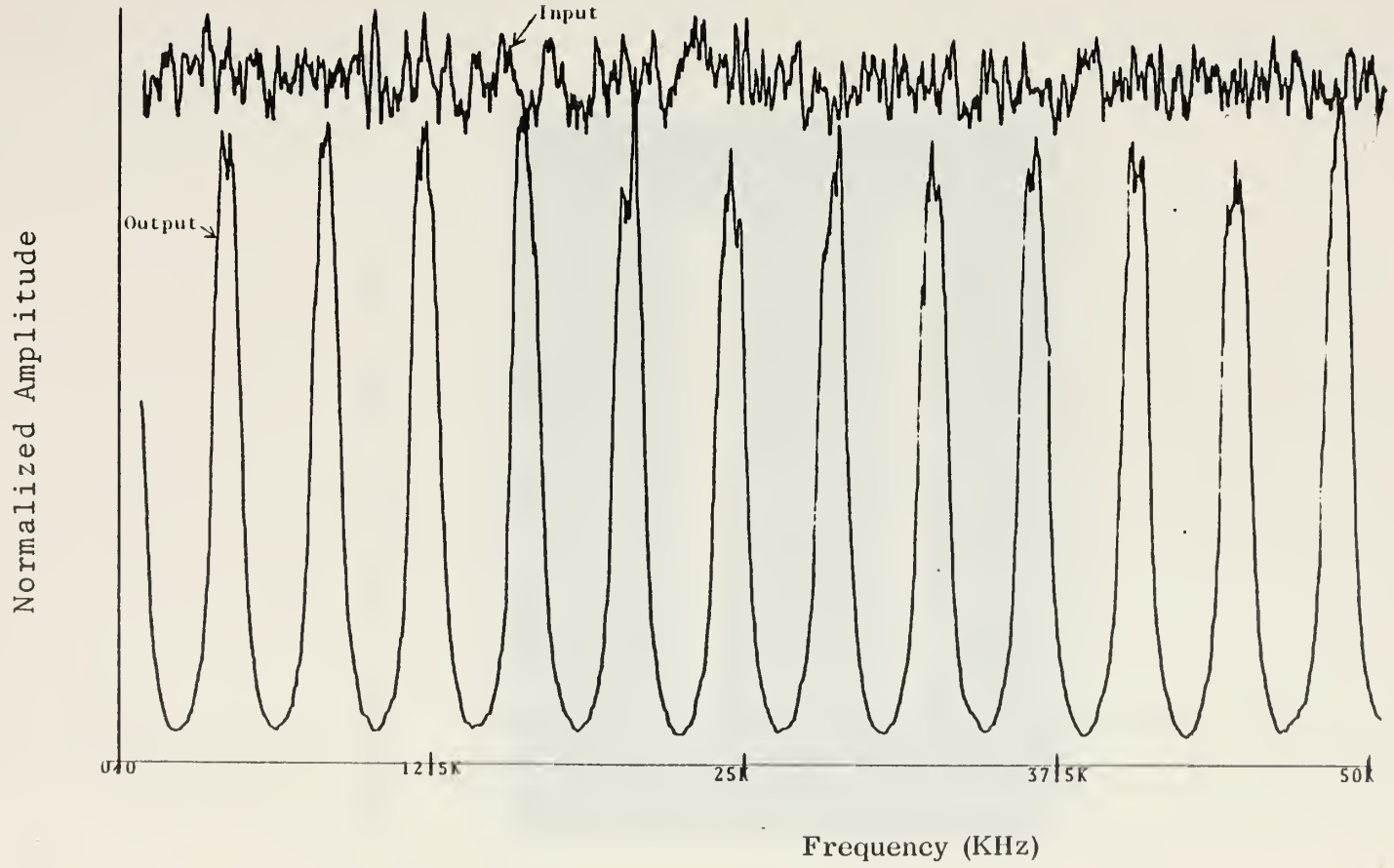

Figure 5.12 Comparison of Input and Output Noise Spectrum

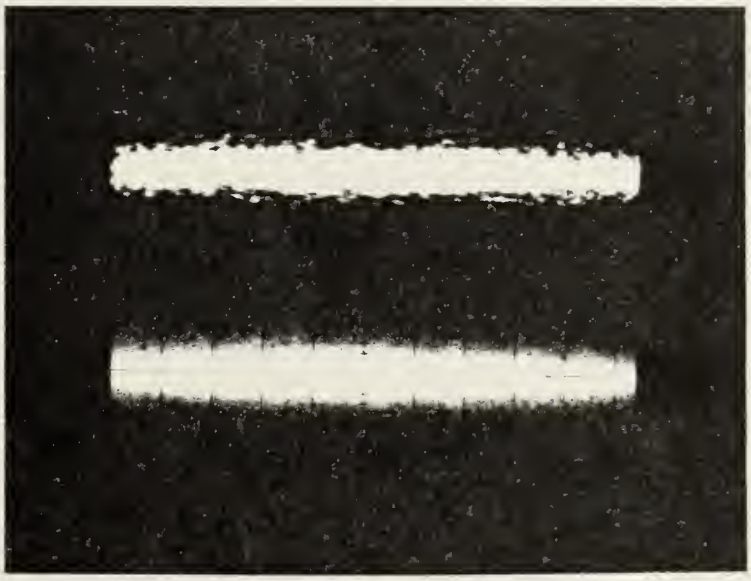

Figure 5.13 Time Domain of Input and Output Noise

D. SIGNAL-TO-NOISE RATIO MEASUREMENTS

It has been determined at this point that the Integrator Comb filter will act well in cancelling much of White Gaussian noise. But, can a signal be detected well enough to determine its presence ; and, if so, what type of signal-to -noise ratio improvment can be obtained? These are very important questions and will be pursued next.

The frequency spectrum of the input pulse train and noise was added with a resistive network as shown in Figure 5.14 below.

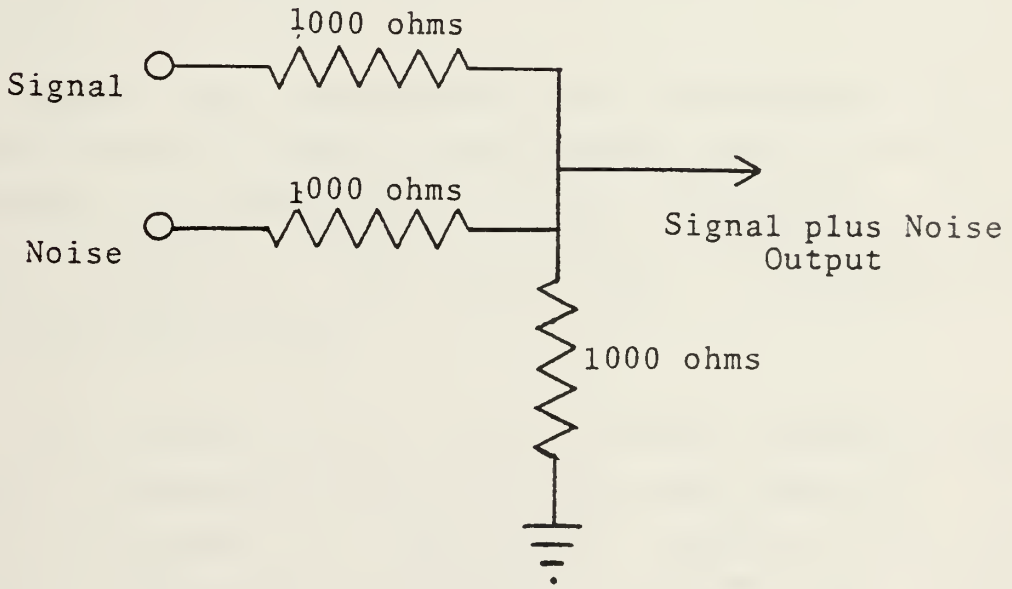

Figure 5.14 Network for adding Signal and Noise

The resistances were necessary to prevent the noise from feeding into the signal source as well as to prevent the signal from feeding into the noise source. The 1.0K ohm resistor to ground was necessary to prevent the relatively low input impedance of the filter from changing too drastically.

Figure 5.15, Figure 5.16, Figure 5.17, and Figure 5.18 are photographs of the signal plus noise input and output. The input signal was decreased from 2 volts peak to peak (figure 5.15) to 0.1 volts peak to peak (figure 5.18). This was done to give an indication of how well the filter will reproduce the signal even though it is buried in a relatively high noise environment. As seen in figure 5.18 the output pulses (bottom trace) are much more noticable than the input pulses.

Figure 5.19 demonstrates the cancellation of the input signal, which is added to the Gaussian noise, when the input frequency is not matched to that of the filter. Note that the output trace (bottom) is only composed of filtered noise whereas the top trace (input) is composed of both the signal and noise.

The previous data gives a visual indication that the signal is reproduced and also gives some indication of how well the signal is reproduced. However, a more precise method in answering the question of how well the signal is reproduced is to compare the signal's input and output frequency spectrum's. The following photographs show the frequency spectrum comparisons of the input and output.

Figure 5.20 is the frequency spectrum plot of the output pulse train alone. It covers a frequency range from zero to 450K hertz. Note that there is a large impulse at

390K hertz. This is due to the sampling clock PRF feeding through the filter; not a characteristic of the pulse train. Further note that the spectrum decreases to approximatly -67 dB at its minimum value which occurs at 390.0K hertz. This is as predicted since the Fourier analysis (as seen in appendix A) predicts that the spectrum will have a SinX/X envelope with the first null occuring at the reciprocal of the pulse width (i.e. 390.0K hertz). Figure 5.21 shows an overlap of both the input and output spectrums. The two curves are very much alike with the exception that the output spectrum (top curve) is approximatly 10 dB higher than the input spectrum (bottom curve). This is due to the filter having a gain of approximatly 10 dB. Figure 5.22 is the same output spectrum of figure 5.20 except that the plot extends only to approximately 20K hertz. Finally, Figure 5.23 shows the input and output plots overlapping. Again note the increase in the peak amplitudes due to the gain of the filter. Thus this comparison of both the time domain and frequency domain proves that the pulse train is reproduced exactly.

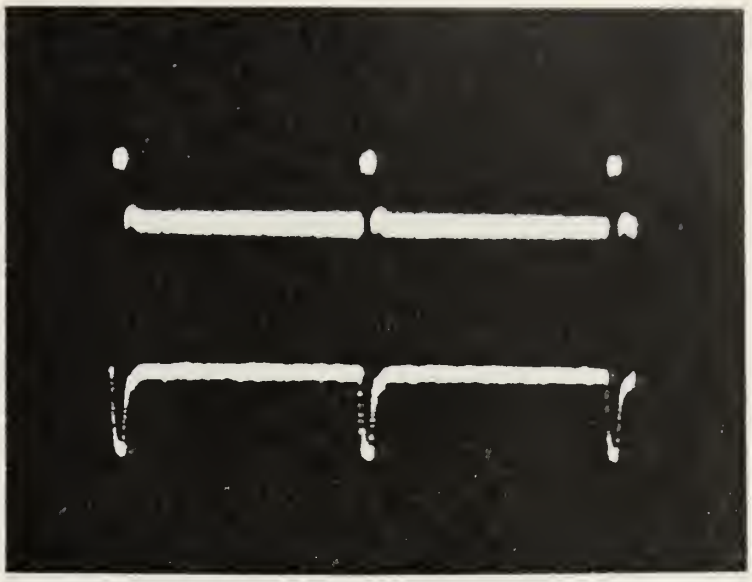

Figure 5.15 Signal Plus Noise

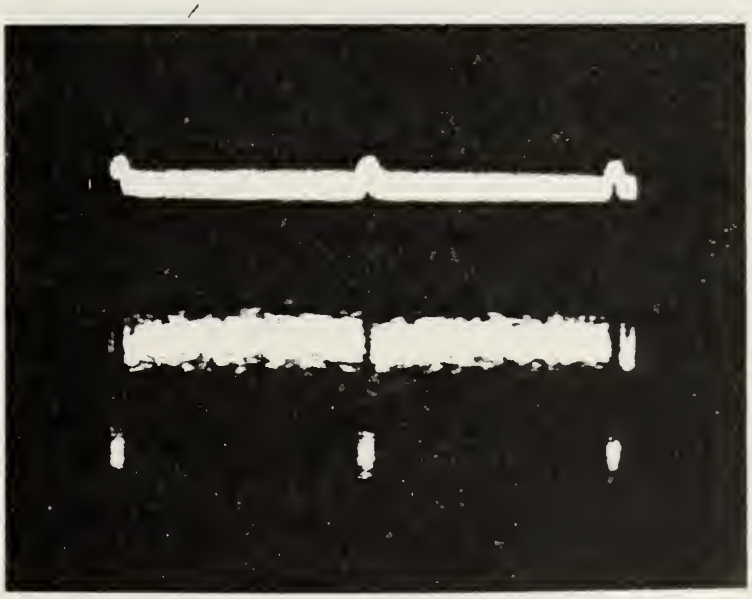

Figure 5.16 Signal Plus Noise

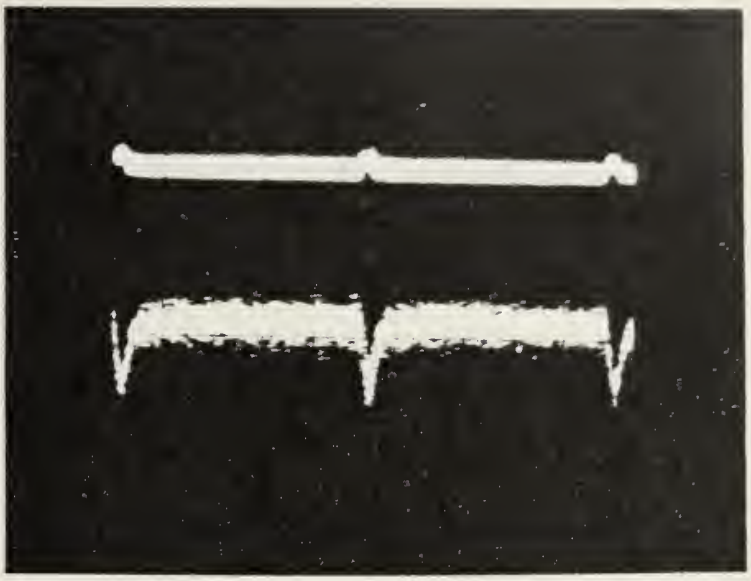

Figure 5.17 Signal Plus Noise

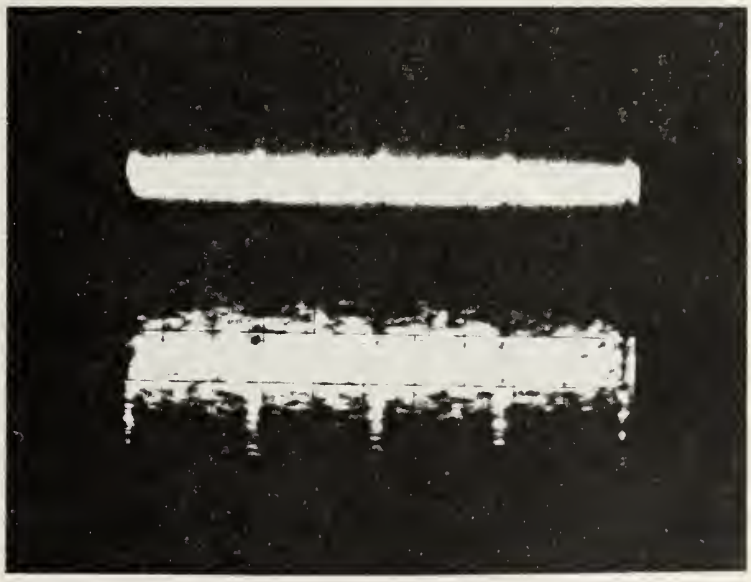

Figure 5.18 Signal Plus Noise

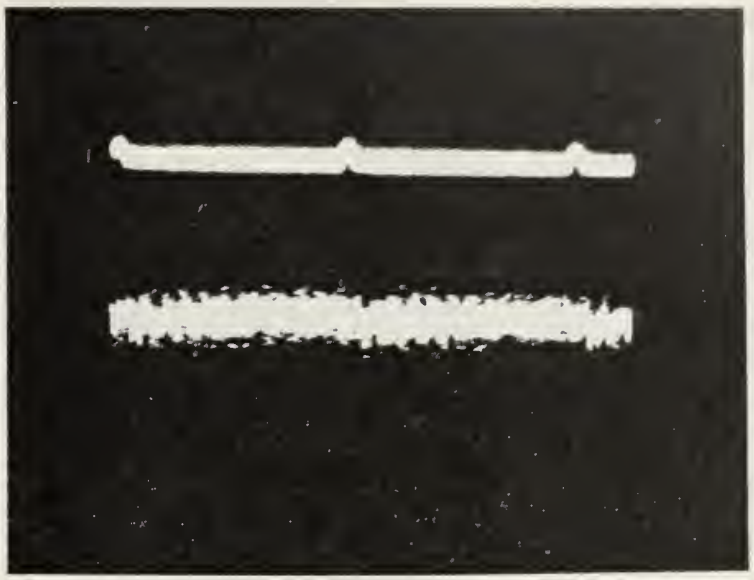

Figure 5.19 Cancellation of Signal Plus Noise

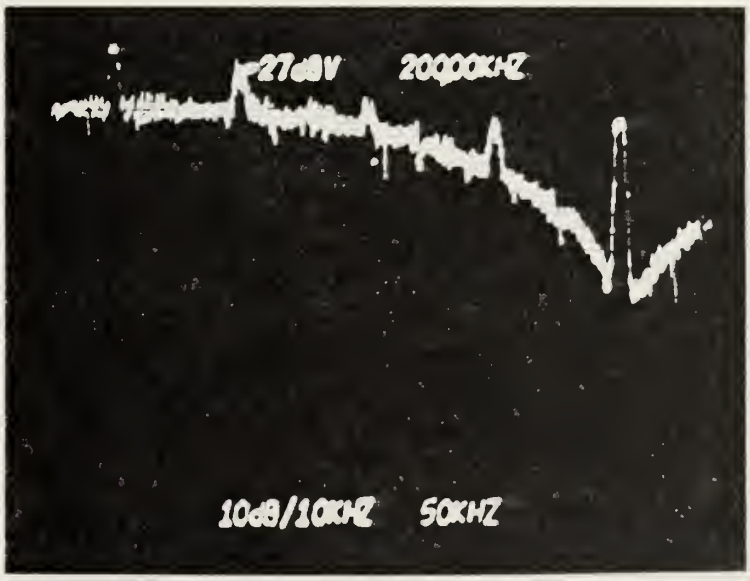

Figure 5.20 Output Signal Frequency Spectrum

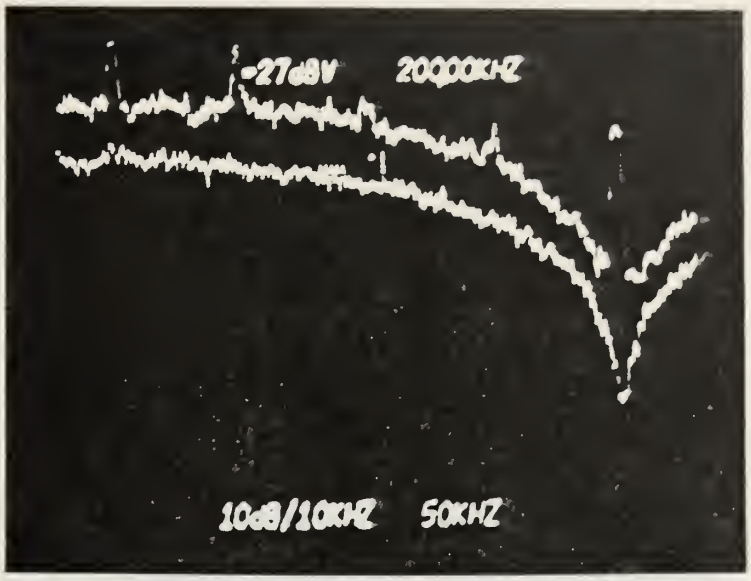

Figure 5.21 Comparison of Input and Output Spectrums

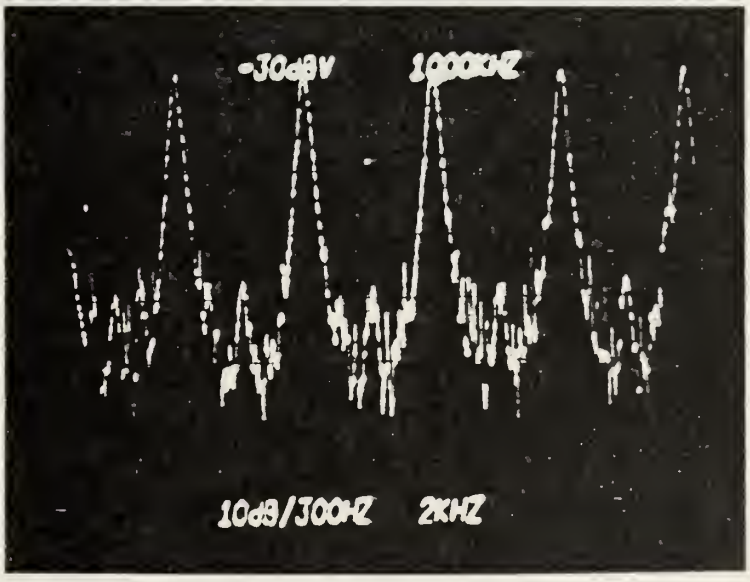

Figure 5.22 Output Frequency Spectrum

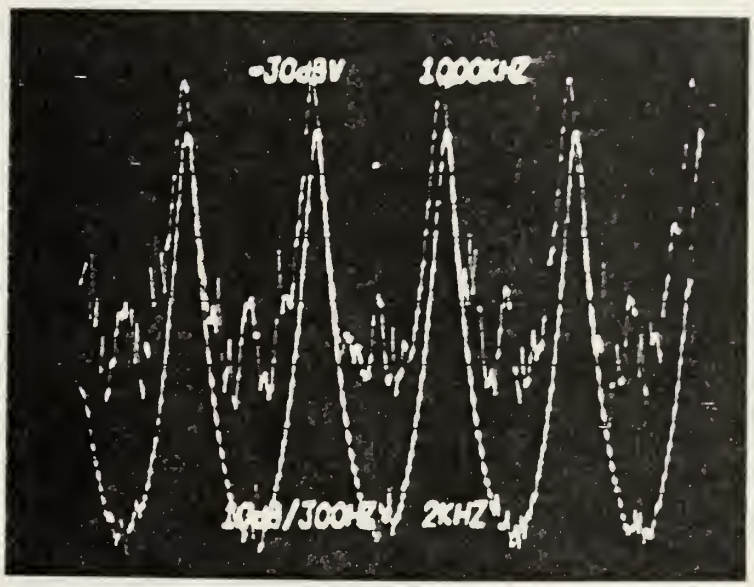

Figure 5.23 Output and Input Frequency Response Comparison

E. FREQUENCY CONSIDERATION

To this point there has been no comparison of signal plus noise in the frequency domain. The following data will show that the input signal is uneffected by a noisy environment and is reproduced exactly by the filter.

Figure 5.24 is a frequency spectrum of the input signal plus noise from zero hertz to 50 K hertz. The spectrum shown is a continious one since Gaussian noise has a continious spectrum; but , in this graph the pulse train spectral components are added to the noise spectrum causing the spectral lines to protrude higher than the noise spectral amplitudes. For a signal - to - noise ratio improvement it will be necessary for the Integrator Comb filter to attenuate the noise spectral components. This is in fact what has been done as seen in Figure 5.25. All the noise spectral components between the signal spectral lines have been attenuated to nearly zero. Note, however, that there is still noise passed through the filter since the pass band teeth have some finite width. Also, the width of the output spectrum teeth appear to be much wider than the filter pass band teeth. This is due, as explained earlier, to the small signal levels. Thus from the previous data, the signal is in fact reproduced exactly since all the spectral components of the pulse train signal are passed through the filter but also along with this reproduced signal there is noise passed through; however, the noise has been reduced considerably.

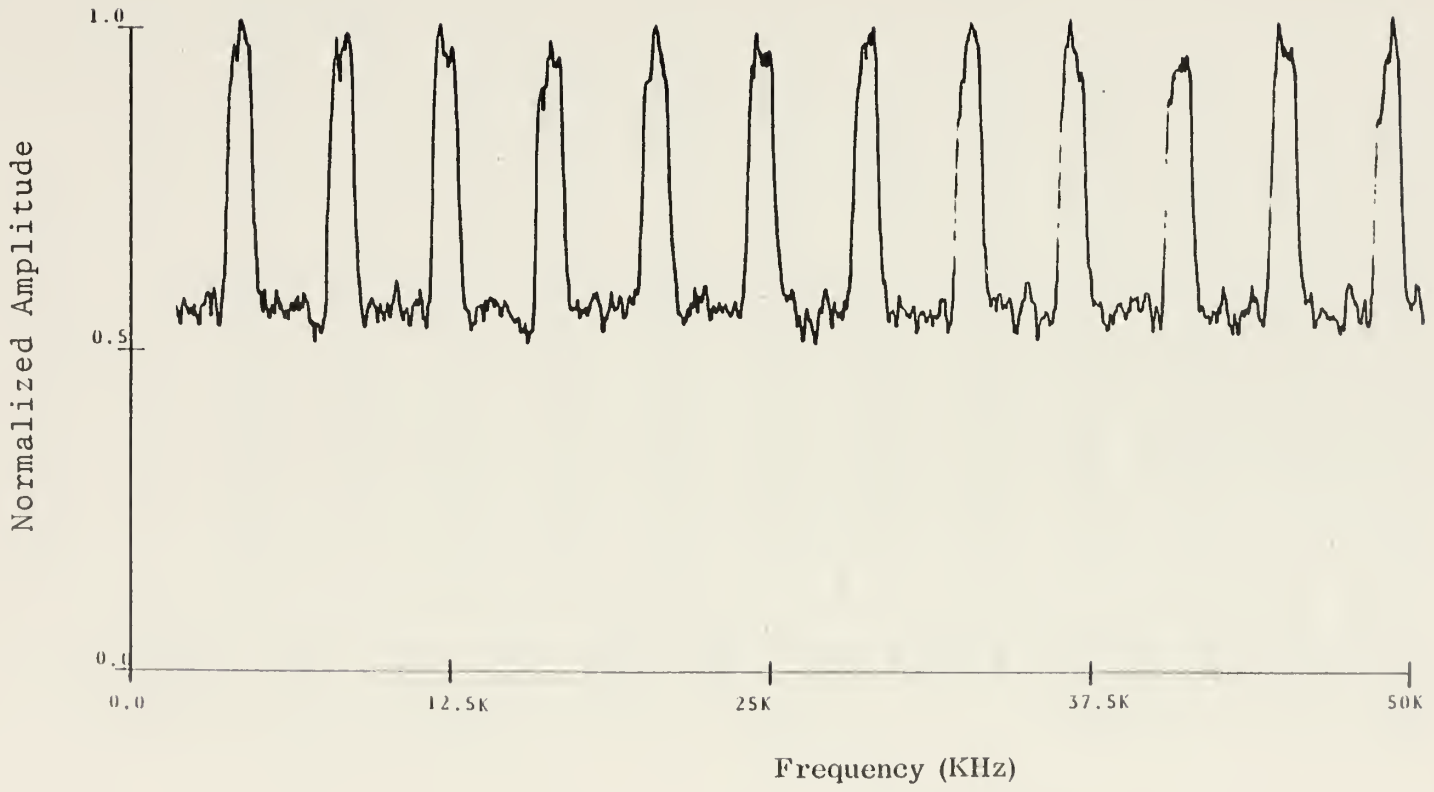

Figure 5.24 Pulse Train Plus Noise Frequency Spectrum

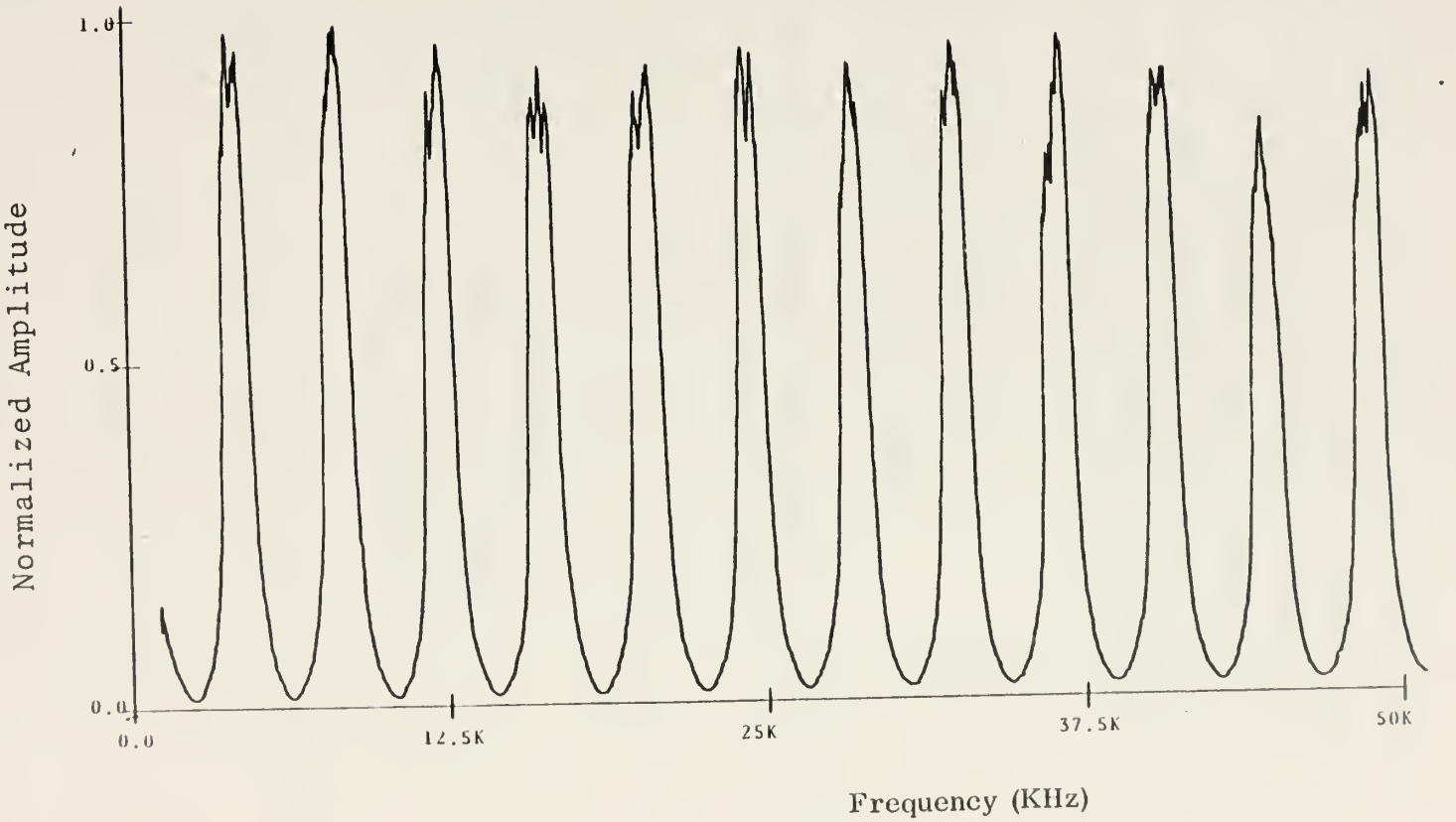

Figure 5.25 Filtered Pulse Train Plus Noise

F. SNR IMPROVEMENT USING A SECOND ORDER FILTER

It is evident at this point that there has been an improvement in signal - to - noise ratio, since the signal has been reproduced exactly and much of the noise has been attenuated. The question still remains as to how much improvement has been obtained. The answer to this question was obtained by making voltage measurements with an RMS voltmeter. The measurements were as follows:

Pulse Train Voltage (RMS)	.104	.880
Noise Voltage (RMS)	.665	1.15
Filter Noise Voltage < RMS)	-	.033

Since these are voltage measurements the signal-to-noise ratio is calculated using equation 3 below.

$$SNR(dB) = 20x(Log_{10} V_{sig} - Log_{10} V_{noise}) \quad 3$$

Thus the values are as given below:

$$SNR_{in} = -16.12dB$$

$$SNR_{out} = -2.32\ dB$$

The difference of the output SNR and the input SNR is the improvement. For these conditions it is:

$$SNR_{improvement} = 13.79\ dB$$

Although a 13.79 dB SNR improvement is not a great feat the fact remains that, for a first generation application of

the Reticon SAD - 100 as an Integrator Recursive Comb filter, it has performed well. Room for improvement in its operating techniques as well as the filter design techniques still remains.

G. FIRST ORDER FILTER SNR IMPROVEMENT CURVES

The work which has been done above was all with a second order integrator filter. The following data was taken with the Reticon SAD-100 operating as a first order filter having numerator coefficients as: $a_0 = a_1 = 1.0$. The b coefficient was variable for this demonstration. The transfer function for this filter configuration is shown below as equation 4.

$$H(z) = \frac{1 + Z^{-1}}{1 + b_1 Z^{-1}} \qquad 4$$

The purpose of this section was to obtain some insight of the SNR improvement ability of the first order filter. The experimental data is shown in Appendix C. This data was plotted and is presented below in figure 5.26.

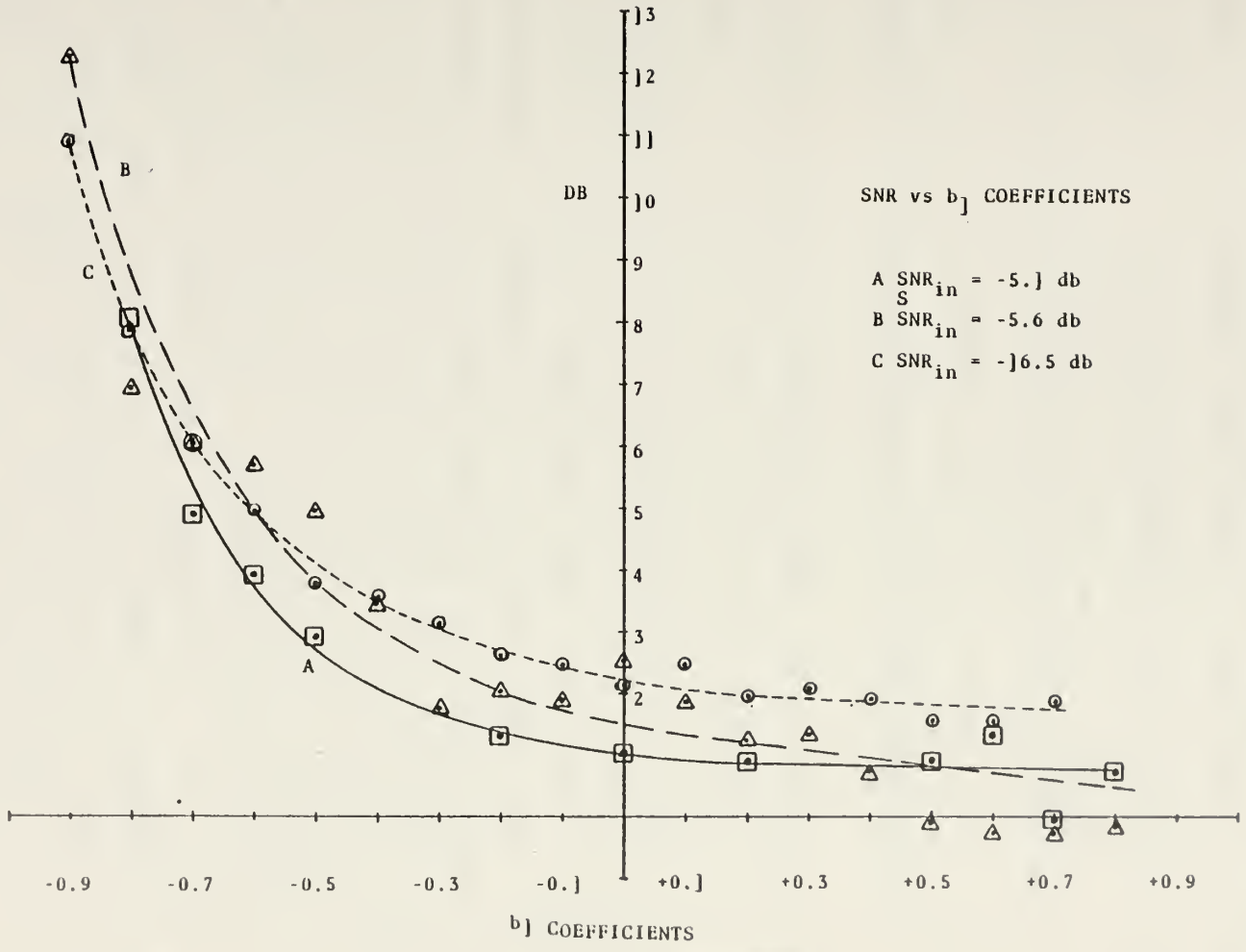

Figure 5.26 SNR Improvement vs b_1 Coefficients

The graph of figure 5.26 above is plotted with the b_1 coefficient on the abscisa as the independent variable and the SNR improvement as the dependent variable. the data was plotted in this manner since the b_1 coefficient determines the shape of the filter passband teeth as well as whether the filter is a canceller (+ b's) or an integrator (- b's). Thus by varying b_1 the filter will either pass more or less noise component through with the pulse train spectral components giving a variation in the SNR improvement.

Three curves are plotted each with varying SNR_{input} values. Although curves A and B only differ by 0.4 db, the input signal and noise voltages doubled in curve B giving approximatly the same input SNR. This was done to see the effects the input amplitude had on the amount of improvement. Curve C is a plot with the input SNR approximatly three times the value of either curves A or B. It was interesting to note that all the curves are within 2db or less of each other as seen in figure 5.27. This was an expected result since the filter pass band teeth are the same for the respective b coefficients regardless of the input signal amplitude. The SNR improvement is much higher for negative b coefficients because of the filter teeth becoming much narrower (i.e. a higher Q integrator circuit) and attenuating more and more of the noise. Since the three curves of figure 5.26 are all relatively close to each other, it was felt that the variations are due to instrumentation measurement errors and the fact that the noise is such a highly random signal that the measurement of the noise changes slightly each time a new measurement is made on the same signal. These small changes in

measurements cause a noticable logarithmic variation due to the nature of the logarithmic conversion characteristic.

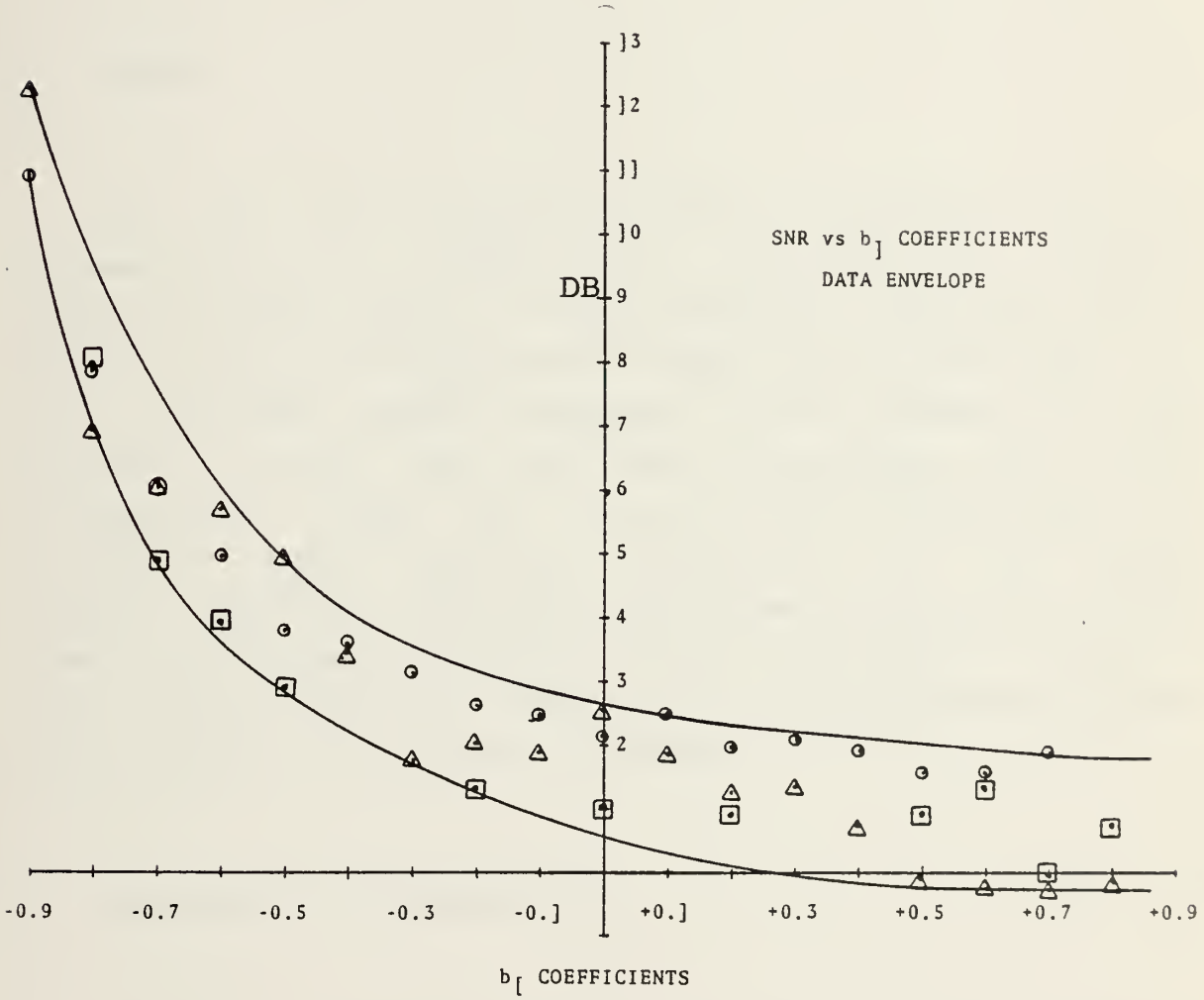

Figure 5.27 Band of Data Variation

VI. APPLICATION OF THE INTEGRATOR TYPE RECURSIVE COMB FILTER 2: SELECTION OF PULSE TRAIN

A. RADAR

Now that the Integrator Recursive Comb filter has been demonstrated as a device with potential to improve Signal-to-Noise ratio, to what practical use could such a device be put? One application which has been discussed in the literature (Recent Advances in the Synthesis of Comb filters) is their use for Radar application for video integrators. They are used in this application to accomplish linear addition (integration) of the radar signals which are consistant from sweep to sweep and at the same time the random signals (noise) will add in a root - sum -square form. The net result is an improvement in the SNR as shown in the previous section.

B. ELECTRONIC COUNTERMEASURES

Another application which is proposed by this report is the use of the Integrator Recursive Comb filter as a Pulse Sorter of Radar pulses to speed up the acquisition of Radar signals in an Electronic Countermeasures situation. This concept of a pulse Sorter has been demonstrated and the results are shown in Figure 6.1. The systems pulse trains added together make up the first four traces. There are four separate traces to show each pulse train as a stationary

signal on the scope. This was done by synchronizing the oscilloscope separately with each input signal and reexposing the same negative to the scope trace, after synchronizing and shifting the position of the stationary pulse train. After the first exposure, the filter output was moved off the scope screen, the next pulse train was synchronized to the scope, (to keep it stationary) the entire trace was moved vertically down on the screen, and the film was reexposed to the screen. Thus, the same negative was exposed four times. The frequencies of each pulse train from top to bottom are: f_1 = 8.46K hertz, f_2 = 1000 hertz, f_3 = 2000 hertz, and f_4 = 1500 hertz. The last trace is the filter output of the captured pulse train (f_1 in this situation). Note the correspondence between the pulse locations in the top trace f_1 and the output trace (bottom trace). This is the captured signal. The others do not pass through the filter since they fall in the filter's stop bands and are attenuated. Thus, by using the Integrator Recursive Comb filter, a particular pulse was sorted from among several and interference reduced from non-synchronous pulse train.

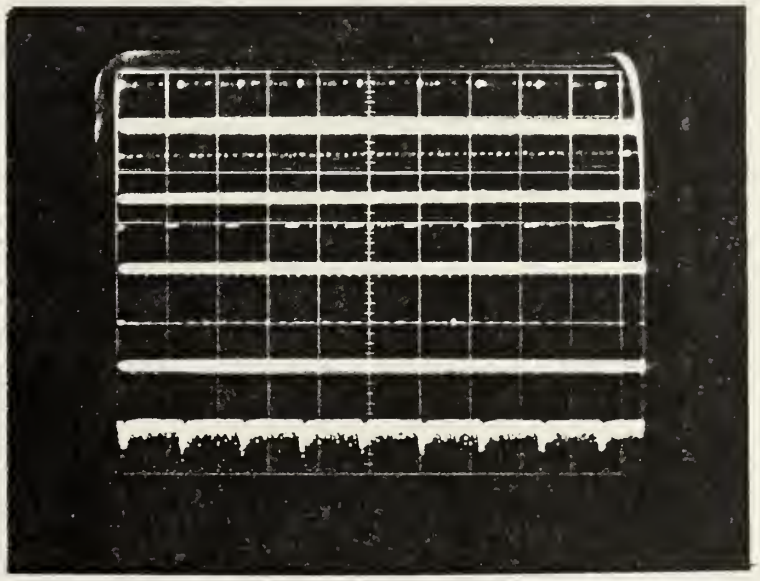

Figure 6.1 Pulse Sorting Illustration

1. Interference considerations from non-synchronous pulse trains

Ideally, the Reticon filtering will not pass through the system at all. But, there are some frequency relationships between the desired passed pulse train and the undesired signal so that the filter will allow for passage of some of the undesired components. The components that will pass are those of the signals that have a whole multiple spectral component of the filter's clock frequency. For example, the frequencies which were used above (f_1 = 8.46 K hertz, f_2 = 1000 hertz, f_3 = 2000 hertz, and f_4 = 1.5 K hertz), f_2, f_3, and f_4 have spectral components that are $8f_2$ = 8Khertz, $4f_3$ = 8Khertz, and $8f_4$ = 12Khertz and will fall within the pass band of the filter teeth. The effects of these components will cause some (as yet undetermined) distortion. The distortion was not noticable in the data taken in this thesis. An indepth study of this distortion would be most interesting as a thesis chapter in the future. Figure 6.2 below shows the spectral components that fall within the filter pass bands and very close to the captured signal (f_1).

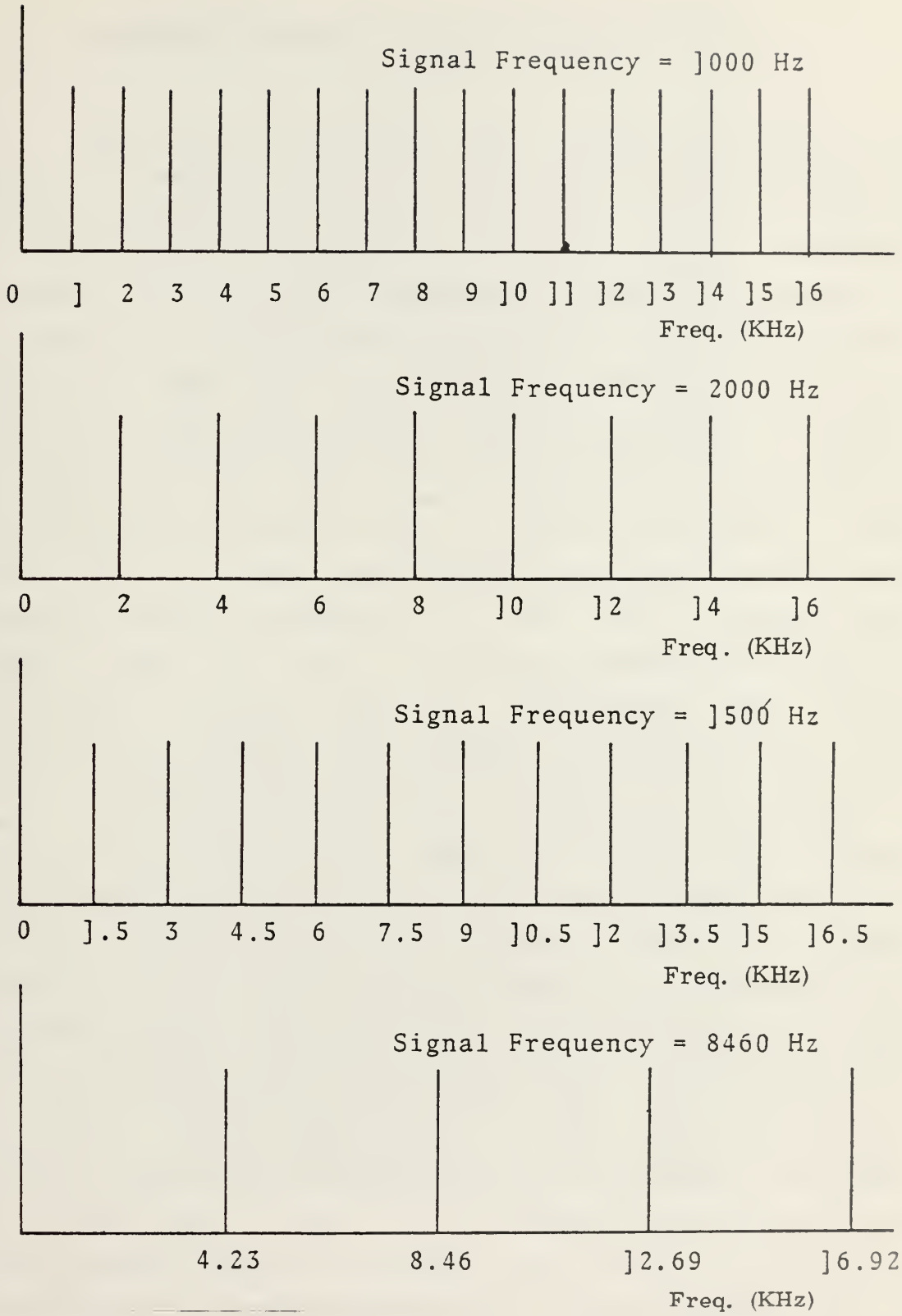

Figure 6.2 Interferring Spectral Components

2. Frequency Spectrum Considerations

The previous figures have demonstrated that the filter can select a specific pulse train signal and pass it while attenuating the others. The signal which is selected by the filter is reproduced at the output; but, how accurately is the signal reproduced? Figure 6.3a shows, on a linear plot, the line spectrum of the input pulse train. This is the signal that was eventually passed through the filter to give the output trace in Figure 6.1 above. Although the filter will pass multiples of signals starting at 406K /96 Hertz, the primary frequency selected for this demonstration was 8.46 K hertz. With this frequency, every other tooth of the comb filter frequency response will contain a spectral component of the 8.46 K Hertz input signal. This was done to ease the comparisons which are made later in this report in determining the filter's selectivity. Figure 6.3b shows the output of the filter using the input signal as shown in Figure 6.3a. Note that there are some very small spectral components at approximately 4K Hertz, 12K Hertz, 20K Hertz, etc. These components are that portion of the comb filter's teeth pass bands that are not filled with spectral lines of the signal. Instead, there are some noise components (possibly filter generated) which fall into these unused teeth and are being passed through. In comparison of these two signals, Figure 6.4 shows an overlay of both the input and output line spectrums. It is important to note that the signals' spectral lines match perfectly and at the proper frequency. This shows that there is no frequency distortion as the signal passes through the filter, but does not give any indication of phase relationship. Note, however, that the spectral amplitudes are very different. This amplitude change is a result of the filtering system gain.

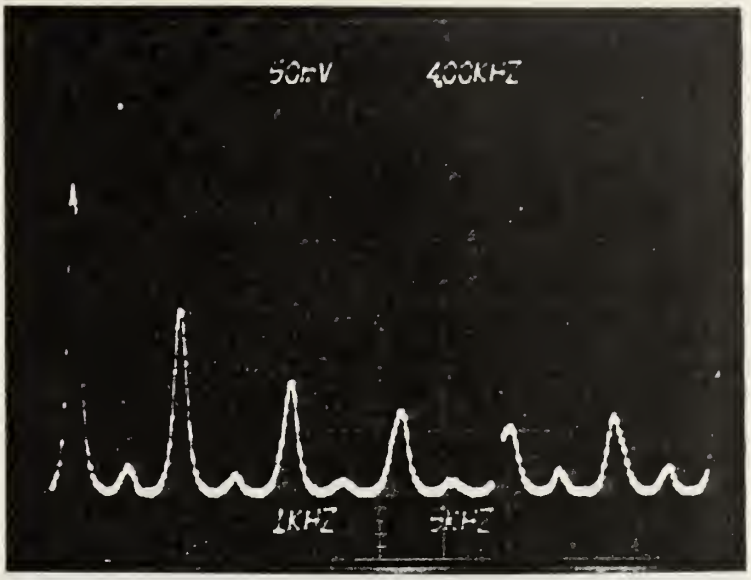

Figure 6.3a Output Frequency Spectrum

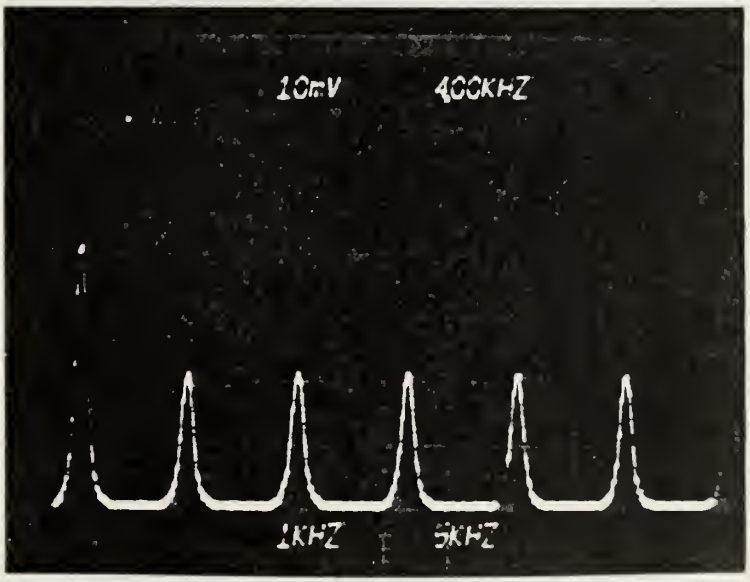

Figure 6.3b Input Frequency Spectrum

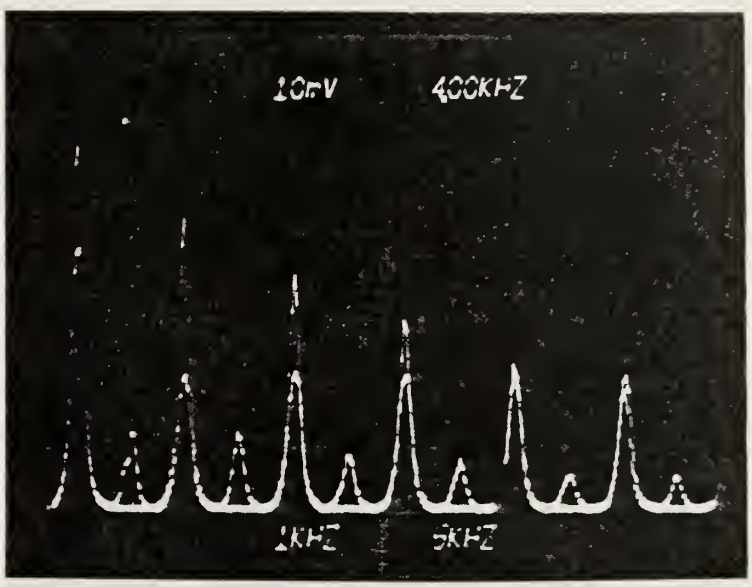

Figure 6.4 Comparison of Input and Output Spectral Components

In summerizing the observations of Figures 6.1,6.2,6.3, and 6.4 is noted that: first, the filter reproduces the input signal without frequency distortion; second, the filtering system amplifies the signal; and third, the filtering system introduces some small amount of noise into the signal. Now that it is known that the filter can reproduce the input pulse train with an added benefit of amplifying it; what will be the effects of two input pulse trains with equal PRF's and amplitude be on the filter? The following data will answer this question. The spectral components of the 8.46K hertz pulse train are shown in Figure 6.5a. It was expected that if a second pulse train of an equal PRF was injected at the filter input, the spectral components would simply add. This effect was demonstrated and is shown in Figure 6.5b.

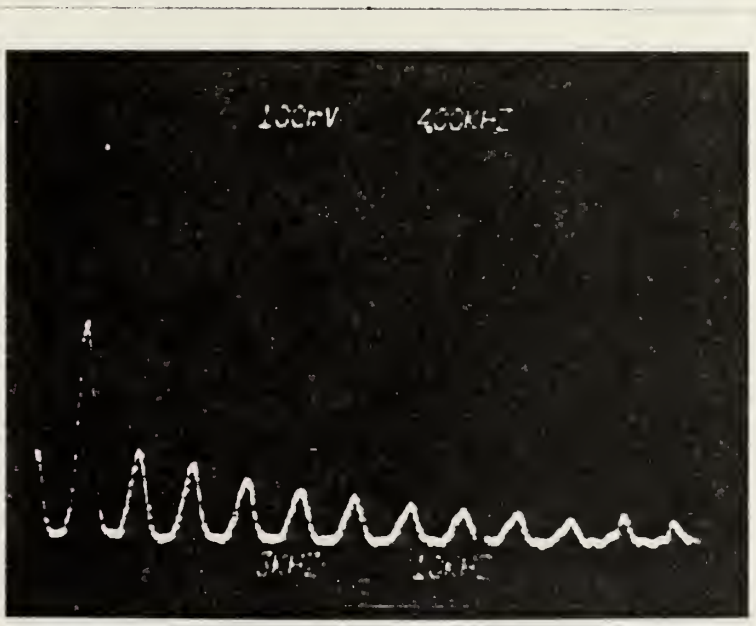

Figure 6.5a Spectral Output with Two Input Signals

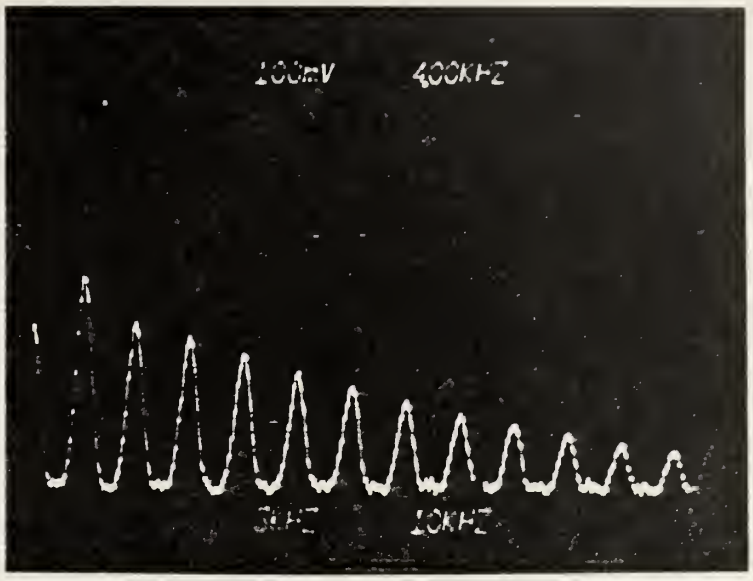

Figure 6.5b Spectral Output with Two Passed Signals

Figure 6.6 shows the overlap of both the curves of Figure 6.5. Note that the two signal spectral components simply add and that their frequency relationship is unchanged.

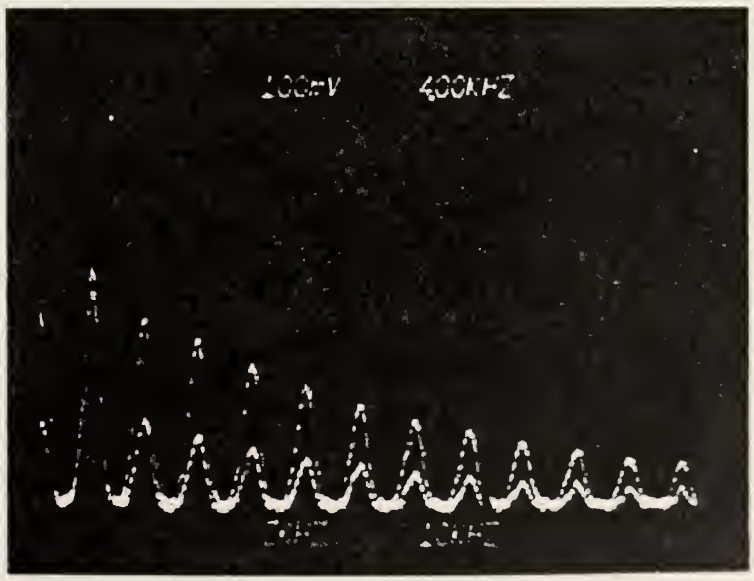

Figure 6.6 Comparison of Figures 6.4 and 6.5

The effects of harmonically related signals were demonstrated in the above data. These effects were used to aid in determining the frequency selectivity of the filter. This was done by using two input pulse trains which were harmonically related: 4.44K hertz and 8.88K hertz. The spectral components of the 8.88K hertz signal are 8.88K hertz, 17.76K hertz, 26.64K hertz, etc. and those of the 4.44K hertz signal are 4.44K hertz, 8.88K hertz, 13.22K hertz, 17.76K hertz, etc. Thus, the line spectrum of the sum of these two signals will reveal that the spectral components of the 8.88K hertz signal should be larger than those of the 4.44K hertz ones because they are an addition of both the 8.88K hertz and 4.44K hertz frequency components. Figure 6.7a shows this effect on the linear spectrum plot. This spectrum is the addition of two signals (8.88K hertz and 4.44K hertz) and was used as the input to the filter. Figure 6.7b shows the filter output. In both pictures, the larger amplitude components represent the summation of the 4.44K hertz and 8.88K hertz spectral components; and the smaller spectral lines between are only the 4.44K hertz spectral lines.

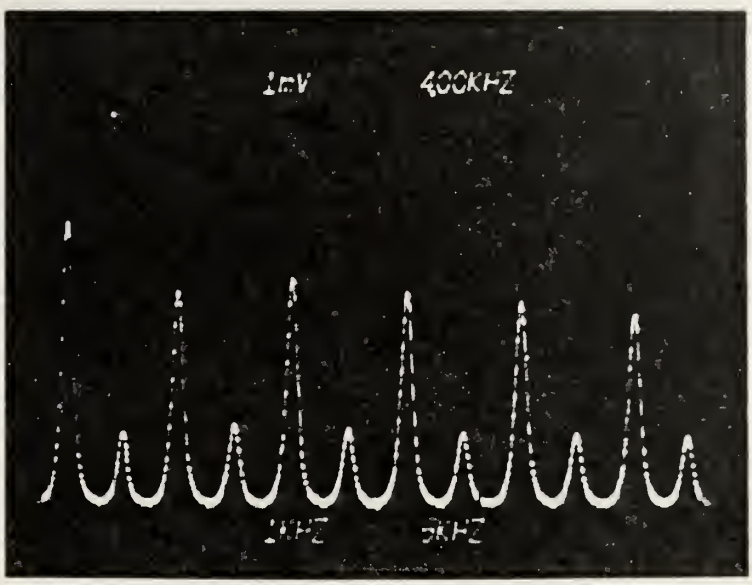

Figure 6.7a Input Spectral Components

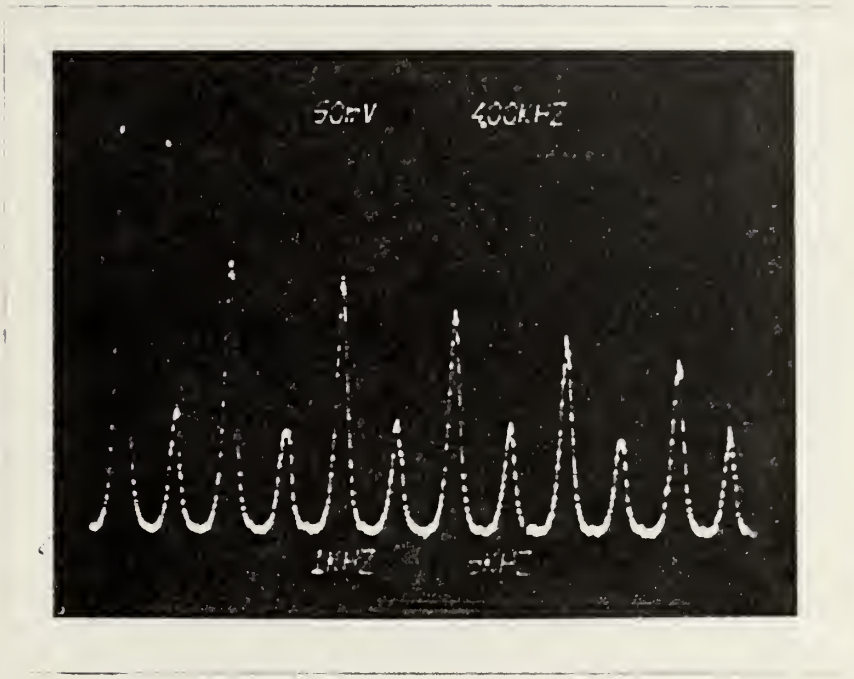

Figure 6.7b Output Frequency Spectrum with Two Input Signals

The differences in spectral component amplitudes was used in determining at what frequency the 8.88K hertz signal was attenuated and not present at the filter output. Then, by taking the difference of the passed signal frequency and the unpassed frequency,the filter selectivity could be determined. Figure 6.8 shows a comparison of the output of the 4.44K Hertz and 8.78K Hertz input signals. Note that the components of the 8.8K Hertz signal are deteriorating and decreasing. Decreasing the signal further to 8.59K Hertz as shown in Figure 6.9 shows that the original 8.88K Hertz is nearly gone with the exception of some 8.0K Hertz and 16K Hertz components. The filter output at 8.59K Hertz was very distorted and the pulse train was undetectable visibly on the oscilloscope. Thus, using this frequency as the limit of the filter's passable frequency, results in a selectivity of 290 Hertz on either side of the passband center frequency.

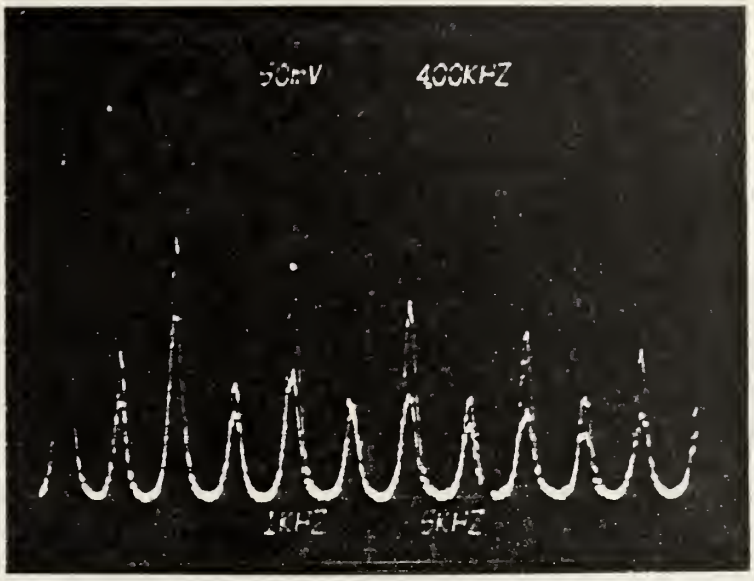

Figure 6.8 Comparison of Two Harmonically Related Signals

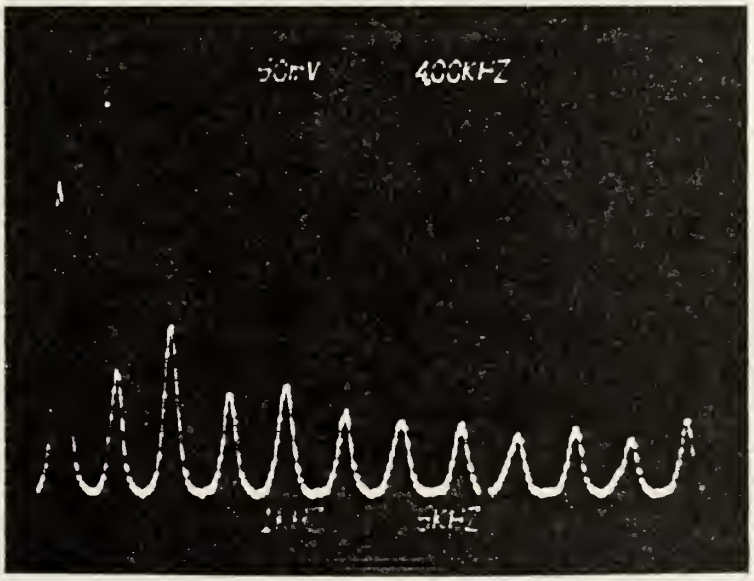

Figure 6.9 Limit of Frequency Selectivity

C. PROBLEMS ENCOUNTERED IN DATA TAKING:

One of the major problems encountered during data taking was the problem of the sampling frequency clock drifting as much as 10K Hertz. Slight adjustment in the circuitry was continuously necessary. Also related to the clock problem was the problem of keeping the clocks in synchronization when the filter was connected in the second order design. However, once synchronised they generally remained so.

The pulse generator was another source of difficulty in that the selected frequency for both the pulse Sorter and the SNR improvement demonstration would drift enough to cause the output to be distorted appreciably.

VII. CANCELLER APPLICATIONS AND DEMONSTRATION

A. BACKGROUND

The most common use of the recursive canceller comb filter is as a cancellation circuit for a Moving Target Indicator (MTI) radar. In this type of system it is important to attenuate the unwanted signals (called clutter) from the radar return spectrum. This clutter results from stationary targets such as; mountains, buildings from the local surroundings, and moving targets such as the leaves on trees which are moving with the wind , the trees themselves swaying with the wind, ocean waves and swells, etc.. It is highly desirable that this narrow band of clutter signals be cancelled and the desired signal targets pass through the filter and eventually give a target presentation on the radar scope. The recursive canceller comb filter is ideal for this application. Since it is periodic, a majority of the narrow frequency-banded clutter, which is periodic due to the pulse repition frequency (PRF) of the radar signals, will be cancelled. Also, the canceller frequency spectrum characteristic has a wide pass band and will pass the doppler shifted moving target. (unless it falls in the filters stop band which is then at the radars' blind speed). Complete cancellation of the clutter will not occur, however, since the stop band of the filter is generally not as wide as the clutter spectrum. If the clutter is a single spectral component, (stationary targets) then the filter will cancel it.

B. CANCELLER FIITFR DEMCNSTRATION

The technique of cancelling an unwanted frequency and passing a wanted signal was demonstrated with the Reticon SAD-100 used previously in this study. The filter was connected as a first order comb filter. The clock frequency was reduced to its lowest possible value of 104.6 KHz. Although the filter is capable of operating at a clock frequency as low as 2 KHz, this frequency was not achievable without physically changing a capacitor and a variable resistor on the printed circuit board that the SAD-100 and its associated circuitry was mounted on. The clock frequency of the filter was reduced to allow cancellation of as low a frequency as possible to simulate the previously discussed clutter spectrum. However, at this clock frequency, the lowest frequency that could be cancelled was DC and multiples of 1.09K Hertz. The frequency response of the filter at f_c =104.6 KHz is shown in figure 7.1. The stop band center frequencies are at whole number multiples of 1.09 KHz as seen in figure 7.1. For demonstration purposes the unwanted and desired signals were arbitrarily chosen to be 2 KHz and 13.1 KHz. Figure 7.2 depicts, in the top oscilloscope trace, the addition of the two signals at the filter input. The bottom trace shows the filter output of the 13.1 KHz signal. Figure 7.3 shows the passage of 13.1 KHz signal and a 1.5 KHz signal. This demonstrates that the filter will pass two simultanious signals and that if the unwanted signal is not at the stop band frequency, it will not be attenuated.

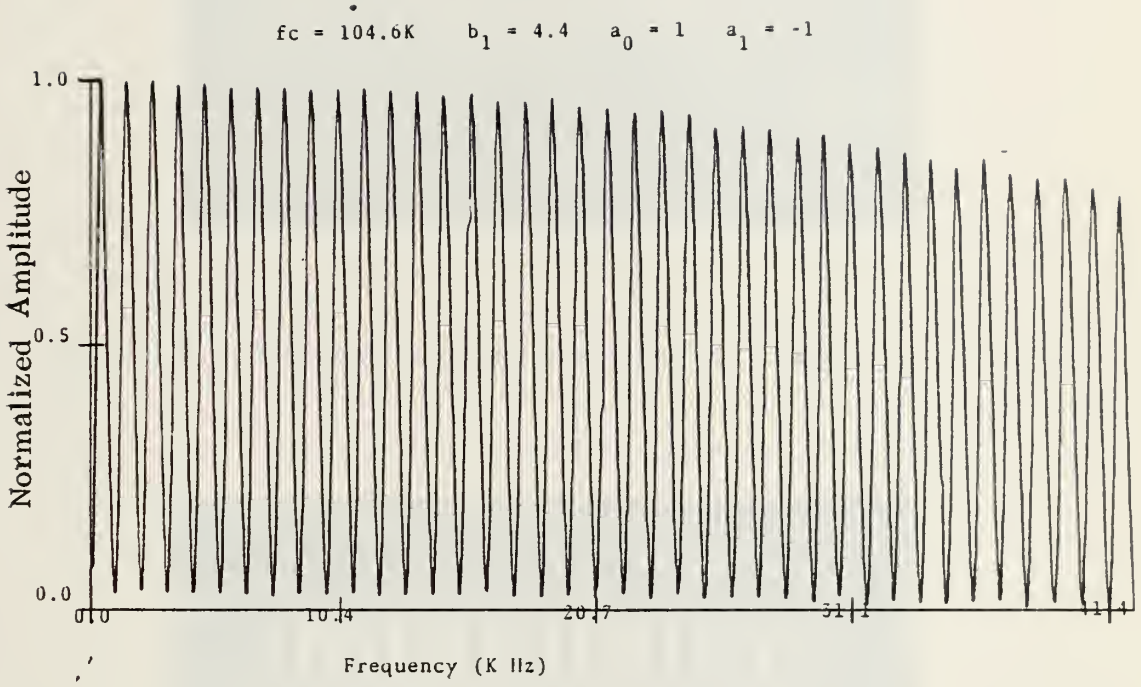

Figure 7.1 Frequency Response f_{clock}=104.6 KHz

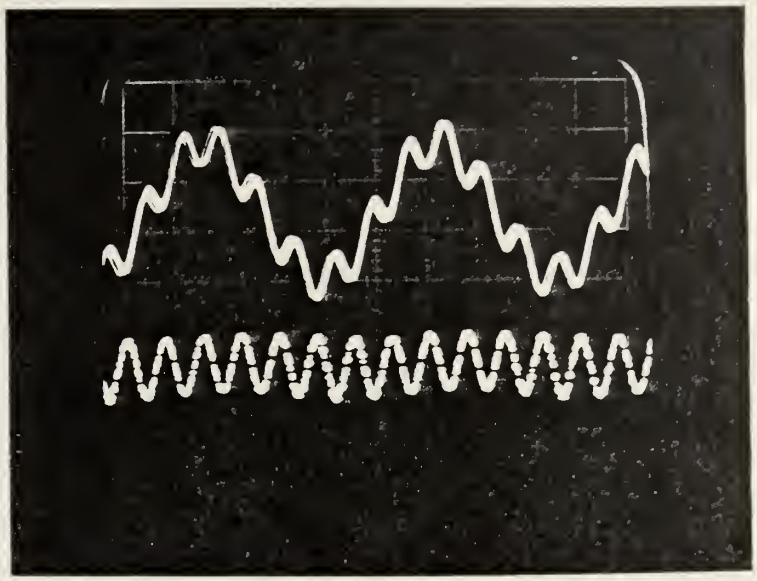

Figure 7.2 Demonstrating the Cancellation of a Signal

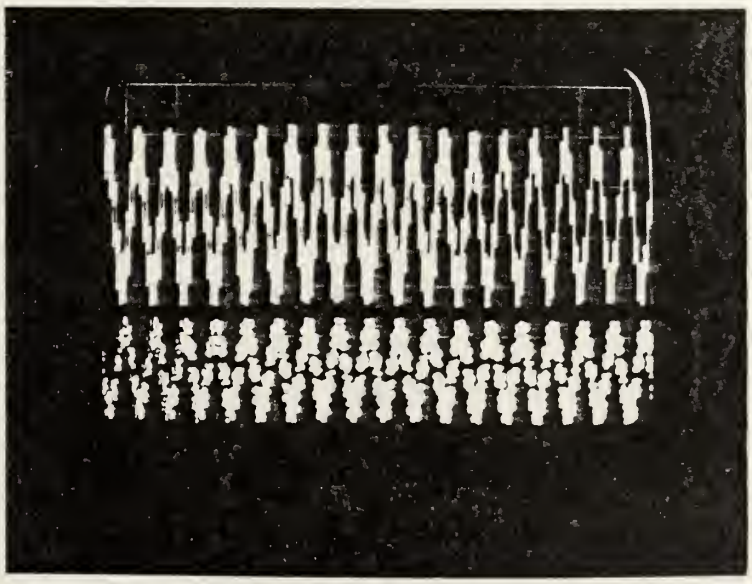

Figure 7.3 Demonstrating the Cancellation of a Signal

VIII. SUMMARY AND RECOMMENDATIONS

Results of this thesis are summarized in three areas: Experiment, Theory, and Applications.

A. EXPERIMENTAL RESULTS

Sampled analog recursive comb filters using a first or second order CTD delay line have been studied experimentally in detail. The filter circuit used for this study was the canonical circuit universally used for the digital recursive filters. The feedforward coefficients in this circuit (a_0, a_1, and a_2) are restricted to a mutual relation of 1, ±2, 1 in order to achieve perfect separation (infinite attenuation) between neighboring comb teeth. However, experimental results revealed that the nulls between comb teeth cannot be maintained. Deterioration of these nulls results with increasing frequency. To combat this problem, it was found that a sample and hold circuit was necessary at the input of the filter. The nulls of the filter frequency response improved in most cases giving nearly perfect attentuation between the neighboring comb teeth.

The major portion of this thesis dealt with the integrator comb filter while a companion thesis (written by Arif Ejas[11]) concentrated on the canceller comb features.

The Reticon-96 bit delay SAD-100 was the device used to implement the comb filter. This device's characteristics were studied extensively and the measurements taken are contained in Chapter 4. This study revealed that sampled analog recursive comb filters deviated from the ideal comb characteristics in that:

1. The peaks of the comb filter frequency response vary with frequency due to the Sin X/X characteristic of the sample and hold circuit, and also with the frequency dependence of the numerator and denominator coefficients of the filter transfer function.

2. A sample and hold circuit was necessary at the front of the canonical filter circuit to improve the nulls in the frequency response.

B. THEORETICAL ANALYSIS

To model the sampled analog recursive comb filter from the existing digital recursive filter theory, it was necessary to consider the following:

1. The feedforward coefficients a_0, a_1, and a_2 must be related by the ratio of 1, ±2, 1 respectively. This was necessary since the coefficients will place a zero on the unit circle in the Z-plane at either Z = +1+j0 or Z = -1+j0, resulting in the desired nulls.

2. The single delay Z^{-1} used in digital recursive filter theory, must be changed to Z^{-n} where n is the number of delay stages in the device. This accounts for the n comb teeth from DC to the sampling frequency (f_s).

3. The filter coefficients are all dependent on frequency due to several causes: sampled and hold effect, frequency rolloff due to limited bandwidth of electronics, and charge transfer inefficiency effect.

In summary, the theoretical transfer function for a second order sampled analog recursive comb filter is:

$$H(z) = \frac{a_0(f) + a_1(f)Z^{-n} + a_2(f)Z^{-2n}}{1 + b_1(f)Z^{-n} + b_2(f)Z^{-2n}}$$

where $a_0 = 1$, $a_1 = \pm 2$, $a_2 = 1$ at low frequency.

Using this modified theory, the theoretical analysis and experimental measurements are in close agreement. However, if proper frequency dependence of the filter coefficients can be obtained, the agreement between theory and experimental measurements will be improved.

C. APPLICATIONS

Three applications have been demonstrated, two for the integrator comb filters and one for the canceller type comb filters:

1. Integrator comb filter
   a. Signal to noise ratio improvement
   b. Pulse sorting
2. Canceller comb filter
   a. Deleting unwanted sinusoids

D. CONTINUATION OF THIS RESEARCH

Suggestions for future work are listed below:

1. Study the frequency dependence of the coefficients. This study would involve more computer simulation and matching of actual data and the computer plots such as those contained in Chapter 3.

2. Physically implementing the pulse sorter at the front end of a wide band receiver to evaluate its use under physical "real world" conditions.

3. Implement the Reticon filter with a chirped clock frequency and evaluate its performance. This type of device would have application in a chirped or jittered PRF radar.

4. Determine the input-output phase relationship of the pulse sorter of Chapter 6 to determine if there is any phase distortion encountered by the filter.

5. Determine the affects of the unwanted spectral components that fall in the filters pass bands on the desired pulse train spectral components for the pulse sorter discussed in Chapter 6.

6. Theoretically compare actual data with the data of figure 5.26 based on area under the comb teeth versus the response attenuation area.

APPENDIX A

PULSE TRAIN FOURIER ANALYSIS

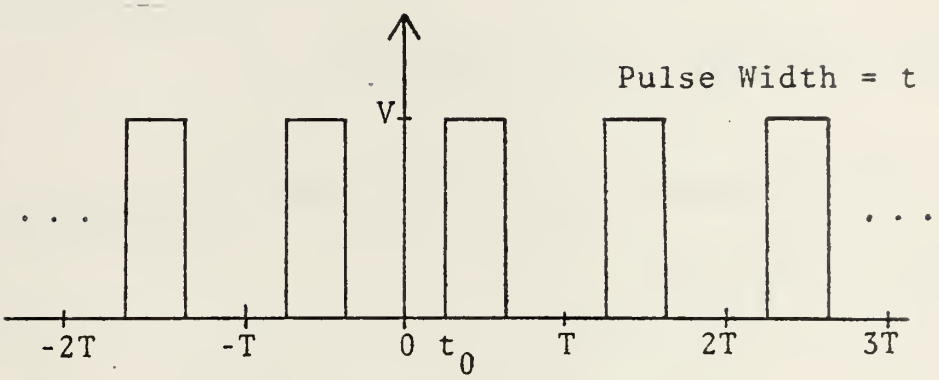

Figure A.1 Pulse Train

$$V = \begin{cases} 0, & 0 \le t < t_0 \\ v, & t_0 \le t \le t_0 + t \\ 0, & t_0 + t < t \le T \end{cases}$$

$$C_k = 1/T \int_{-T/2}^{T/2} f(t)\, e^{-jk w_o t}\, dt$$

$$C_k = 1/T \int_{0}^{t_o} 0\,dt + 1/T \int_{t_o}^{t_o+t} V e^{-jk w_o t}\, dt + 1/T \int_{t_o+t}^{T} 0\,dt$$

$$C_k = V/T \int_{t_o}^{t_o+t} e^{-jk w_o t}\, dt =$$

$$V\, e^{-jk w_o t} / -jk w_o T \Big|_{t_o}^{t_o+t} =$$

$$C_k = V/-jkw_oT\left(e^{-jkw_o(t_o+t)} - e^{-jkw_o t_o}\right)$$

Rewriting C_k:

$$V/-jkw_oT\left(e^{-jkw_o(t_o/2 + t/2)}\, e^{-jkw_o(t_o/2 + t/2)} - e^{-jkw_o(t_o/2 +t/2)}\, e^{-jkw_o(t_o/2 - t/2)}\right)$$

$$= V/-jkw_oT\left(e^{-jkw_o(t_o/2 +t/2)}\right)\left(e^{-jkw_o(t_o/2 + t/2)} - e^{-jkw_o(t_o/2 - t/2)}\right)$$

$$= V/-jkw_oT\left(e^{-jkw_o(t_o/2 +t/2)}\right)\left(e^{-jkw_o t_o/2}\right)\left(e^{-jkw_o t/2} - e^{+jkw_o t/2}\right)$$

using the Trig. Identity:

$$\mathrm{Sin}X = (1/2j)\left(e^{jX} - e^{-jX}\right)$$

$$= 2V/kw_oT\left(e^{-jkw_o(t_o + t/2)}\right)\left(e^{+jkw_o t/2} - e^{-jkw_o t/2}\right)/2j$$

$$= 2V/kw_o\left(e^{-jkw_o(t_o + t/2)}\right)\left(\mathrm{Sin}kw_o t/2\right)$$

$X = kw_0 t/2$

Therefor:

$$C_k = \frac{Vt}{T}\left(e^{-jkw_o(t_o + t/2)}\right)\left(\frac{\mathrm{Sin}kw_o t/2}{kw_o t/2}\right) \qquad 1$$

Solving for the absolute value of C_k:

$$\left|C_k\right| = (Vt/T)\,(\,\mathrm{Sin}X/X)$$

Similarily solving for the DC value of the pulse train:

$$C_0 = a_0 = 1/T \int_0^T f(t)\,dt = 1/T \int_{t_o}^{t_o+t} V\,dt$$

$$C_0 = (1/T)\,Vt \Big|_{t_o}^{t_o+t}$$

$$C_0 = (1/T)\,V(\,t_0 + t - t_0)$$

Therefore:

$$C_0 = (1/T)\,Vt$$

APPENDIX B

COMPUTER PROGRAM FOR PLOTTING H(Z)

```
      READ(5,200)A0,A1,A2,B1,B2
200   FORMAT(7F6.3)
      PI=3.141592654
      DEL=0.1
      HMAX=0.0
      DO 5 I=1,961
      K=I-1
      IF(I-1)2,2,4
2     GG=1.0
      GO TO 1
4     GG=ABS(SIN(PI*K*416.67/400000)/(PI*K*416.67/400000))
      G=GG
1     CONTINUE
      C=COS(2*PI*K*DEL)
      S=SIN(2*PI*K*DEL)
      CC=COS(4*PI*K*DEL)
      SS=SIN(4*PI*K*DEL)
      XR=A0+A1*C+A2*CC
      XI=A1*S+A2*SS
      YR=1+B1*C+B2*CC
      YI=B1*S+B2*SS
      R=XR*YR+XI*YI
      RI=XR*YI-XI*YR
      D=YR**2+YI**2
      H(I)=(SQRT(R**2+RI**2)/D)*GG
      IF(H(I)-HMAX)6,3,0
3     HMAX=H(I)
```

```
6       CONTINUE
5       CONTINUE
        DO 9 I=1,961
        K=I-1
        F(I)=K*0.4
        A(I)=H(I)/HMAX
9       CONTINUE
        CALL INIT
        CALL XFRM(4)
        CALL YFRM(4)
        CALL NPTS(961)
        CALL PLOT(F,A)
        CALL PAUSE
        CALL FIN
        END
```

APPENDIX C

EXPERIMENTAL DATA FOR SNR GRAPHS

Coeff.	Noise Volts (RMS)		Signal Volts (RMS)		SNR (DB)		
b_1	V_o	V_i	V_o	V_i	In	Out	Improv.
+0.8	0.061	0.038	0.036	0.021	-5.36	-4.58	+0.78
+0.7	0.059	0.405	0.035	0.024	-4.51	-4.55	-0.04
+0.6	0.056	0.375	0.035	0.202	-5.37	-4.00	+1.37
+0.5	0.056	0.039	0.036	0.226	-4.76	-3.84	+0.92
+0.2	0.055	0.037	0.039	0.023	-3.90	-2.99	+0.91
0.0	0.063	0.039	0.039	0.022	-5.18	-4.17	+1.02
-0.2	0.068	0.037	0.043	0.020	-5.37	-3.98	+1.39
-0.5	0.079	0.039	0.062	0.022	-5.07	-2.13	+2.95
-0.6	0.097	0.038	0.083	0.021	-5.25	-1.31	+3.94
-0.7	0.118	0.042	0.114	0.023	-5.21	-0.30	+4.91
-0.8	0.114	0.038	0.195	0.021	-5.36	+2.63	+7.99

*Data plotted as dots with squares around them in Figure 5.26.

Coeff.	Noise Volts (RMS)		Signal Volts (RMS)		SNR (DB)		
b_1	V_o	V_i	V_o	V_i	In	Out	Improv.
+0.8	0.126	0.082	0.066	0.044	-5.53	-5.68	-0.15
+0.7	0.115	0.082	0.060	0.044	-5.43	-5.67	-0.24
+0.6	0.119	0.085	0.060	0.044	-5.72	-5.96	-0.24
+0.5	0.120	0.085	0.063	0.045	-5.58	-5.61	-0.03
+0.4	0.123	0.085	0.070	0.044	-5.70	-4.91	+0.79
+0.3	0.125	0.085	0.077	0.045	-5.60	-4.26	+1.34
+0.2	0.125	0.085	0.076	0.045	-5.62	-4.38	+1.24
+0.1	0.135	0.085	0.088	09045	-5.60	-3.77	+1.84
0.0	0.134	0.085	0.094	0.045	-5.62	-3.08	+2.54
-0.1	0.135	0.085	0.088	0.045	-5.62	-3.72	+1.90
-0.2	0.150	0.085	0.099	0.045	-5.62	-3.61	+2.01
-0.3	0.152	0.085	0.098	0.045	-5.60	-3.81	+1.79
-0.4	0.162	0.085	0.125	0.044	-5.70	-2.25	+3.45
-0.5	0.196	0.085	0.181	0.045	-5.58	-0.69	+4.89
-0.6	0.219	0.085	0.218	0.044	-5.72	-0.04	+5.68
-0.7	0.244	0.082	0.295	0.044	-5.43	+1.65	+7.08
-0.8	0.320	0.082	0.425	0.044	-5.53	+2.46	+7.99
-0.9	0.575	0.085	1.300	0.044	-5.72	+7.09	+12.28

*Data plotted as dots with triangles around them in Figure 5.26.

Coeff.	Noise Volts (RMS)		Signal Volts (RMS)		SNR (DB)		
b_1	V_o	V_i	V_o	V_i	In	Out	Improv.
+0.7	0.204	0.150	0.038	0.023	-16.5	-14.6	+1.86
+0.6	0.206	0.150	0.037	0.023	-16.5	-14.9	+1.56
+0.5	0.207	0.150	0.037	0.023	-16.5	-14.9	+1.59
+0.4	0.212	0.150	0.039	0.023	-16.5	-14.6	+1.93
+0.3	0.220	0.150	0.042	0.023	-16.5	-14.4	+2.09
+0.2	0.228	0.150	0.043	0.023	-16.5	-14.5	+1.99
+0.1	0.236	0.150	0.047	0.023	-16.5	-14.0	+2.46
0.0	0.235	0.150	0.045	0.023	-16.5	-14.3	+2.18
-0.1	0.236	0.150	0.047	0.023	-16.5	-14.0	+2.46
-0.2	0.242	0.150	0.049	0.023	-16.5	-13.9	+2.61
-0.3	0.261	0.150	0.056	0.023	-16.5	-13.4	+3.11
-0.4	0.280	0.150	0.063	0.023	-16.5	-12.9	+3.52
-0.5	0.312	0.150	0.073	0.023	-16.5	-12.7	+3.80
-0.6	0.353	0.150	0.094	0.023	-16.5	-11.5	+4.98
-0.7	0.410	0.150	0.123	0.023	-16.5	-10.5	+6.02
-0.8	0.525	0.150	0.197	0.023	-16.5	-8.51	+7.96
-0.9	0.905	0.150	0.480	0.023	-16.5	-5.51	+10.9

*Data plotted as dots with circles around them in Figure 5.26.

LIST OF REFERENCES

1. Hayt, W. H. Jr. and Kemmerly, J. E., Engineering Circuit Analysis, p. 503 to 526, McGraw-Hill Inc, 1971.

2. Taub, H. and Schilling, D. L., Principles of Communication Systems, p. 1 to 10 and 480 to 481, McGraw-Hill Inc., 1971.

3. Rabiner, L. R. and Gold, B., Theory and Application of Digital Signal Processing, p. 1 to 46 and 205 to 228, Prentice - Hall, Inc., 1975.

4. Skolnik, M. I., Introduction To Radar Systems, p. 113 to 162 and 445 to 446, McGraw - Hill Book Company, 1962.

5. Boyd, J. A. and others, Electronic Countermeasures, p. 30-15 to 30-21, Prepared for U.S. Army Corps under Contract DA-36-039 SC-71204, 1961.

6. Holmes, S. V., Lcdr USN, Theory of Operation and Application of Sampled Analog Devices in Recursive Comb Filters, p. 142 to 187, Doctor of Philosophy Thesis, NPGS Monterey, Ca., 1976.

7. Freund, B. R., Implementation of Comb Filters by Sampled Analog Techniques, p. 1 to 69 and 90 to 135, Masters of Science Thesis, NPGS Monterey, Ca., 1975.

8. Saetre, L. T., Sampled Analog Recursive Comb Filter and their Application to MTI-Radar, p. 1 to 91, Master of Science Thesis, NPGS Monterey, Ca., 1975.

9. Iamsa-ad, V., Charge-Coupled-devices for Analog Signal Processing - Recursive Filter Study, p. 4 to 18, Masters of Science Thesis, NPGS Monterey, Ca., 1974.

10. Ejas, A, Theory of Sampled Analog Recursive Comb Filters and their Canceller Applications, p. 1 to 120, Electrical Engineer Thesis, NPGS Monterey, Ca., 1976.

11. White, W. D. and Ruvin, A. E., " Recent Advances In The Synthesis of Comb Filters", IRE Natl. Conv. Record, v. 5, p. 186 to 199, 1957.

12. Reticon Corperation, " Preliminary Data Sheet SAD-100 Serial Analog Delay", p. 1 to 3, 1974.

INITIAL DISTRIBUTION LIST

		No. Copies
1.	Library, Code 0212 Naval Postgraduate School Monterey, California 93940	2
2.	Department Chairman, Code 62 Department of Electrical Engineering Naval Postgraduate School Monterey, California 93940	1
3.	Assoc. Professor T.F. Tao, Code 62 TV Department of Electrical Engineering Naval Postgraduate School Monterey, California 93940	6
4.	Lt. Frank Piazza USNR 1203 Leahy Rd. Monterey, California 93940	3

Thesis
P4864 Piazza
c.1 Theory and applications of CTD recursive comb filters.

4 APR 78 S1822
18 JUN 79 25203

Thesis
P4864 Piazza
c.1 Theory and applications of CTD recursive comb filters.